# Ruby Graphite Project

## Beaverhead County, Montana

# 2022 Technical Report

**January 31, 2023**

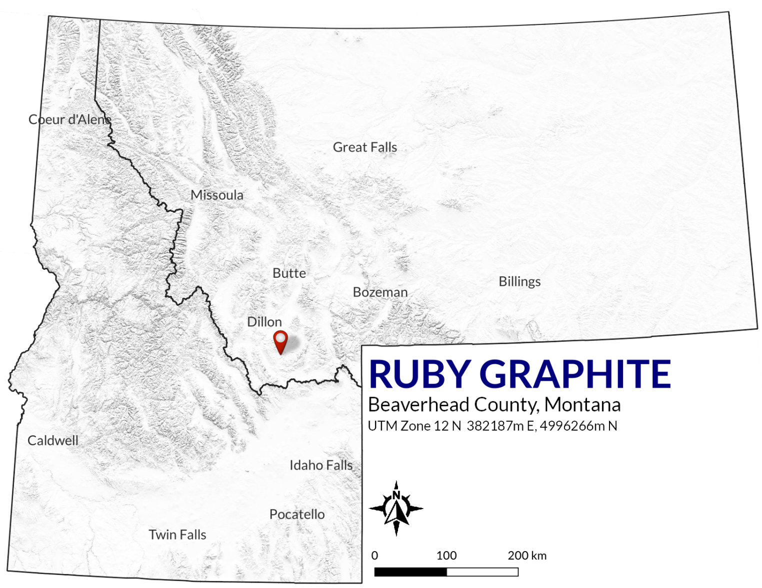


*Prepared for:*

**Reflex Advanced Materials**
905 West Pender Street
Vancouver, BC V6C 1L6
+1 (416) 768-6101

*By:*

Emma Kerins, B.Sc
Scott Close, M.Sc P.Geo

**Ethos Geological**
902 North Wallace
Bozeman, MT 59715
+1 (406) 291- 4198
www.ethosgeological.com

ETHOS GEOLOGICAL

REFLEX ADVANCED MATERIALS

# Table of Contents

## List of Figures

## List of Tables



## List of Appendices

*This page intentionally left blank*

# 1 Summary

The Ruby Graphite Project is located in the Blacktail Mining District in Beaverhead County, Montana, USA. The Project comprises 96 lode claims and three private land parcels under mineral lease to Ruby Graphite Holdings LLC, which is under option to be acquired by Reflex Advanced Materials Corp., totalling approximately 1,864.76 acres. Excellent infrastructure, year-round road access, and proximity to potential existing processing facilities in Dillon, Montana, create an excellent opportunity for near-term advancement and production.

Exploration and mining from 1901 to 1950 produced 2400 tons of graphite (Cg) at an estimated range of 14-27% Cg. Activities focused on graphite-bearing veins and fissures from the historic Ground Hog and Bird's Nest Mines. The Project remained undeveloped for more than sixty years until Graphite Corp. negotiated a mining lease for the Smith estate in 2012 and staked mining claims. The lease and claims were dropped in 2014, leased and restaked anew in 2016 by Ruby Graphite Holdings LLC, who then optioned the Project to Reflex Advanced Materials in 2022.

The Project comprises vein, flake and disseminated graphite mineralization hosted within Archean gneisses and marbles. The parent rock (protolith) for these rocks were likely an ancient sequence of marine and shore facies muds, silts and carbonates that underwent high temperature and pressure metamorphism during accretion and formation of the North American craton.

A unique type of concentrated vein graphite occurs at Ruby that is only recognized in several other localities world wide; a vein concentration that is relatively pure. The graphite occurs as crystalline lumpy or clotty graphite, and large acicular, flake-like masses with comb and rosette structures.

Reflex commissioned Ethos Geological ("Ethos") of Bozeman, Montana to perform field work during 2022, which included field mapping, soil sampling, outcrop sampling, ground electromagnetic surveys, and several Induced Polarization (IP) line surveys. Ethos was also charged with preparing the Report incorporating historic and new data on the Project.

Detailed field mapping identified several distinct gneiss units and their contacts with the marble. Soil sampling exposed lithologic differences and helped delineate important structures in areas lacking outcrop. Representative outcrop samples were collected and assayed, using their geochemistry to characterize the protolith; assay results are expected in Q1 2023.

EM and IP geophysical surveys identified several northeast-striking conductors that sit along trends of historic mineral workings; spatially coincide with the gneiss-marble contacts; and are located within newly identified areas. Both geophysics and the structural mapping imply that graphite-bearing horizons may be more widespread and continuous than previously recognized. Future exploration should target margins of the marble units and along structural fold hinges.

The Authors propose IP geophysics and a 3500m core drilling program in 2023 to target several large chargeable, conductive, and geologic anomalies identified by the work performed in 2022. Additionally, channel sampling across known and unmined exposures of graphite and tight ground EM survey arrays will help further delineate surface mineralization. Additional soil grids and structural mapping will aid definition and projection of important geologic contacts in areas lacking surface exposures.

# 2 INTRODUCTION

This report was prepared for Reflex Advanced Materials Corp. (Reflex) by Ethos Geological and documents the new historical information currently available for the Ruby Graphite Project ("Ruby" or the "Project") located in southwestern Montana, U.S.A.

The Project was originally mined by the Crystal Graphite Company in the early to mid 1900's and has remained dormant since. Ruby Graphite Holdings LLC (RGH), a private company based in Phoenix, Arizona, owned by Gregory and Joan Bell, acquired the claims and private mineral lease in 2016. The Project was then optioned by Reflex in September 2022.

Predicted increased usages of graphite and the need to meet increasingly stringent environmental controls and restrictions in the coming years will lead to significantly higher graphite prices (Bennett, 2022). Reflex contracted Ethos to lead the exploration effort, identify potential graphite-bearing areas, and develop a geological model of the stratigraphy and structure.

Over the course of the geologic work, Ethos performed the following studies:

- Detailed geological field mapping;
- Sampled a variety of rock types at 25 locations and submitted them for geochemical analysis to support lithology and structure mapping;
- Soil survey, collecting 201 samples at 25-m spacing along three lines, analyzed them for pH and geochemical analysis for identification of lithology changes across the Project;
- Detailed photogrammetry and elevation modeling conducted with an unmanned aerial vehicle (UAV or drone);
- Using a GEM-2 Ski by Geophex Ltd., a multifrequency electromagnetic (EM) handheld survey tool, acquiring approximately 100 line-km of surface EM data at 200 m spacing; and
- Contracted KLM Geoscience LLC to conduct an Induced Polarization (IP) survey along three lines, each approximately 1500 m long at 50-m dipole spacing, for identifying potential graphite-bearing intervals by searching for electrically conductive and chargeable anomalies.

## 2.1 Terms of Reference

Any 'historical' or 'potential' estimates contained in this document are not in accordance with the mineral resources or mineral reserves classifications contained in the CIM Definition Standards on Mineral Resources and Mineral Reserves, as required by National Instrument 43-101 ("NI 43-101"), as the purpose of this report is to obtain evidence and testing to confirm or deny the potential mineral targets.

Accordingly, Ethos Geological is not treating any included historical or potential estimates as current mineral resources or mineral reserves as defined in NI 43-101, and such estimates should not be relied upon without further testing and confirmation.

The terms "ore" or "resources" or "tonnes" in this report are being used in a descriptive and representative sense for historical accuracy, and are not to be misconstrued as representing any current economic viability.

Unless otherwise mentioned, all coordinates in this report are provided in the Universal Transverse Mercator WGS84 Zone 12 projection datum. Currency used in this report is provided in U.S. Dollars, unless stated otherwise. For this report, units of measurement are presented primarily in metric units.

## 2.2 Abbreviations

Abbreviations utilized in this report include:

| | |
|---|---|
| BLM | U.S. Bureau of Land Management |
| C | Carbon |
| Cg | Graphitic carbon |
| cm | Centimeter |
| CFR | U.S. Code of Federal Regulations |
| DEQ | Montana State Department of Environmental Quality |
| EM | Electromagnetic |
| FLPMA | Federal Land Policy and Management Act |
| ft | Foot |
| g | Gram |
| Ga | Billion years ago |
| GPS | Global positioning system |
| ha | Hectare |
| in | Inch |
| IP | Induced Polarization |
| kg | Kilogram |
| km | Kilometer |
| m | Meter |
| mm | Millimeter |
| Mt | Million tonnes (metric) |
| Ma | Million years ago |
| NI 43-101 | National Instrument 43-101 |
| NOITL | Notice of Intent to Locate a Lode Mining Claim |
| PoO | Plan of Operations |
| ppm | Parts per million |
| RGH | Ruby Graphite Holdings, LLC |
| SRHA | Stock Raising Homestead Act of 1916 |
| t | Tonne (metric) |
| $t/m^3$ | Tonnes per cubic meter |
| UAV | Unmanned Aerial Vehicle |
| USGS | U.S. Geological Survey |
| UTM | Universal transverse mercator |
| VLF | Very low frequency |

## 2.3 Statement of Qualified Persons

I, Scott Close, do hereby certify:

1. I am a Geoscientist employed by Ethos Geological, with an office at 902 North Wallace, Bozeman, Montana, USA;
2. I am a graduate of Montana State University (2004) with a Bachelor of Science degree in Earth Science, and a graduate of Simon Fraser University in Burnaby, British Columbia (2006) with a Master of Science degree in Earth Science;
3. I have practised my profession continuously since 2004;
4. I am presently the President and Chief Geologist of Ethos Geological Inc., a geological and mineral exploration consulting firm based in Montana, USA, and have been so since May 2008;
5. I am a registered Professional Geologist and a member in good standing with the Association of Professional Engineers and Geoscientists of British Columbia since July 2012;
6. This report is based on publicly available reports, maps, and on original interpretation;
7. My relevant experience for the purpose of this Technical Report is over continuous work and research in the field of geology and mineral exploration, of which the majority was spent as an independent consultant for mineral targeting, mineral resource estimation, ore body modelling, and mineral resource auditing;
8. I have read the definition of “qualified person” set out in National Instrument 43-101 (NI 43-101) and certify that by reason of my education, affiliation with a professional association and past relevant work experience, I fulfil the requirements to be a "qualified person" and am independent from the issuer;
9. I have overseen authorship of this report and I am responsible for this report in its entirety;
10. I state that, as the date of the certificate, to the best of my qualified knowledge, information and belief, the Report contains all scientific and technical information that is required to be disclosed to make the Report not misleading;
11. I have no personal knowledge, as of the date of this certificate, of any material fact or material change that is not reflected in this Report;
12. I have read the NI 43-101 professional codes of practice that set minimum standards for Public Reporting of minerals Exploration Results, Mineral Resources and Ore Reserves, and this Report has been prepared in compliance with those instruments and forms.

Dated this January 31, 2023

***"Scott J. Close"***

Scott J. Close, M.Sc., P.Geo
#158157 EGBC

Ethos Geological
902 North Wallace
Bozeman, MT U.S.A. 59715
scott@ethosgeo.com

# 3 Reliance on Other Experts

This Report has been prepared by Ethos Geological for Reflex Advance Materials Corp. This Report relies heavily upon field work, analyses, experience, and historical information compiled in a 2018 unpublished report on the Ruby Graphite Project by Gregory Bell and Brad Van Den Bussche.

The information and conclusions within this Report are also based on:

- Assumptions, conditions, and qualifications as set forth in this report;
- Data, reports, and other information supplied by RGH and Reflex; and
- Other third-party assays and analyses.

Public sources, including those for regional geology, analogs of similar and proximal deposits, technical documents, and other supporting documentation are referenced. Copies of documents obtained by the Authors, including those unpublished or unreleased or not readily available through public sources are available upon request.

# 4 Project Description and Location

## 4.1 Location

The Ruby Graphite Project is located in the Blacktail Mining District in Beaverhead County, Montana, USA. The Project sits in the southwestern Ruby Mountain Range, approximately 14 miles (22 km) southeast of Dillon, Montana (Figure 1).

The center of the Project is approximately 382187 E, 4996266 N in Mercator Zone 12 N (EPSG:32612). The Project covers portions of Township 8S, Range 8W, Sections 24 and 25, and Township 8S, Range 7W, Sections 20, 21 and 28 through 33 (Figure 2).

## 4.2 Project Description

The Project comprises private and public lands totaling 1,864.76 acres (754.65 ha), including 96 lode claims totaling 1,763.82 acres (713.79 ha) and 100.94 acres (40.85 ha) of private land under the Smith Mining Lease. Numerous historic adits, shafts, exploration trenches, discovery pits and several derelict structures are located within the Project area.

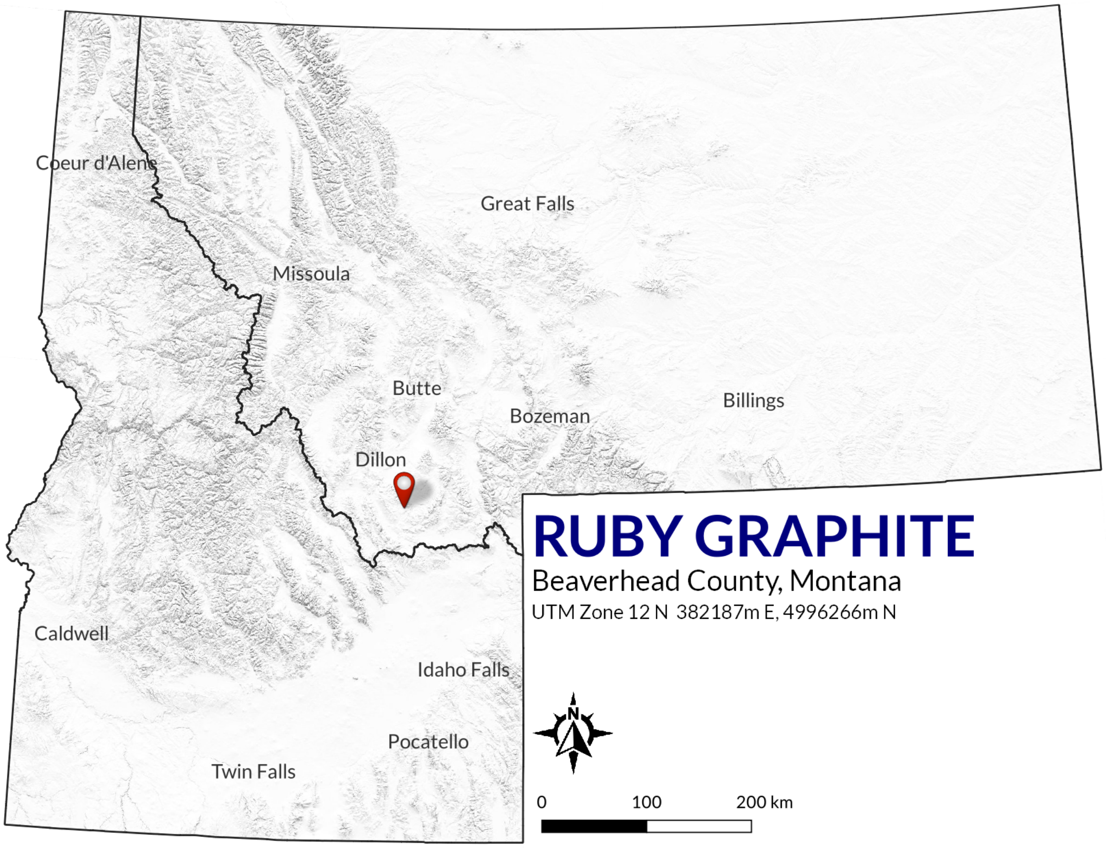


**Figure 1. Location of the Ruby Graphite Project, Montana, USA.**

## 4.3 Project Ownership, Mineral Tenure, Agreements and Encumbrances

The unpatented lode claims sit on a combination of private and public lands owned by Timber Creek LLC and the Bureau of Land Management (BLM), respectively (Figure 2). Three patented land parcels, the Smith Cabin, Mill Site, and Ground Hog, which account for roughly 5% of the Project area, are owned by the Smith family and under a mineral exploration and mining lease by RGH (Table 1).

All 96 contiguous lode claims and associated private leases are held by RGH and optioned by Reflex (Figure 2) as per an agreement finalized in October 2022. The Option is subject to a 2% net smelter returns royalty and a balloon payment of $3M on the commencement of commercial production. To fully exercise the Ruby Option, Reflex will be required to issue an aggregate of 1,000,000 common shares to the optionor on the occurrence of certain project milestones, incur an aggregate of $1.325M in exploration expenditures on the Project, and pay aggregate cash consideration of $1M to RGH designees.

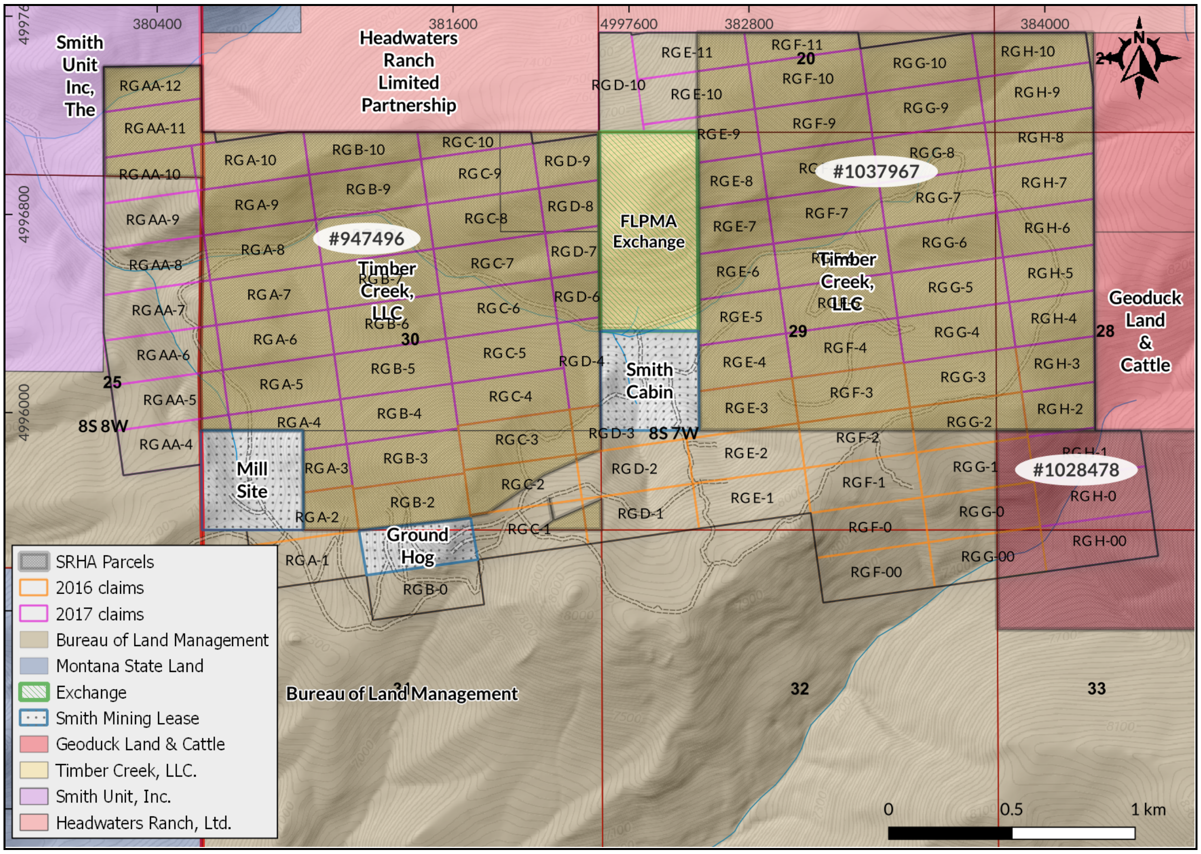


**Figure 2. Land status map for the Ruby Graphite Project showing lode mining claims (small rectangles), private land leases (stippled); contiguous private real estate parcels (labelled with ovals); and private and government administered lands.**

**Table 1. Summary of mineral rights for Reflex's Ruby Graphite Project.**

| Project Name | Mineral Ownership | Surface Ownership | Size (acres) | Size (hectares) |
|---|---|---|---|---|
| Smith Mining Lease | Private | Private | 100.94 | 40.85 |
| 2016 Lode Claims | Subsurface- BLM | Mixed BLM, Private | 453.01 | 183.33 |
| 2017 Lode Claims | Subsurface- BLM | Mixed BLM, Private | 1310.81 | 530.47 |
| **Total Controlled Project Area** | | | **1864.76** | **754.65** |

### 4.3.1 Smith Mining Lease

In 2016, RGH negotiated and executed the Smith Mineral Exploration and Mining Lease (the "Smith Mining Lease") with the heirs of the estate of the late Ralph I. Smith. The lease is comprised of three parcels of land:

1. Smith Cabin Site, consisting of the NW ¼ of the SW ¼ of Section 29, Township 8 S, Range 7 W, being 40 acres (16.19 ha) more or less;
2. Mill Site, consisting of Lot 4 (SW ¼ of the SW ¼) of Section 30, Township 8 S, Range 7 W, being 41.07 acres (16.62 ha) more or less; and
3. Ground Hog Lode, a patented mining claim located partially in the SE ¼ of the SW ¼ and in the SW ¼ of the SE ¼ of Section 30 and in the NE ¼ of the NW ¼ and in the NW ¼ of the NE ¼ of Section 31, all in Township 8 S, Range 7 W, being 19.87 acres (8.04 ha) more or less.

The Smith Mining Lease comprises 100.94 acres (40.85 ha) of land. Primary term of the lease is twenty-five years, renewable for an additional twenty-five-year term and continued indefinitely until the cessation of mining and/or milling operations. The Smith Mining Lease provides the right to:

- Conduct all customary mineral exploration activities including, but not limited to geological mapping, soil sampling, rock chip sampling, environmental baseline data acquisition, geophysical surveys on the ground and by aircraft, trenching, drilling, coring and excavation of test pits for bulk samples;
- Develop and mine minerals in accordance with all Federal and State regulations;
- Use the property for any shafts, openings, pits, and stockpile-grounds which are sunk or made for the mining, removal, and/or stockpiling of minerals from any adjoining or nearby projects;
- Process minerals on the property including waste disposal;
- Construct new structures as required for the purposes of mineral exploration, mining and processing operations or facilities;
- Access the property on existing roads;
- Use of the existing easements to the Axes Canyon and Van Camp Canyon Roads;
- Construct new roads on the property as required;
- Drill wells for water on the property;
- Appropriate and use surface water from the Mill Site and Ground Hog claim; and
- Lay and maintain all necessary water lines, among other provisions.

The Smith Mining Lease became effective June 1, 2016. The initial annual lease rental payment was $2,000, and this rental payment increases to $4,000 by year three. In addition, an advanced royalty payment of $10,000 was due by the fourth anniversary date, increasing to $20,000 per year thereafter. A 3% royalty on Net Smelter Return (NSR) is payable on production and sale of minerals mined from the Smith property, but not on cross-mined production. Half of the royalty may be purchased for $1,500,000 and will reduce the royalty to 1.5% of NSR.

Gregory Bell performed a chain-of-title search in 2018 (personal communication) and has verified records beginning with the initial land patents issued by the U.S. Government to Pearl I. Smith, settlement of the Pearl I. Smith estate, consolidation of the deeds under Smith's son, Ralph I. Smith, and distribution of Ralph I. Smith's estate to his dependents.

### 4.3.2 Federal Mining Claims

Rights to explore and mine locatable Federal minerals are acquired by staking individual mining claims. A lode claim is for vein-type deposits and is restricted to a size no larger than 1500 feet (457 m) long and 600 feet (183 m) wide, for a maximum size of 20.66 acres (8.36 ha). A locatable mineral is a legal term and includes valuable minerals that are subject to the U.S. Mining Law of 1872, that is not leasable and not salable. Graphite is a locatable mineral on most of the lands considered for the Ruby Graphite Project.

Initially, 23 federal lode mining claims were staked by RGH in 2016 and recorded with Ruby Graphite Holdings LLC as the claimant. Locations of these unpatented claims are shown by Figure 2. With these claims, a contiguous block of mineral control was established with the Smith Mining Lease lands.

Additional claims were located and staked in 2017 by Backcountry Geoscience, LLC. under hire to RGH as the claimant, consisting of 73 federal lode mining claims positioned to the north of, and contiguous with, the initial 23 mining claims. Locations of these unpatented claims are shown by Figure 2.

Because some of the claims encounter the edges of the Smith Mining Lease lands or other lands adjacent to the claims, not all claims have the maximum allowable size of 20.66 acres (8.36 ha).

Annual maintenance fees must be paid prior to September 1 of each year to maintain the claims for the following year. Currently the annual maintenance fees are $165 per claim and these have been paid to the BLM until August 31, 2023. Ownership of unpatented mining claims in the U.S. is in the name of the holder (locator or claimant), with ownership of the minerals belonging to the United States of America, under the administration of the U.S. Bureau of Land Management (BLM). Under the Mining Law of 1872, the claimant has the right to explore, develop and mine minerals on unpatented mining claims without payments of production royalties to the federal government.

### 4.3.3 Stock Raising Homestead Act - Surface Ownership

Within the Project area sit lands originally acquired under the Stock Raising Homestead Act (SRHA) of 1916. These lands are split estate; containing segregated private surface ownership and subsurface Federal mineral rights.

Figure 2 displays three such parcels within the Project Area: SRHA Patent Nos. 947496, 1037967 and 1028478. The first two parcels are approximately 640 acres (259 ha) or one square-mile in size. These first parcels were patented in 1924 and 1930, respectively, and are known as the “Bucher” and “Dixon” blocks, respectively. These were both purchased by Fred W. Brown and Helen C. Brown from the original owners; the lands are now administered by their daughter, Judy A. Brown.

The third parcel was patented in 1929, and is known as the “Carter” land block. This block is owned by the Geoduck Land and Cattle LLC of Seattle, WA.

Because these split estate lands have private surface ownership, special processes must be followed in order to stake federal mining claims, access, and explore for the subsurface minerals. First, a Notice of Intent to Locate a Lode Mining Claim (NOITL) must be filed with the BLM followed by a copy submitted to the landowner. After a 30-day waiting period, the NOITL grants the applicant access to the lands for mineral exploration purposes for 90 days. Future access, exploration and disturbance must be coordinated with the BLM under a Plan of Operations if an access agreement cannot be made with the private landowner.

### 4.3.4 FLPMA Exchange Land

Within the Project Area, an 80-acre (32.37-ha) parcel of land in Section 29, T8S, R7W designated on Figure 2 as 'FLPMA Exchange' has a split estate, with the land having private surface ownership and Federal mineral estate. These lands were acquired and patented by the Brown estate through a land exchange with the Federal government pursuant to Section 206 of the Act of October 21, 1976, titled "The Federal Land Policy and Management Act" (FLPMA). The land exchange reserved to the United States "all the mineral deposits in the lands so patented, and to it [the United States], or persons authorized by it, the right to prospect for, mine, and remove such deposits from the same under applicable law."

Mineral-rights acquisition under this FLPMA Exchange land is currently designated by the BLM Master Title Plat to be "Not Open to Mineral Location." RGH submitted a petition to the BLM for terminating the mineral withdrawal for the parcel of land, however the petition was denied. A formal land use planning decision to open and restore the lands to mineral entry will be required, but the BLM has no immediate plans to do so.

There is no assurance that the BLM will issue a land use planning decision in favor of opening the land to mineral entry in a timely manner. However, if it does, then RGH will pursue acquisition of mineral rights to these lands. In the meantime, RGH has been granted permission to explore the FLPMA Exchange land as part of the Project Area for the approved Plan of Operations.

## 4.4 Permitting and Environmental Review

### 4.4.1 Permitting

Many of the activities related to permitting of new mining operations, assignments, or amendments on these lands are delegated to the BLM. This includes the entire period of operation from exploration to mine planning, construction, operation, and reclamation through final closure. Permit requirements are described in the BLM H-3809 Handbook. Responsibilities for permitting include:

- Processing Notices of Intent and Plans of Operations;
- Assessing and withholding reclamation bonds ($1000-$5000/acre disturbed, up to $5/foot drilled);
- Issuing Permits;
- Reviewing annual reports and operating plans for conformance;
- Reviewing and assessing plans for verifying reclamation cost estimates;
- Reviewing and administering permit amendment proposals;
- Reviewing deactivation and closure plans;
- Evaluating operations for reclamation release; and
- Developing reclamation rules and amendments as needed.

Ten (10) NOITLs were submitted and processed for the Ruby lands to locate lode mining claims on SRHA lands with private surface ownership. Eight (8) were accepted, six (6) of which comprise Timber Creek LLC lands, and two (2) of which comprise Geoduck Land and Cattle lands.

A Plan of Operations (PoO) was submitted by RGH to the BLM (#MTM 109814) on June 7, 2017 for the initial 23 claims. The additional 73 claims were added to the Plan of Operations on September 20, 2017. The PoO was approved on January 18, 2018, after an Environmental Assessment was conducted and a Finding of No Significant Impact (FONSI) was issued, granting permission for geologic mapping, rock sampling, geophysical and geochemical surveys. The lands involved include BLM managed surface and mineral estate, as well as privately held surface that was patented under the Stock Raising Homestead Act where subsurface minerals were reserved to the federal government and are managed by the BLM. This decision is in accordance with the performance standards listed at 43 CFR 3809.420.

A person or company may not engage in mineral exploration in the State of Montana without first obtaining an exploration license from the Department of Environmental Quality (DEQ). The BLM coordinates the PoO approval with the DEQ, and a reclamation bond is jointly determined. The bond for the currently approved PoO is $2,340.

### 4.4.2 Environmental Review

Environmental Assessments and/or Environmental Impact Statements are required for any substantial physical disturbance of lands in this area, which includes road building, exploration drilling and trenching, mining proposals, and are often required for expansions or substantial changes to existing operations. The National Environmental Policy Act (NEPA) governs the environmental assessment and impact statement procedure. Operator responsibilities include providing technical assistance in the environmental review process to local units of government, other BLM Divisions, other state and federal agencies, and private industry.

### 4.4.3 Inspection

Inspections of mining and reclamation progress are conducted prior to and upon the closure date of any Notices of Intent (NOI) or Plans of Operations (PoO) as situations warrant. Reclamation sites are visited to ensure standards are met for successive growing seasons.

### 4.4.4 Reclamation

When an area is no longer scheduled to be disturbed, reclamation is initiated. These sites are inspected the first year. Inactive sites are evaluated for likelihood of re-disturbance.

Vegetation establishment is initiated (i.e. seeding, fertilizing, mulching) after the area is no longer scheduled to be disturbed. When repair or replanting is needed, sites are inspected again. Prior to the remittance of a Reclamation Bond, all sites must be similar to an approved reference area.

### 4.4.5 Enforcement

Site visits and communication between reclamation staff and company personnel occur as needed. If problematic or non-compliance reclamation issues arise, BLM staff work with a Company to resolve them. Enforcement action authority is also provided through the BLM.

# 5 ACCESSIBILITY, CLIMATE, LOCAL RESOURCES, INFRASTRUCTURE & PHYSIOGRAPHY

## 5.1 Accessibility

The Ruby Graphite Project is easily accessed year round from the town of Dillon, Montana, sitting along US Interstate 15. The route to the Project from Dillon comprises approximately eight miles of two-lane asphalt road, and six miles of gravel and dirt road, the final two suitable for an SUV or truck. There are two locked gates passing through private land, however, the Company has obtained access as part of the Smith Mining Lease through easements executed by the various surface owners and the Smiths in 1994 (Bell and Van Den Bussche, 2018).

Dillon is accessible by freeway from all major cities of Montana, Idaho and Utah. Commercial flights are available in nearby cities including Bozeman, Butte, Missoula, and Idaho Falls. Additionally, Dillon has a local airport supporting private and charter air traffic.

Dillon is located on the Union Pacific (UP) Railroad line, North America's largest railroad enterprise, covering the western two-thirds of the United States. A strategic stop on the UP line is Reno, Nevada, where the Tesla lithium-ion battery mega-factory is located. Products may be shipped by rail from Dillon to Reno at a distance of approximately 800 miles (1,300 km). The UP can carry freight to any of the shipping ports in Washington, Oregon and California.

The Burlington Northern Santa Fe (BNSF) Railway passes through Butte, which operates in the Pacific Northwest. Freight could be transported from Dillon to Butte, and then transferred to the BNSF to complete travel to Washington or Oregon.

Additional rail lines are located 14 miles (23 km) west of the Project at Barretts, exclusively accessed via gravel roads, thereby minimizing impact to the public. Barretts has a talc-processing mill which has and maintains a shipping facility.

## 5.2 Climate

The 10-year average temperature in Dillon is 44°F (6.6°C). December is the coldest month ranging from 11°F to 30°F (-1°C to -12°C) and July is the warmest ranging from 50°F to 84°F (10°C to 29°C).

The average wind speed is nine mph with sustained highs averaging 22 mph and gusts averaging up to 28 mph. Wind gusts as high as 60 mph or greater have been recorded in Dillon. Sustained winds tend to be lower in the summer and greater in the spring. Wind direction is typically from the south-southwest.

The area is relatively arid; 10-year annual precipitation in Dillon averages 11 inches per year. The wettest months, April through October, average 1.3 inches of precipitation per month, with frequent thunderstorms. Snow occurs in Dillon November through February.

The Project area is between 1,600 to 2,800 ft (500 to 900 m) higher elevation than Dillon, therefore weather is more extreme on the Project with respect to temperature, wind and precipitation. Dillon is located at 5,200 ft (1,600 m) and the Project area is between 6,800 to 8,000 ft (2,100 to 2,400 m).

## 5.3 Local Resources

As per the 2020 United States Census report, the town of Dillon, Montana, has a population of 4,403. Dillon hosts full municipal services (fire, water, police), an airport at an elevation of 5,220 ft (1,590 m) with two non-commercial airstrips, and the Barretts Hospital. Education centers in Dillon include elementary, middle and high schools, and the University of Montana-Western.

The city of Butte, an hour drive north of Dillon, and its university, Montana Tech, form a state-wide center for, and a long history of, mining engineering and technology. Mining remains an important part of the economy in western Montana, therefore, several mining equipment and supply businesses are located in Butte, Helena, Bozeman and Missoula.

## 5.4 Infrastructure

The Project is classified as a Brownfield exploration project because previous disturbances have occurred, and modern mining practices have not been implemented in the Project area. Historic mining infrastructure exists on the Project, however, altogether new infrastructure is required for future function.

The nearest railway is a Union Pacific north-south line. The rail line is part of a regional north-south corridor running between Butte, Montana and Salt Lake City, Utah, and provides local access to sidings in Dillon and an inland port facility in Butte (Montana Rail Link).

### 5.4.1 Roads

There are several different routes via roadways open year round to access Dillon from larger Montana and Idaho cities, including the Interstate 15 corridor. There currently exists a rough dirt road for access to the Project. The dirt and gravel roads are suitable for mobilization of drilling equipment and crews, but ultimately will need to be upgraded by grading and ditching. Additionally, the road will need to be properly graveled and compacted to make it all-weather accessible. Also under consideration for project development is construction of a new route to the Project. A potential corridor west of the Project has been identified for construction of about 3 miles (5 km) of new road if mining access is required. If an alternate route were to be constructed, it would be designed to bypass the current road easement, making access less of an issue for the future.

### 5.4.2 Power

There is currently no electrical power to the Project. There is residential power located approximately 2.4 miles (3.8 km) west; along the same corridor identified for the alternate access road. Three-phase power is present along Blacktail Road, 3 miles (4.8 km) further west. A major power upgrade could be facilitated from the nearest substation located 10.6 miles (17 km) west of the Project.

### 5.4.3 Water

Water is available at the Mill Site (Figure 2) from two sources. A spring runs through the Mill Site patented claim, but its flow is likely not great enough to support an ore processing mill. The second source is a steel-cased water well 175 feet (50 m) from the foundation of the old mill structure. The diameter of the steel pipe is compatible to provide sufficient flow for the mining and milling operations; however, flow rates from the water well have not been verified.

The Smith Mining Lease provides access to the water rights associated with this patented claim, and additional wells could be drilled if required. Additionally, there is a spring near the Smith Cabin, and an improvement of this site could provide a water source for drilling at the Bird's Nest prospect.

### 5.4.4 Phone and Internet

The majority of the Project area has limited cell phone reception; access improves along ridgelines and hilltops. Hardline phone and internet service could be run to location along with new electrical power supply, if necessary.

## 5.5 Physiography

The Project is located within the Ruby Mountain Range, bounded by the valleys of the Beaverhead River to the northwest, Ruby River to the northeast, and Blacktail Deer Creek to the southwest. All streams flow northerly to the Jefferson River, a major tributary of the Missouri River.

The terrain is rugged with gneiss and marble outcrops. Vertical relief rises from Blacktail Deer Creek valley at 5,500 ft (1,680 m) to 7,978 ft (2,432 m) at the peak of Crown Point located within the Project Area at the southeast quarter of Section 30, T8S, R7W.

The northern portion of the Project comprises the higher-elevation, north-facing slope of Van Camp Canyon and is pine and fir timbered. The southern portion of the Project comprises a lower-elevation, south-facing slope covered by sagebrush and prairie grass (Figure 3).

**Figure 3. Physiography of the Ruby Graphite Project.**

# 6 HISTORY

## 6.1 Historical Ownership and Development

Historical and recent activities at the Ruby Graphite Project include:

- 1887 to 1901, graphite was discovered and work began on the original mining claims;
- 1901 to 1919, early development work as Crystal Graphite Company;
- 1920 to 1937, post WW-I efforts with low-rate production for local sales;
- 1939 to 1946, during WW-II under a new lease and management;
- 1947 to 1957, as Montana Graphite Inc.
- 2012-2014, Graphite Corp. staked and dropped claims and performed limited mineral exploration activities;
- 2014-2021, RGH staked claims and performed limited exploration activities; and
- 2022, RGH and Reflex (this Report).

Graphite was first discovered at the Project Area in 1887 by Charles E. Robbins, who staked the eight original mining claims in 1890, and worked them for nine years (Unknown, Western Mining World, 1901). In 1899, Pearl I. Smith organized the Crystal Graphite Company, and in 1900 Smith filed Certificates of Location with the County for several mining claims, including the Ground Hog claim (Smith, 1900).

From 1903 through 1918, graphite was mined and sold, but production stopped once World War I ended. By 1919, all mining operations had ceased. Pearl I. Smith obtained 40-acre land patents for the Mill Site and for the Smith Cabin site in 1918 and 1919, respectively, including all minerals and water rights. Smith continued to operate the graphite mine at a low level of activity after WW-I.

In 1938, the graphite-associated lands and claims were granted to Ralph I. Smith. In 1939, at the beginning of WWII, Ralph Smith and the Crystal Graphite Co. reopened the mine. In 1947, the mine was leased to Montana Graphite Inc. with Ralph I. Smith as president and Project owner (Cameron and Weis, 1960). The mining operation restarted in 1948, and in 1949 a mill was constructed with funds from a loan by Reconstruction Finance Corp. (RFC). Montana Graphite Inc. ceased in 1957.

The Project remained undeveloped for more than sixty years until Graphite Corp. negotiated a mining lease for the Smith estate in 2012, permitting the right to perform exploration activities on the Ground Hog, Mill Site, and Smith Cabin patented lands (Bell and Van Den Bussche, 2018).

In 2012, Graphite Corp. staked and registered 83 lode claims on land adjacent to and near the Smith mineral lease. These claims were located exclusively on BLM lands to the south and west of the current Project area (Figure 4).

Graphite Corp. failed to raise the funds for their planned exploration program and abandoned the claims and mining lease in 2014.

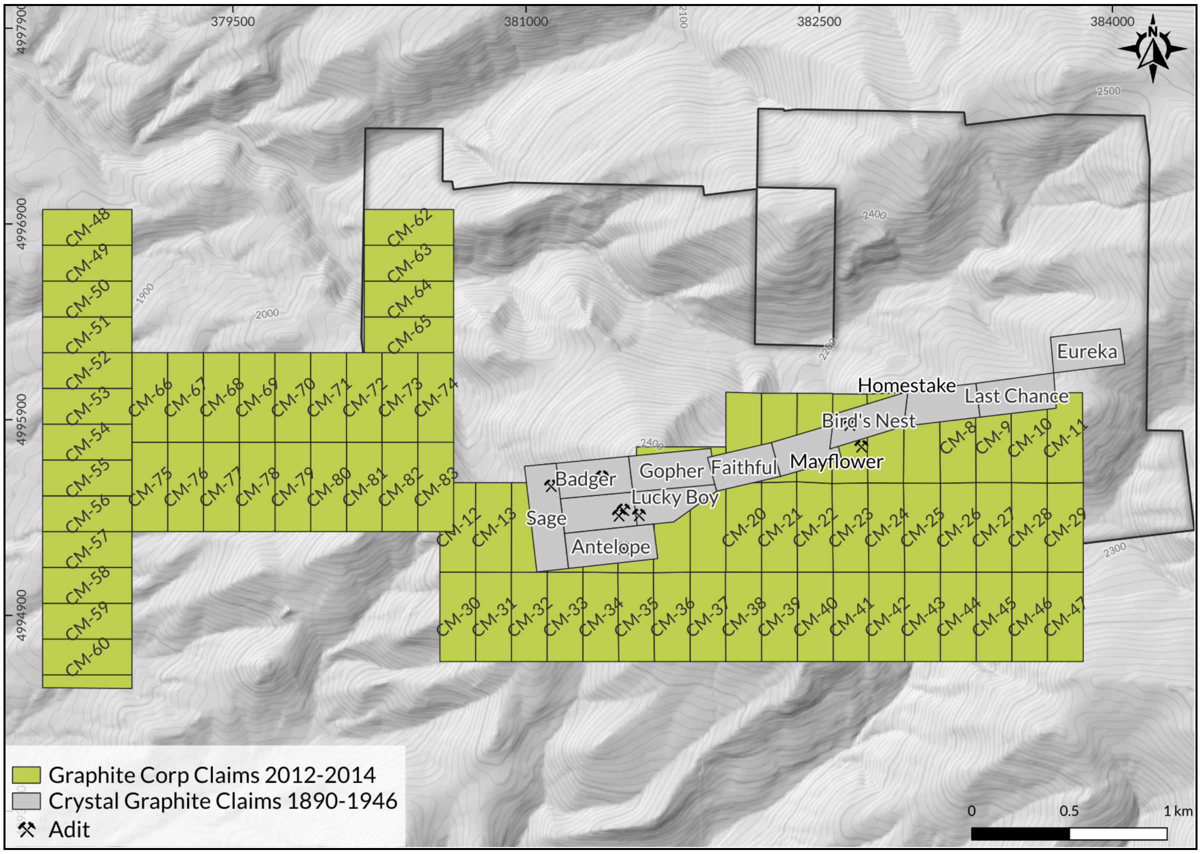


**Figure 4. Historic lode claims of the Crystal Graphite Co. and Graphite Corp.**

## 6.2 Historic Production

Most of the historic production from the Ruby area was produced from the Ground Hog mine, which refers to an area that includes the Ground Hog surface pit, Ground Hog east pit, Smith Level Adits 1 and 2, Dubie Level, Hoy Level and Antelope Level (Figure 5). No recorded production, but sufficient activity, also exists northwest of the Ground Hog area at the site of a surface pit and adit (Badger and Sage). Early production also occurred from the Bird's Nest claim. Most historic workings have caved-in or have since been intentionally condemned by governing agencies for safety purposes.

For the majority of the production time span mining was performed by hand-cobbing without the benefit of power tools and shipments were likely transported on foot or by pack animals. According to an interview conducted in 1942, pneumatic power tools were in use, enabling underground drilling and blasting:

> *"The present operators are hand-sorting the graphite and shipping it to industrial points in the East in the form it is mined. With the method of mining used, hand sorting is not difficult. The stope is cut in the waste of the hanging wall, and the graphite is left on the foot wall. It is then scraped and dug out of the vein, as far as can be reached by hand scrapers on sheets of canvas. It is then dumped into sacks and carried out of the mine."*

Between 1902 and 1950, it is estimated that 2,400 tons (2,200 tonnes) of graphite was produced and shipped from the Project. Perry (1948), reported that the first 50 tons of graphite were sourced from the Bird's Nest claim, but It is unclear if all adits at the Bird's Nest mine were involved in production.

The bulk of remaining production was sourced from the Ground Hog claim (Perry, 1948). According to mapping performed in 1945 by the mine operators and sampled by RFC, mine workings from the Ground Hog Claim included more than 3,500 feet (1,070 m) of drifts, crosscuts, shafts, and raises, together with several stopes, prospect pits, and two adits each 75-feet (23-m) long (Armstrong and Full, 1950).

A 250 ft (76 m) long adit was driven 200 ft (61 m) below the Badger discovery pit, which was cut after the 1945 map was prepared (Cameron and Weis, 1960), and is referred to as the Sage adit in the present report. No production has been recorded from this adit. The Sage adit has been secured by the government by pulling the hillside down around a culvert pipe and placing a locked gate at the entrance. It has been deduced that the Sage adit was constructed by Montana Graphite Inc. between 1948 and 1949, and is therefore the most recently constructed working.

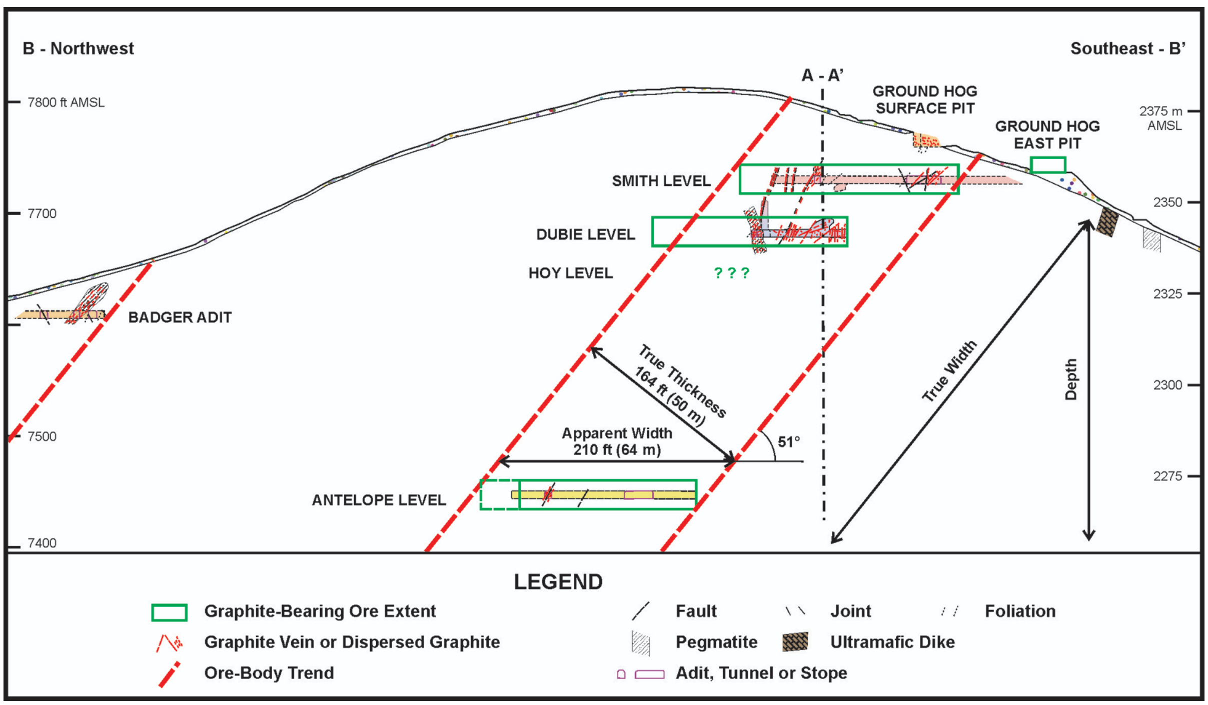


**Figure 5. Cross Section of Ground Hog Mine Complex (Bell and Van Den Bussche, 2018).**

The estimated grades at Bird's Nest and Ground Hog are 14.5% Cg and 32%, respectively (Bell and Van Den Bussche, 2018), and are not NI 43-101 compliant. The estimated grades were calculated by Bell (2018) using reported production tonnes, volumes of mapped underground workings from the Crystal Graphite Company and other reports by the USGS(Table 2) (Armstrong and Full, 1950; Perry, 1948). The following equation was used to calculate grade:

$$\frac{[Production\ (tons, Table\ 2) \times product\ grade \times 0.908\ tonne/ton] \times 100}{[planar\ area\ of\ adit \times 2m\ assumed\ tunnel\ height \times density\ of\ ore\ (2.65\ t/m3)]} = \%\ Cg.$$

**Table 2. Summary of graphite production at the Project from 1902 to 1950 (Bell and Van Den Bussche, 2018).**

| Period | Company | Operation | Graphite Grade | Production (tons) |
|---|---|---|---|---|
| 1902 | Crystal Graphite Co. | Bird's Nest Claim | 14.5% Cg | 50 |
| 1918 – 1919 | Crystal Graphite Co. | Ground Hog Claim | 26.5% Cg | 2150 |
| 1920 – 1937 | Crystal Graphite Co. | Post WW-I, Pre WW-II | | 50 |
| 1939 – 1946 | Crystal Graphite Co. | Reorganized | | 150 |
| 1948 – 1950 | Montana Graphite Inc. | Milling Existing Material | | 22 **not sold* |
| Total | | | | **2400** |

## 6.3 Historic Sampling

Thirty-two channel samples were collected by Crystal Graphite Co. in 1945 at the Ground Hog mine complex, specifically at the Ground Hog Surface Pit, Smith Portal No. 1, Smith Portal No. 2, Dubie Portal, and Antelope Portal (Giulio, 1945). Table 3 shows the samples taken at each location and carbon assay values completed independently by RFC and Crystal Graphite Co.'s internal laboratory (Bell and Van Den Bussche, 2018).

**Table 3. Channel samples collected at the Ground Hog mine complex by Crystal Graphite Co. in 1945.**

| Ground Hog Surface Pit | | | |
|---|---|---|---|
| Sample ID | width (ft) | RFC %C | Fenner %C |
| 20 | 5 | 7.8 | 6 |
| 21 | 4 | 4.5 | 7.92 |
| 22 | 8 | 8.6 | 9.12 |
| **Weighted Avg 7.7% C** | | | |

| Antelope Portal | | | |
|---|---|---|---|
| Sample ID | width (ft) | RFC %C | Fenner %C |
| 30 | 6.5 | 7.8 | 8.01 |
| 31 | 5 | 9.3 | 10.56 |
| 32 | 5 | 8.3 | 7.52 |
| **Weighted Avg 8.5% C** | | | |

| Smith Portal No. 1 | | | |
|---|---|---|---|
| Sample ID | width (ft) | RFC %C | Fenner %C |
| 23 | 4.5 | 11.4 | 11.6 |
| 24 | 4 | 13.3 | 14.62 |
| 25 | 5 | 11.1 | 11.97 |
| 26 | 5 | 17.2 | 14.64 |
| 27 | 4.5 | 13.8 | 15.19 |
| 28 | 6 | 12.8 | 13.12 |
| 29 | 4.5 | 12.5 | 12.5 |
| **Weighted Avg 13.24% C** | | | |

| Smith Portal No. 2 | | | |
|---|---|---|---|
| Sample ID | width (ft) | RFC %C | Fenner %C |
| 18 | 7.5 | 16.7 | 16.08 |
| 19 | 4 | 10 | 11.88 |
| **Weighted Avg 13.67% C** | | | |

| Dubie Portal | | | |
|---|---|---|---|
| Sample ID | width (ft) | RFC %C | Fenner %C |
| 1 | 3.5 | 10.9 | 12.09 |
| 2 | 3 | 8.8 | 10.58 |
| 3 | 6 | 10.2 | 9.57 |
| 4 | 5.5 | 11.9 | 11.75 |
| 5 | 10 | 9.9 | 10.02 |
| 6 | 6 | 10.8 | 14.77 |
| 7 | 7.5 | 12.9 | 12.75 |
| 8 | 4 | 7.6 | 7.56 |
| 9 | 6.5 | 9.5 | 9.68 |
| 10 | 2 | 10.7 | 9.05 |
| 11 | 2 | 29.4 | 28.82 |
| 12 | 7.5 | 24.5 | 22.96 |
| 13 | 6 | 17.3 | 16.61 |
| 14 | 3 | 4.3 | 4.38 |
| 15 | 4 | 9.2 | 10.04 |
| 16 | 3.5 | 7.1 | 8.94 |
| 17 | 1 | 24.5 | 28.22 |
| **Weighted Avg 16.4% C** | | | |

In 2012, five rock samples were collected by Graphite Corp. Specific locations, sample type and descriptions were not provided in conjunction with assay results. All samples exceeded 10% graphite with multiple samples exceeding the 20% limit of detection (Table 4, Goss, 2013). ACME Labs in Vancouver, BC conducted the analysis using Inspectorate code C-GP-OR and/or ACME code 2A09.

In 2016, nine rock samples were collected by Gregory Bell and Peter Ellsworth. Samples were selected to represent various locations across the Project area, and are not necessarily representative of average graphite resources or grades. The selected samples were photographed, cleaned of foreign organic matter using a stiff wire brush. The samples were then re-photographed, weighed, dimensions measured, and described. The samples collected by Gregory Bell were shipped to the SGS Canada Inc. laboratory at Lakefield, Ontario. The samples collected by Peter Ellsworth were sent to ALS Minerals. Various preparation procedures and sampling methods were utilized.

**Table 4. 2012-2016 select rock sampling and results (Graphite Corp. samples are not NI 43-101 compliant).**

| **Historic Sampling** | | | | | | **Whole-Rock ICP Analysis (g/t)** | | | |
|---|---|---|---|---|---|---|---|---|---|
| **Collected By** | **Sample ID** | **Location** | **Lab** | **Year** | **Cg %** | **Fe g** | **Ni g** | **Co g** | **V g** |
| Greg Bell | RG Badger Rubble | RG Badger Rubble | SGS | 2016 | 1.01 | 18,400 | 4.09 | 3.19 | 6.04 |
| Greg Bell | RG Smith #1 Outcrop | RG Smith #1 Outcrop | SGS | 2016 | 0.82 | 6,740 | 5.25 | 0.99 | 2.41 |
| Greg Bell | RG Bird's Nest Adit | RG Bird's Nest Adit | SGS | 2016 | 4.84 | 11,700 | 3.65 | 1.52 | 2.82 |
| Greg Bell | RG F-1 Pit | RG F-1 Pit | SGS | 2016 | 11.6 | 11,400 | 5.26 | 1.29 | 2.3 |
| Greg Bell | RG G-0 Outcrop | RG G-0 Outcrop | SGS | 2016 | 0.59 | 3,890 | 3.51 | 0.41 | < 1 |
| Peter Ellsworth | EG RG-1 | Old Mill stockpile | ALS | 2016 | 8.18 | *null* | *null* | *null* | *null* |
| Peter Ellsworth | EG RG-2 | Badger rubble | ALS | 2016 | 1.08 | *null* | *null* | *null* | *null* |
| Peter Ellsworth | EG RG-3 | Dubie portal waste rock | ALS | 2016 | 1.08 | *null* | *null* | *null* | *null* |
| Peter Ellsworth | EG RG-4 | F-1 | ALS | 2016 | 4.29 | *null* | *null* | *null* | *null* |
| Graphite Corp | AB-20120912-02 | *unknown* | ACME | 2012 | 10.5 | *null* | *null* | *null* | *null* |
| Graphite Corp | AB-20120912-05 | *unknown* | ACME | 2012 | >20 | *null* | *null* | *null* | *null* |
| Graphite Corp | AB-20120912-13 | *unknown* | ACME | 2012 | >20 | *null* | *null* | *null* | *null* |
| Graphite Corp | AB-20120912-17 | *unknown* | ACME | 2012 | 13 | *null* | *null* | *null* | *null* |
| Graphite Corp | AB-20120912-18 | *unknown* | ACME | 2012 | >20 | *null* | *null* | *null* | *null* |

Additionally, a metallurgical test was conducted to characterize the graphite concentrate in terms of flake size distribution and total carbon grades of different size fractions. The economic viability of graphite is determined predominantly by flake size distribution and concentrate grade. A froth flotation test was conducted, which simulates the separation and concentration of graphite from the host rock (Bell and Van Den Bussche, 2018).

Five samples collected by Greg Bell in 2016 were subject to metallurgical testing, and received by SGS Canada Inc. in February 2017 (Table 4). Three of the samples were below the cutoff threshold of Cg (approximately 2% Cg) and were not included in the froth flotation test. A composite of the qualifying two samples (Bird's Nest and F-1 samples) was subject to a single flotation test using two reagents; fuel oil #2 (diesel) as the collector and Methyl Isobutyl Carbinol (MIBC) as the frother.

The flotation test consists of two grinding processes, followed by four cleaning stages. A total of 91.9% of the graphite was recovered in the 4th cleaner concentrate at a grade of 97% Ct. (Table 5). Carbon losses are expected to decrease during closed circuit operation since some of the carbon units in the intermediate tailings stream will be recovered into the concentrate. In this study;

> *"The combined concentrate grade of 97% C(t) exceeded the range of 85% to 95% C(t) that is typically targeted in this type of scoping level flotation test, which suggests that the Birds Nest Adit and the F-1 Discovery Pit material can be upgraded to very high concentrate grades with very limited primary grinding and regrinding, thus minimizing the degree of flake degradation" (SGS Minerals Services, 2017).*

The final cleaner concentrate was submitted for a size fraction analysis to evaluate the quality of the graphite concentrate with regards to flake size distribution, and concludes;

> *"The combined mass recovery into the jumbo and large flake categories of +80 mesh yielded 40.0%. The medium sized flakes of -80 mesh/+150 mesh made up 17.3% of the mass. The remaining 42.7% of the mass reported to the -150 mesh size fractions. While the -150 mesh size contained a significant amount of mass, 26.2% reported to the +200 mesh and +325 mesh size fractions, thus rendering this material suitable for battery applications with regards to particle size" (SGS Mineral Services, 2017).*

**Table 5. Concentrate values from froth flotation single batch cleaner test.**

| Product Concentrate | Assay | Recovery |
|---|---|---|
| | Ct % | Ct % |
| Rough | 73.8 | 96 |
| 1st Cleaner | 92.1 | 95.1 |
| 2nd Cleaner | 96.1 | 94.3 |
| 3rd Cleaner | 96.8 | 92.8 |
| 4th Cleaner | 97 | 91.9 |

The 2017 SGS metallurgical study indicated that the composite sample of the Bird's Nest and F-1 Discovery Pit can be easily upgraded to 99.9% purity and that the flake size is also suitable for commercial use.

# 7 GEOLOGICAL SETTING & MINERALIZATION

## 7.1 Regional Geology

The region hosts a complex series of tectonic deformation events including the collision of land masses that became severely deformed, affected by increased pressure and temperature through metamorphism, and underwent various processes of uplift, faulting, and folding. Subsequent erosion exposed the rocks that are currently seen at the surface.

The region is comprised of Archean rocks overlain by Phanerozoic strata and recent Quaternary sediments. The Archean basement of southwestern Montana, part of the northernmost Wyoming Province, is exposed in foreland block uplifts. Orogenesis accompanied the assembly of Archean terranes in the northwestern United States during Paleoproterozoic time. An ocean-arc terrane conjoined the Archean continental blocks at the northwest margin of the Wyoming craton 1.9-1.8 Ga (Mueller at al., 2002, Figure 6). The collisional tectonics reworked the craton margin and deformed the terranes by addition of material to a tectonic plate through subduction (accretion) (Figure 7).

A series of northeast trending thrust faults formed during this collisional phase,bounding the Dillon suture zone and Madison mylonite zone, and part of the greater Trans-Montana fold and thrust belt (Figure 6). The Dillon Block comprises a continental margin assemblage, as it was accreted due to the Trans-Montana fold and thrust belt that formed along the margin of the Medicine Hat Block and the Wyoming Craton (Sims et al., 2004).

The accreted terranes to the north of the Wyoming craton are interpreted as having been amalgamated prior to collision along the Dillon suture zone. Convergence is attributed to closing of the Paleoproterozoic ocean between the accreted terranes and the craton (Sims et al., 2004). Subsequent transtension during the Mesoproterozoic occurred along the trans-Rocky Mountain fault and produced structural basins that acted as depocenters (Winston, 1986).

Uplift of these ancient rocks occurred during the Laramide and Sevier orogenies of Late Cretaceous-early Paleogene time, and produced basement-cored uplifts in southwestern Montana. The Sevier thrust front lies at the western margin of the Dillon Block. Late Cretaceous-Paleogene intrusions are spatially related to Sevier structures and presumably owe their origin to Sevier orogenesis (Schmidt et al., 1990). Paleoproterozoic structures were reactivated during late Cretaceous tectonic and igneous activity, resulting in a general north-east strike to all folds and faults.

During the Neogene, block faulting (basin and range structures) formed in Southwestern Montana by extensional deformation and subsequent reactivation along Proterozoic faults. The eastern limit of Basin and Range extension lies to the east of the Dillon Block.

In Southwest Montana, the late Paleogene to Quaternary experienced various periods of glaciation, lakes covering vast extents, and large rivers carving out valleys. These events caused deposition of alluvial sediments and erosion, exposing basement rocks not previously exposed at the surface (Smith, 2020).

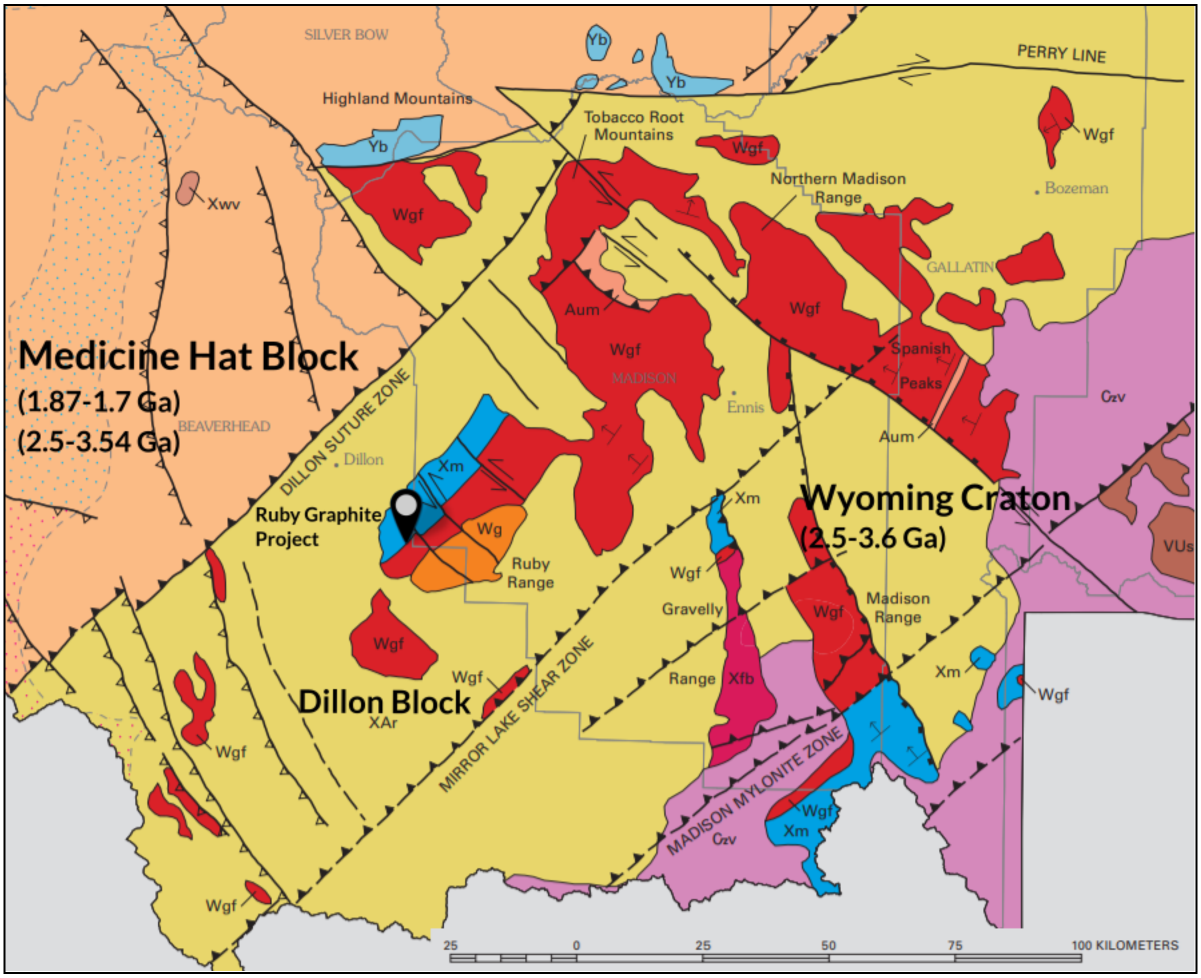


**Figure 6. Terrane map of southwest Montana, including regional northeastern trending thrust faults and local northwest trending strike-slip faults (Sims, et al., 2004).**

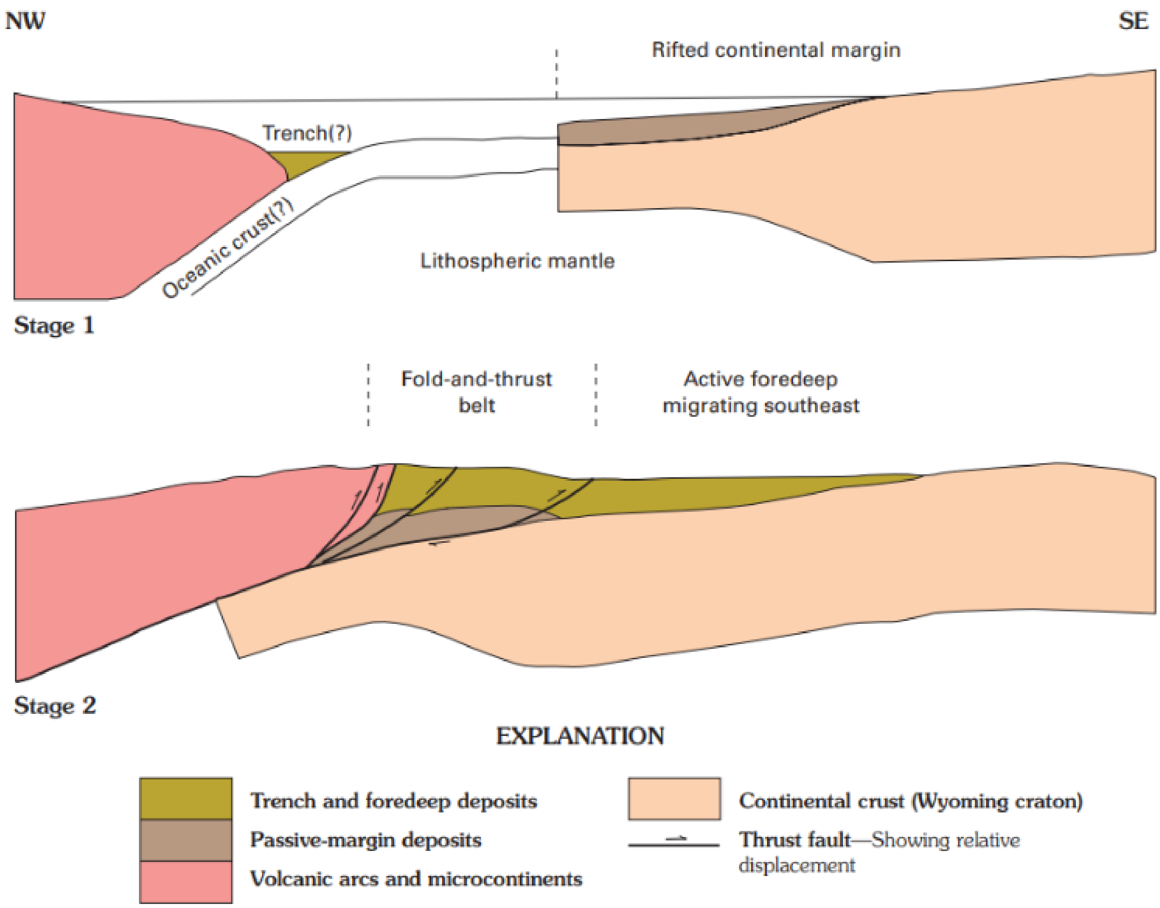


**Figure 7. Evolution of the Trans-Montana fold and thrust belt. Stage 1: Passive, rifted continental margin of Wyoming craton approaching a subduction zone in paleoproterozoic time. Stage 2: Subduction of the continental margin results in thrusting of basement rocks. Modified from (Sims, et al., 2004). The Dillon Block lies within the Fold-and-thrust belt.**

Regional geology rock descriptions for the Dillon 1 x 2 Quadrangle Map (Ruppel et al., 1993) (Figure 8) specific to the Ruby Graphite Project include:

**Am: Marble (Archean)** - Medium-gray to dark-brown, coarsely crystalline, carbonate-rich rocks present as layers that range from less than 1 m to more than 500 m thick. Rock composed mainly of calcite and dolomite and contains subordinate amounts of quartz, diopside, tremolite, and forsterite.

**Asg: Interlayered Schist and Gneiss (Archean)** - Composed mainly of quartz-feldspar-biotite gneiss, granitic gneiss, and amphibolite.

**Aqfg: Quartzofeldspathic Gneiss (Archean)** - Complexly interlayered granitic, tonalitic, quartz-feldspar-biotite, and hornblende-plagioclase gneiss (Vitaliano and Cordua, 1979). In the Ruby Range the gneiss appears to underlie main metasedimentary successions (James 1990). Rb-Sr age determined from these rocks is 2.76 Ga (James and Hedge).

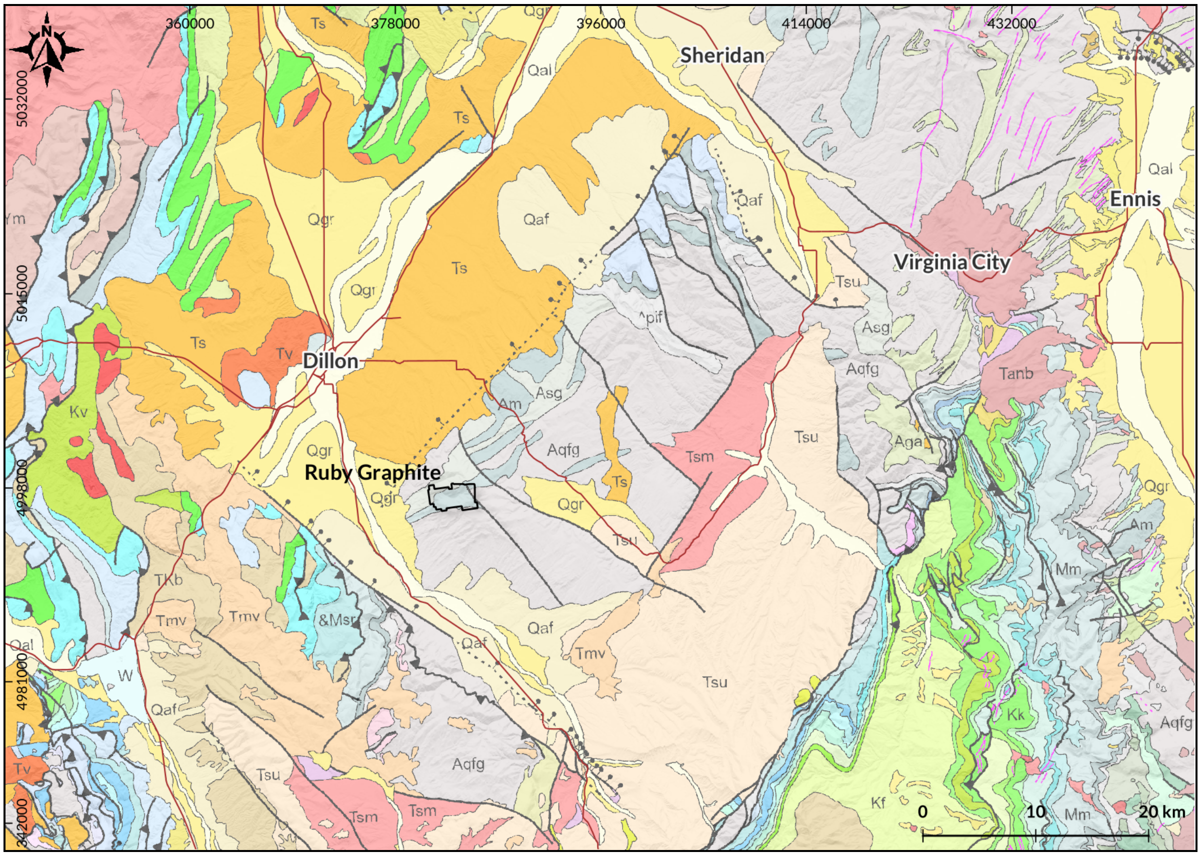


**Figure 8. Regional geology of southwestern Montana, including the Ruby Range (Vuke et al., 2007). The Ruby Graphite Project is lying within the marble and Archean quartzofeldspathic gneiss.**

## 7.2 Regional Structure

The Ruby Range is northeast trending, North-South range bounded by thrust faults, and along which the Dillon Block was uplifted during the early Paleogene (Garihan, 1979, Figure 6). The Trans-Montana Orogeny, as defined by Sims et al., 2004, distinguishes deformation associated with tectonism and crustal suturing of the Paleoproterozoic Wallace Terrane and attached Archean Medicine Hat Block to the Wyoming craton (Sims et. al., 2004).

Northeast-southwest trending ductile shear zones developed during the Trans-Montana Orogeny, including the Dillon Suture Zone between 1.9-1.8 Ga, which bounds the Dillon Block to the north (Figure 6). The Dillon Block consists of imbricated thrust slices of crystalline Archean rocks and paleoproterozoic passive continental-margin supracrustal rocks. The northwest trending wedges of faulted and folded Paleozoic rocks lie unconformably on Archean basement units. Subsequent faulting and uplift occurred in the late Cretaceous-Early Paleogene during the Laramide and Sevier orogenies. Many Archean structures were reactivated during this deformational event.

## 7.3 Project Geology

The Project was mapped by Heinrich in 1960, Okuma in 1971, and Ethos Geological in 2022. Additionally, Armstrong and Full published maps of historic workings, prepared by the operator of the Crystal Graphite Mine in 1945 (Armstrong and Full, 1950).

Sedimentary sequences often express high variability of grain sizes and facies distributions, as is commonly seen across the property. The Authors use strict descriptive rock terms in place of interpretive names formerly provided by Okuma (1971) and Heinrich (1960), such as the "Cherry Creek Group", “Dillon Granite Gneiss” and “Pre-Cherry Creek” and instead, assign a name that is consistent with the rock regardless of interpretation. The names include the abundant minerals in increasing succession and the rock type.

The rocks present at the Project comprise several gneisses, schists and marbles. The northern Project area hosts schists ranging from biotite-rich to sillimanite-rich, Plagioclase Hornblende Gneiss, and marble. The central and southern portion of the Project has marble units alternating with the dominant Quartz Plagioclase K-Feldspar Gneiss gneiss containing lenses of gneiss varieties.

The gneisses and the schists differ in appearance. Gneisses are coarser grained and contain more feldspar and quartz minerals, and express weaker foliation. The gneisses also exhibit several different subtypes based on mineral composition. Schists contain a higher percentage of biotite and amphibole, and display finer foliation. The marbles are often tightly folded and either coarse or fine grained. Diabase dikes transect all units with a northwest-southeast trend, intruding into or following pre-existing northwest-trending faults (Heinrich, 1960). Bedding and foliation consistently strike northeast and dip from 40° to 60° to the northwest (Figure 9).

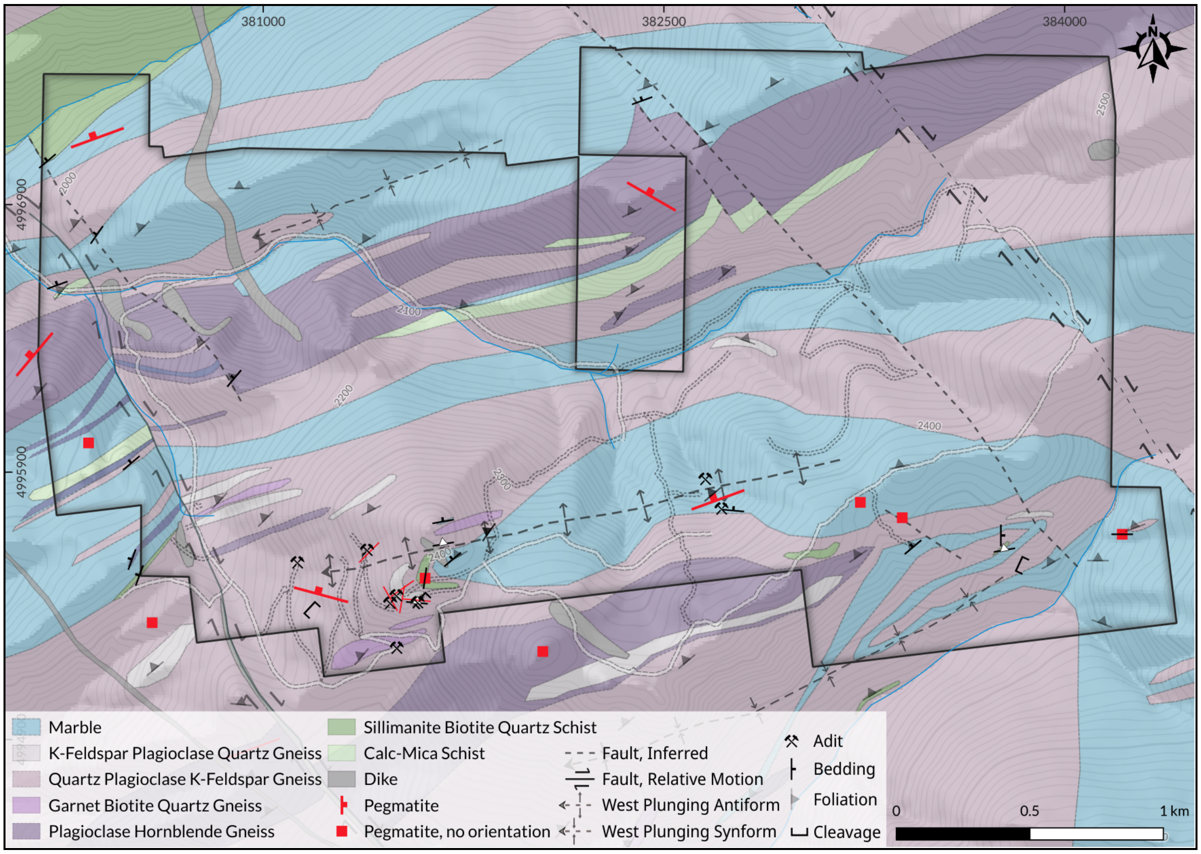


**Figure 9. Geologic map of the Ruby Graphite Project showing major lithologies, structures and faults.**

## 7.3.1 Gneiss

The gneisses outcrop in alternating and gradational sequences. The Quartz Plagioclase K-Feldspar gneiss is the dominant unit at the Project, however it comprises variations that have been subdivided based on composition and appearance. Repetition of the gneisses occurs at both outcrop and Project-wide scales. Overall, the gneisses have varying abundances of quartz, feldspars, biotite, hornblende, and garnet. They have moderate foliation and vary in thickness from one meter to tens of meters. The Rb-Sr age determined from these rocks is approximately 2.76 Ga (James and Hedge, 1980).

### *7.3.1.1 K-Feldspar Plagioclase Quartz Gneiss (Akpq)*

This unit outcrops over most of the Project area, most notably in the southern half, and adjacent to the Quartz Plagioclase K-Feldspar gneiss. This unit is resistant, forming conspicuous white outcrops due to the high percentage of plagioclase. It is coarse-grained, and foliation may be well developed (Figure 10). The composition is quartz dominated (30-50%) with lesser K-feldspar and plagioclase (20-40%) and accessory biotite, muscovite and garnet. The garnet is often euhedral, up to 4 cm as individual crystals and in reddish-brown bands, lobes or clusters.

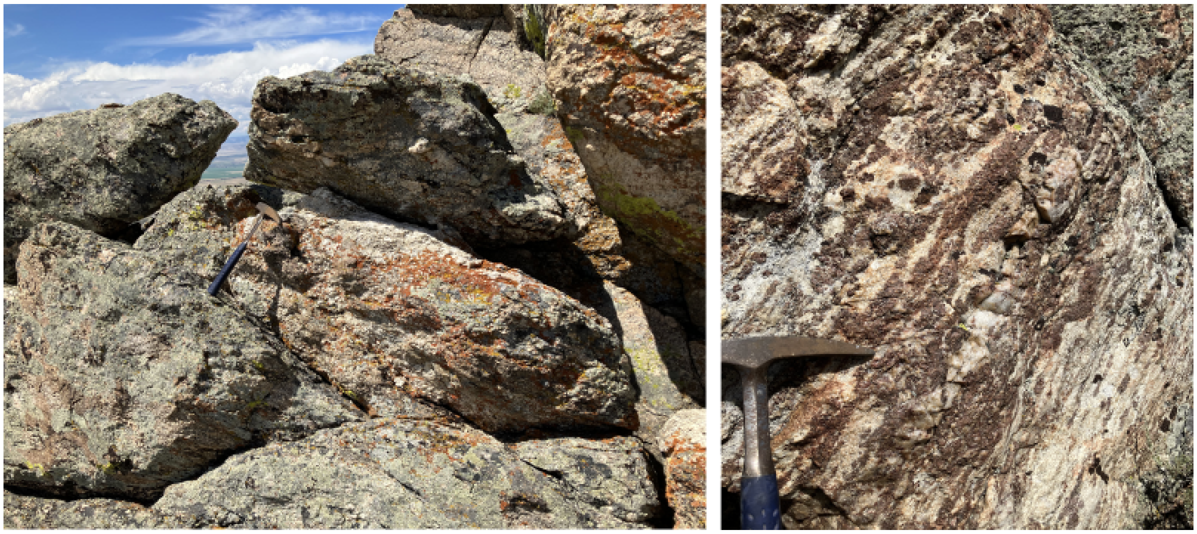

**Figure 10. K-Feldspar plagioclase quartz gneiss in outcrop (left) and with dark garnet crystals (1-4 cm) in bands ~5cm thick (right).**

### *7.3.1.2 Quartz Plagioclase K-Feldspar Gneiss (Aqpk)*

The Quartz Plagioclase K-Feldspar gneiss is the most common unit at Ruby and likely extends throughout the greater region. It is a thick, resistive unit and comprises much of the hillside to the northwest of Timber Creek, near the Ground Hog area, and on the hillside to the north of the Smith Cabin. The unit is pink and white, moderately foliated, and medium grained with thin mineral banding. The composition is dominated by K-feldspar, plagioclase, and quartz with trace amounts of biotite, tremolite, scapolite, and garnet. A dark pink-orange weathered surface is its distinguishing feature in outcrop (Figure 11). The protolith is possibly a well-sorted arkosic sandstone.

**Figure 11. Quartz plagioclase K-feldspar gneiss showing distinct pinkish-white color (left), blocky outcrop (right).**

### *7.3.1.3 Garnet Biotite Quartz Gneiss (Agbq)*

This gneiss has an intermediate composition with alternating bands of dark and light (felsic and mafic) minerals. It is darker than the dominant Quartz Plagioclase K-Feldspar gneiss; medium to dark brown with strong foliation and thin bands, fine to coarse grained, and the composition includes quartz, biotite, feldspar, garnet, with trace amphibole and sillimanite (Figure 13). Sequences are thin (usually a few meters thick). Opaque quartz veins (one to five cm) and large crystalline lobes are common within the layers. The weathered surface is a distinguishable medium to dark brown (Figure 12). The protolith is possibly a poorly sorted sandstone or siltstone.

**Figure 12. Garnet biotite quartz gneiss; often present with crystalline quartz lobes.**

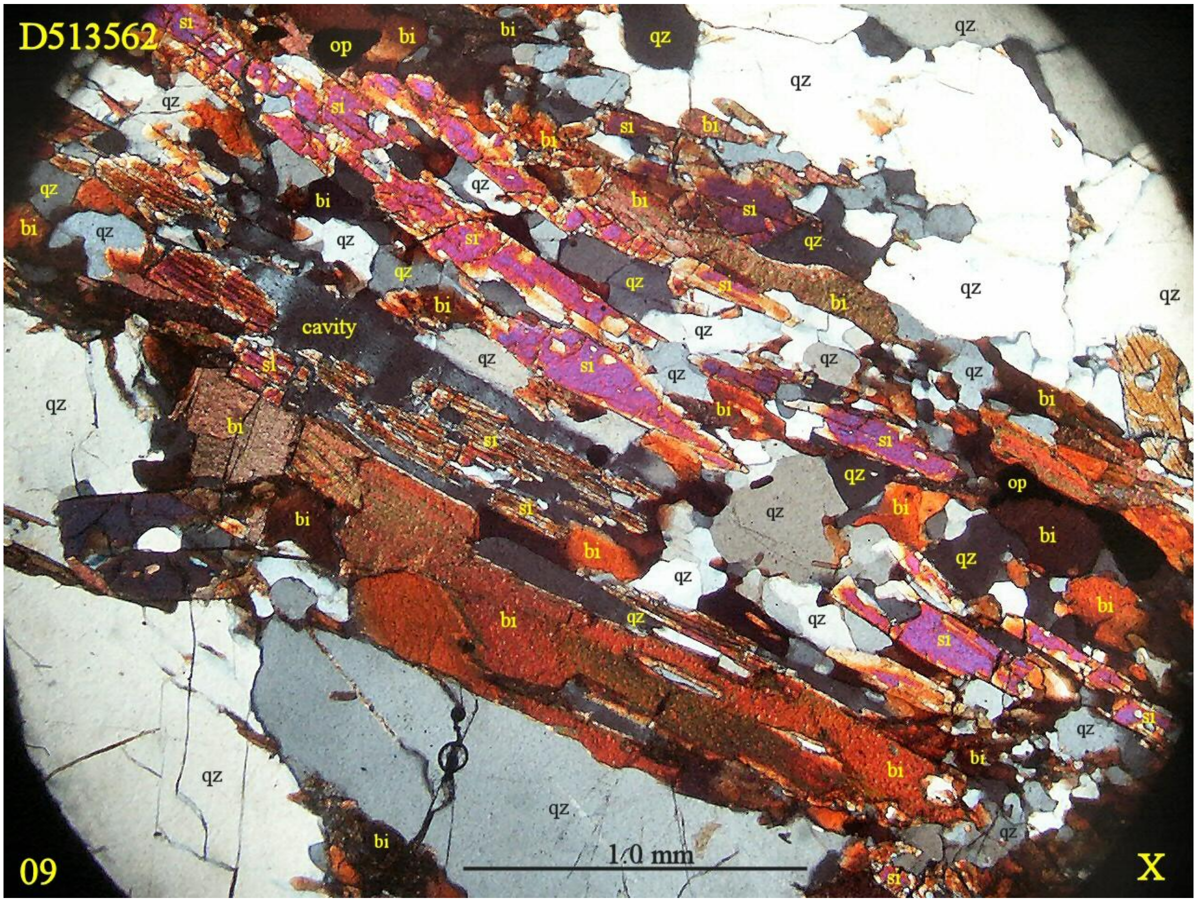


**Figure 13. Photomicrograph of garnet biotite quartz gneiss; Lens of biotite (bi), sillimanite (sl), and interstitial quartz (qz) with minor opaques (op) between two quartz-rich bands (Payne, 2023).**

### *7.3.1.4 Plagioclase Hornblende Gneiss (Aam)*

The Plagioclase Hornblende gneiss outcrops on the ridge to the west of the major fault near the western extent of the Project in thin repeating units (less than one meter thick), dipping to the northwest. It also outcrops on the slope to the north of the Smith Cabin in thicker units (five to ten meters thick). The unit is a black, fine to medium grained mafic gneiss with a composition of hornblende (55-60%) with plagioclase (35-40%) that is partially altered to sericite, and contains trace amounts of quartz, sphene, apatite, and garnet (Figure 15). It has weak foliation and thin mineral banding segregates the feldspar and hornblende (Figure 14). The protolith is possibly a sandstone or siltstone of mafic minerals, or a mid ocean ridge basalt that was deposited within the sedimentary package.


**Figure 14. Rock and hand samples of plagioclase hornblende gneiss.**

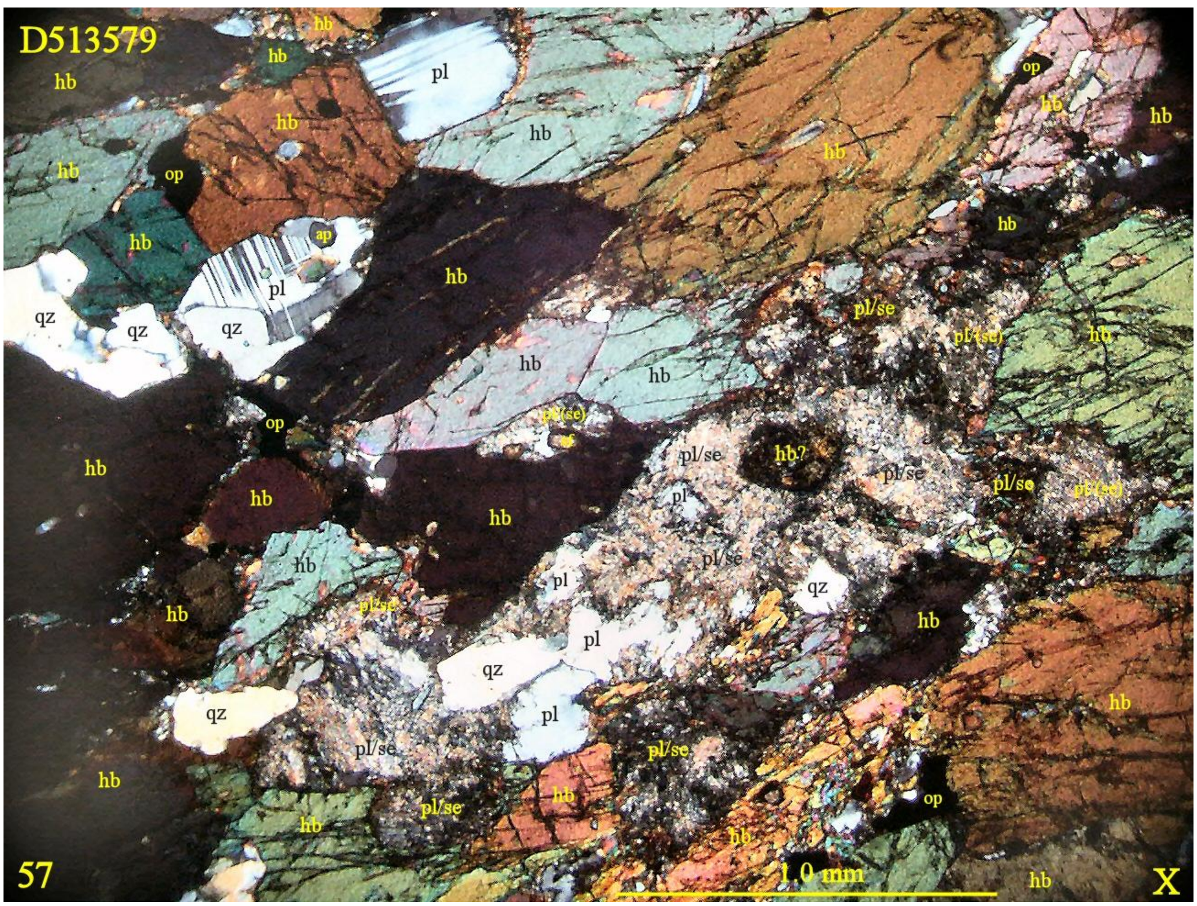


**Figure 15. Photomicrograph of plagioclase hornblende gneiss; Intergrowth of hornblende (hb), lesser plagioclase in part altered to sericite (pl/se), accessory quartz (qz), trace apatite (ap) and sphene (Payne, 2023).**

### 7.3.2 Schist

#### *7.3.2.1 Sillimanite Biotite Quartz Schist (Asbq)*

The sillimanite biotite quartz schist outcrops in the Ground Hog area and near Timber Creek. This unit is uncommon and recessive, with few outcrops on the Project. The unit is dark gray, brown to black, and medium grained to very coarse grained with strong schistosity and foliation. Quartz and biotite are intergrown, each composing 30-35% of the rock with lesser garnet, sillimanite, plagioclase and K-feldspar (Figure 16). The protolith is possibly a siltstone.

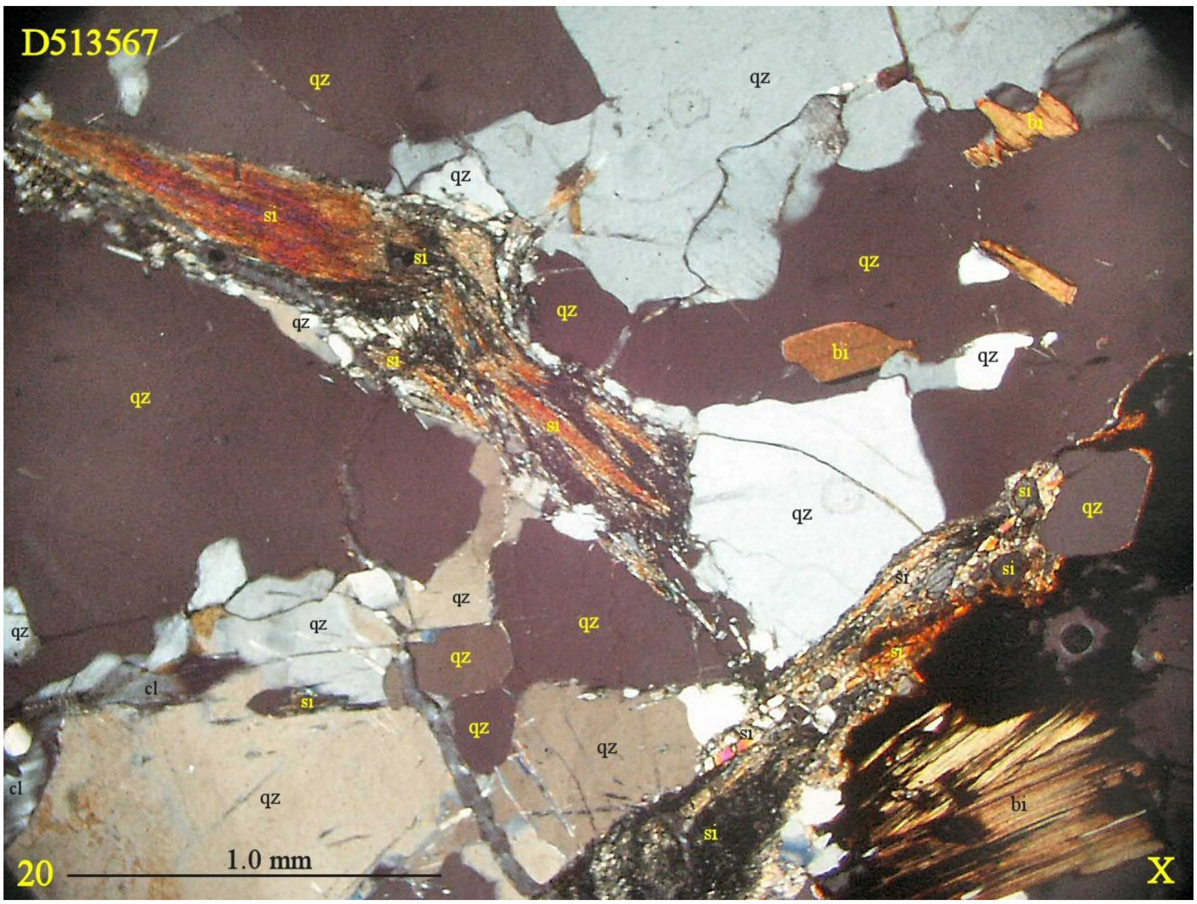


**Figure 16. Photomicrograph of sillimanite biotite quartz schist; Quartz (qz) with lenses of extremely fine grained, acicular to locally prismatic sillimanite (sl), a patch of biotite (bi), minor disseminated biotite flakes, and a discontinuous seam of chlorite (cl)-(sillimanite) (Payne, 2023).**

#### *7.3.2.2 Calc-Mica Schist (Acms)*

The Calc-Mica Schist outcrops sparsely and inconsistently on the north side of the Smith Cabin as lenses within the Plagioclase Hornblende gneiss and Quartz Plagioclase K-Feldspar gneiss. The unit is proximal to the marble and uncommon. Calc-mica schist appears similar to the Sillimanite Biotite Quartz schist and reacts with the hydrochloric acid. The protolith is possibly a calcareous siltstone.

## 7.3.3 Marble (Am)

The carbonate strata form conspicuous units due to their resistance to weathering. It is identifiable by medium gray, dark brown, light gray, and white colors (recrystallized, metamorphosed calcareous rocks). Freshly broken marble ranges in color from white to yellowish-gray to gray, and sometimes orange-pink to reddish-orange. Two distinct marble varieties are common on the Project, however it is currently unclear whether these are different marble units, or if they are spatially variable due to different degrees of metamorphism. The varieties are described below, however, they are not subdivided within the geologic map.

### *7.3.3.1 Fine Grained Marble*

The more common variety is very fine grained calcite that frequently outcrops in folded beds and ranges from one meter to 500 meters thick. This unit was partially recrystallized to finer subgrain aggregates due to variable strain (Figure 17). The marble is 60-70% calcite and contains disseminated clinopyroxene that is moderately to strongly replaced by tremolite. Subhedral to euhedral primary tremolite grains are less common and unassociated with clinopyroxene, and can contain wispy seams of limonite and thin beds of fine calcareous sand.

**Figure 17. Fine grained marble. From left to right; (left) outcrop of marble with characteristic lichen and weathering pattern, (middle) tight folding within fine grained carbonate, (right) foliated marble with pegmatite.**

### *7.3.3.2 Coarse Grained Marble*

The second variety of marble is composed of >95% medium to coarse grained (sparry) calcite with crystal size ranging 2-10 mm that form an intergrowth of equant or anhedral grains and a submosaic texture. There can be disseminated subrounded grains and clusters of clinopyroxene, disseminated anhedral grains of garnet, K-feldspar, muscovite with accessory disseminated graphite <1mm, defining a weak foliation. Small fractures contain limonite and extremely fine grained calcite. This variety of marble has been seen in association with skarn composed primarily of clinopyroxene (Figure 18).

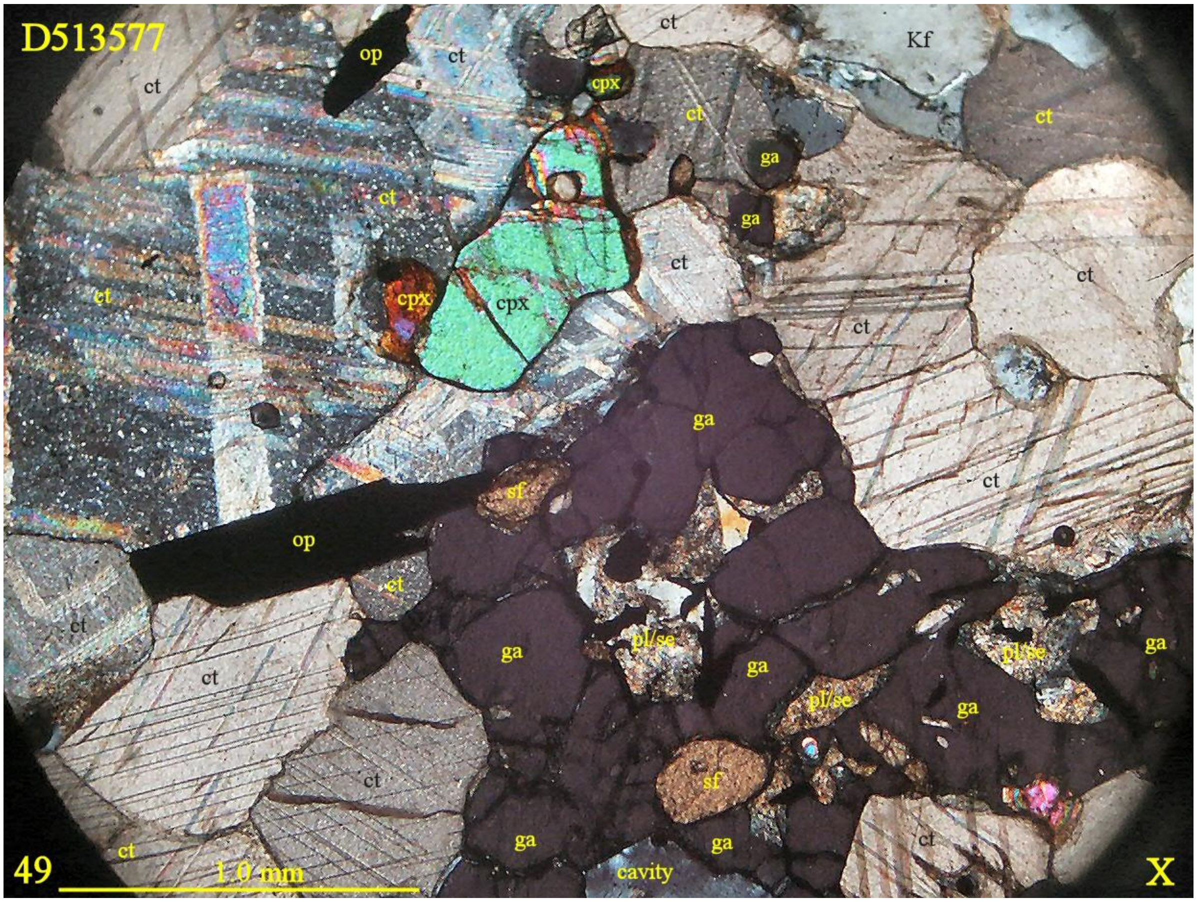


**Figure 18. Photomicrograph of coarse grained marble; Cluster of garnet (ga) with interstitial plagioclase altered strongly to sericite (pl/se) and two grains of sphene (sf); enclosed in calcite (ct) with accessory tabular opaque (op), subrounded clinopyroxene (cpx), and anhedral K-feldspar (Kf) (Payne, 2023).**

### 7.3.4 Pegmatite (Muscovite Plagioclase K-Feldspar Megacryst Granofels)

Several bodies of a feldspar-rich, very coarsely crystalline rock occur in discrete sites throughout the Project. The genesis of these pegmatites is currently unknown; they possibly formed during regional metamorphism through metasomatism, or represent isolated clean sandstone protolith or felsic dikes prior to metamorphism.

This unit often sits concordant with the gneiss in lobes, ranging from a few centimeters to several meters in width. Crystal size and distribution is highly variable in this unit, often forming clusters of large euhedral feldspar among finer-grained feldspar and quartz (Figure 19). K-Feldspar with minor plagioclase megacrysts are intergrown with finer grained K-feldspar, plagioclase and quartz composing the groundmass. Minor biotite, muscovite, garnet, sillimanite and graphite can be found within the groundmass (Figure 20).

**Figure 19. Pegmatites in outcrop; (left) characteristic, large feldspar crystals, (right) pegmatite near Ground Hog.**

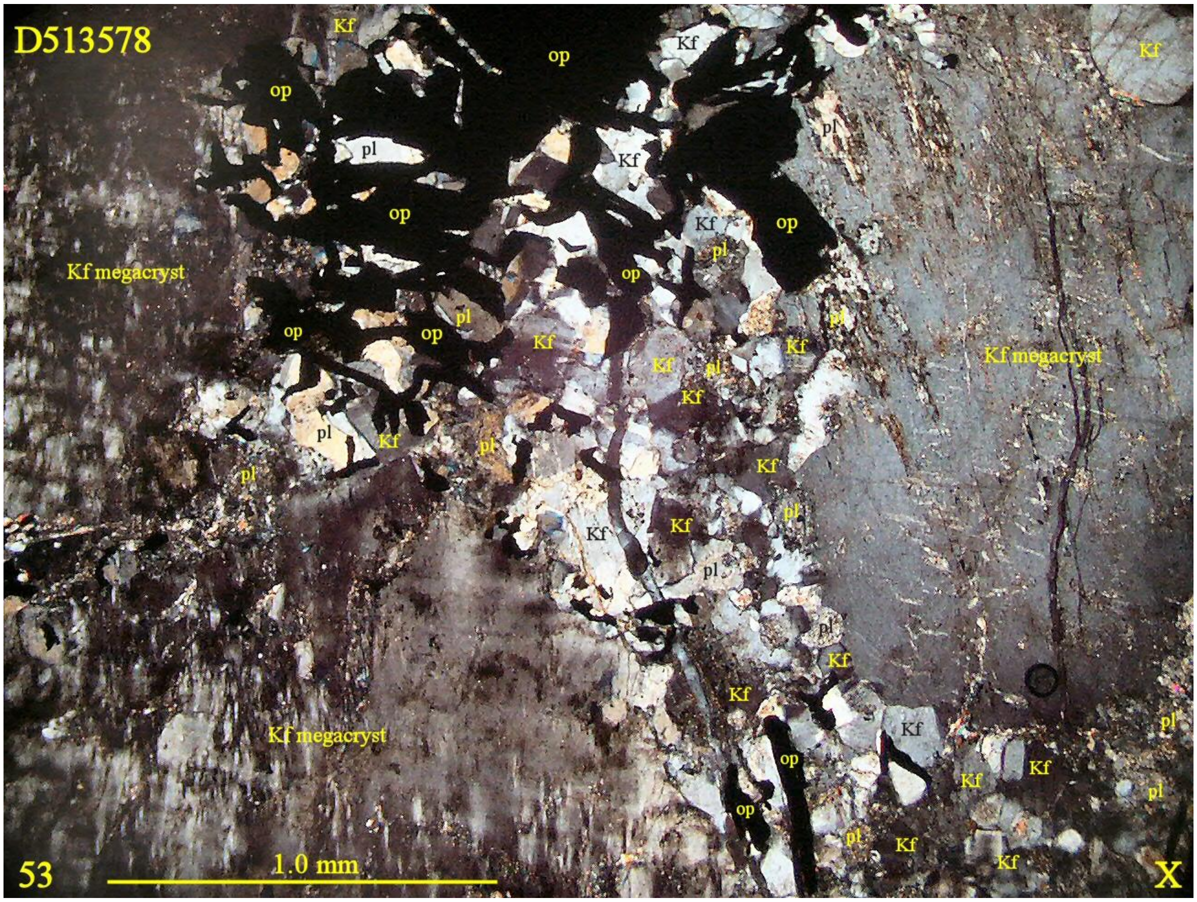


**Figure 20. Photomicrograph of pegmatite; Cluster of tabular opaque (op) mineral (graphite) with interstitial K-feldspar (Kf) and plagioclase (pl); surrounded by K-feldspar megacrysts (one with a few elongate inclusions of plagioclase altered moderately to sericite), with a band of much finer grained K-feldspar-(plagioclase) containing a few tabular to irregular grains of opaque mineral (Payne 2023).**

### 7.3.5 Diabase Dikes (Serpentine Olivine Tremolite)

Diabase dikes are common across the Project and have a general trend of northwest-southeast (striking approximately 300 degrees), and cut the Archean units. Some of the dikes are concordant with major faults. The dikes are generally up to five meters wide and can extend for tens of meters at the surface, although the Axes Canyon dike is over 6 miles long and as much as 600 feet thick (Heinrich, 1960). They are generally free of large vegetation and weathers to rubbly surfaces. Outcrops are usually dark gray to black, and sometimes dark green (Figure 21).

The crystalline mafic unit is usually ophitic, but ranges from aphanitic to phaneritic. These dikes are ultramafic in composition with olivine in equant anhedral grains frequently altered to serpentine, tremolite forming equant to prismatic grains, talc, clinopyroxene, and minor spinel (Figure 22). Fractures are filled with light brown or colorless serpentine and minor magnetite. The dikes have experienced significant alteration, especially of olivine to serpentine and magnetite, and spinel to magnetite and sparse chlorite. The weathered surface is distinctly reddish brown.

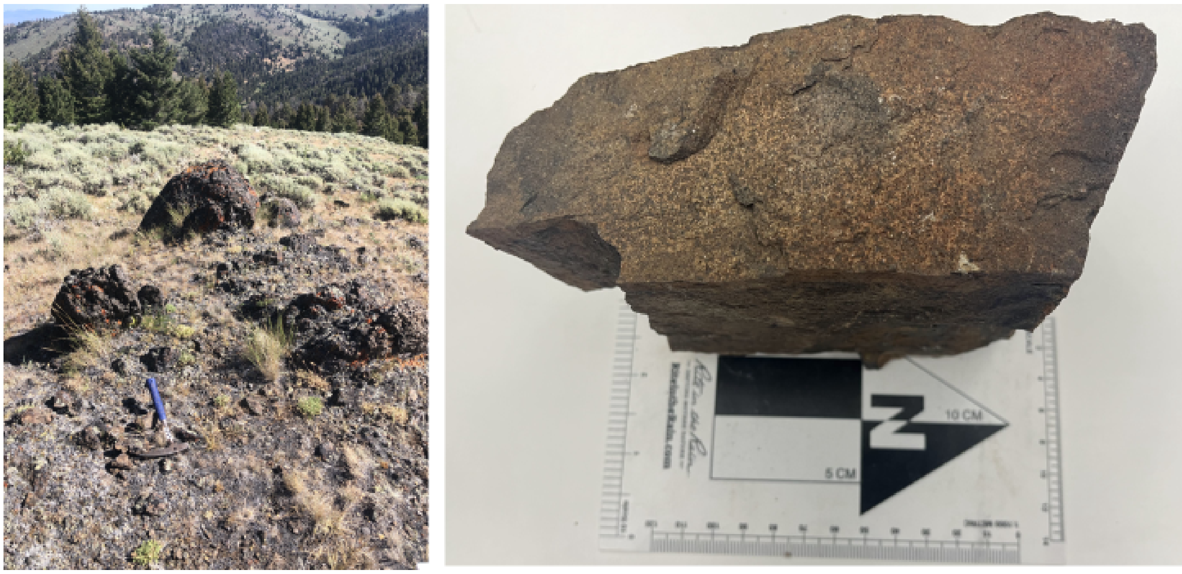


**Figure 21. Diabase; (left) outcrop striking northwest and cutting stratigraphy; (right) hand sample of diabase.**

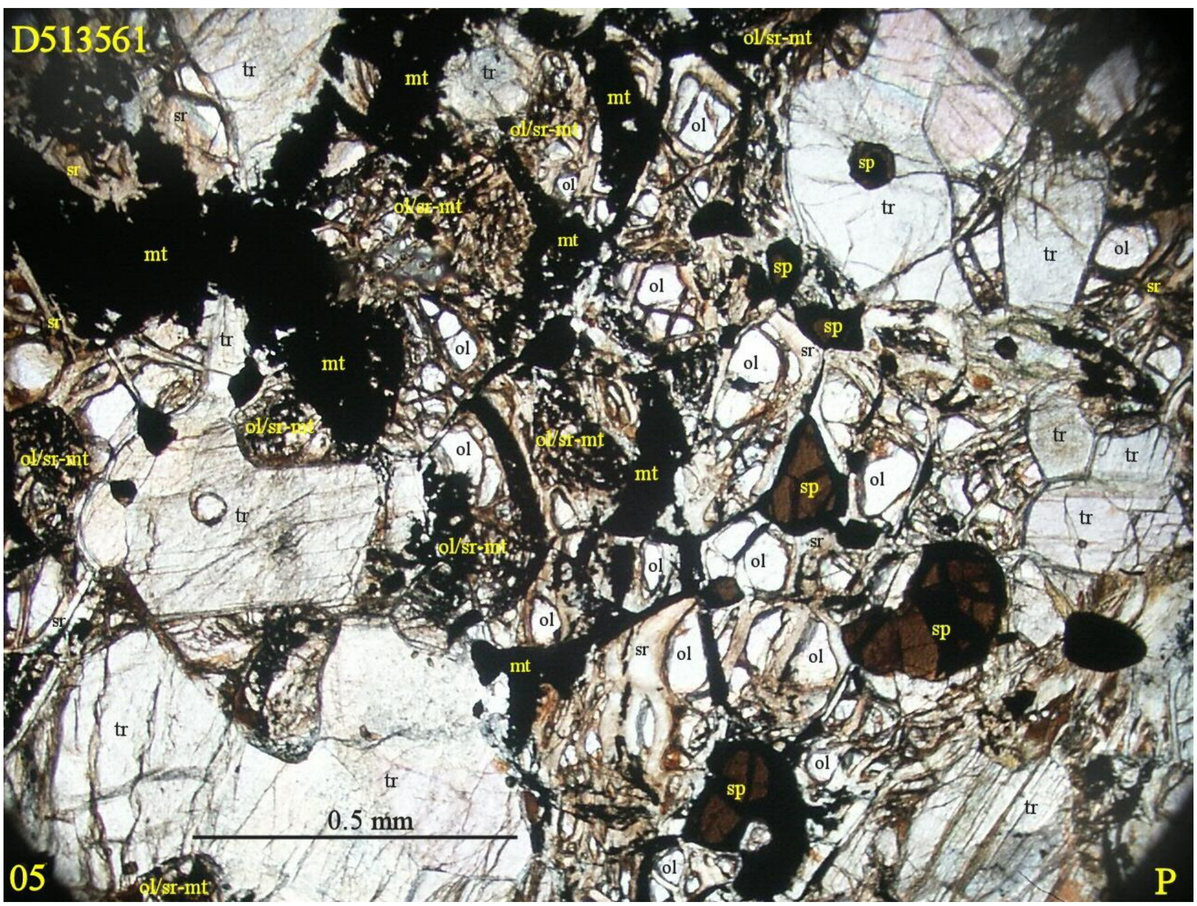


**Figure 22. Photomicrograph of diabase dike; Intergrowth of tremolite (tr) and olivine (ol) (fractured strongly and replaced by light brown to colourless serpentine (sr)), disseminated grains of spinel (sp) (partly altered to magnetite (mt); abundant veins and patches of serpentine-magnetite (sr-mt) (Payne, 2023).**

## 7.4 Project Mineralization

Surface graphite mineralization is observed at the Ground Hog Mine area, Bird's Nest Mine, F-1 pit, G-0 outcrop and on the southeast side of Timber Creek (Figure 23). Mineralization occurs most commonly near contacts of the marble with gneiss or pegmatite, and also as disseminated flake graphite. Graphite does not preferentially mineralize within a unit, rather, graphite occurs within discrete veins and can include acicular, comb, and rosette structures, and less commonly as disseminated flake graphite within the coarse-grained marble (Figure 24, 25).

The geologic focal point of the Project is a northeast-southwest trending bench of marble which terminates at its western extent, the plunging nose of an antiform. This marble bench extends from the Ground Hog area to beyond the Bird's Nest mine to the east.

The Ground Hog adits are located in gneiss near the contact with the marble, with additional adits, the Sage and Badger, to the west. At Ground Hog, graphite occurs in veins as lump or chip graphite and as interstitial graphite flooding the matrix and hosted within gneiss. Historic mining targeted the graphite visible at surface and extraction underground.

The Bird's Nest deposit appears to have been mined along a graphite seam in the gneiss, immediately overlain by carbonates and small discrete pegmatites. The pits to the north of the main mine targeted the continuation of the seam at depth. The graphite at Bird's Nest is acicular, flaky, and clotty within veins and flooding the matrix.

At the F-1 discovery pit and G-0 outcrop the graphite is hosted in thin veins (<10 cm). Southeast of Timber Creek, marble float hosting vein, lump, and interstitial flake graphite (<2 mm) was discovered in 2022.

Surface mineralization is most commonly conspicuous as graphite-bearing veins, formed by partial volatilization or precipitation from carbon-bearing fluids. The Authors have postulated that carbon is sourced from the marble and mobilized by high-grade metamorphism. The carbon within the marble was likely deposited in a calm, shallow marine environment as microbial mats or carbon bearing sediments forming limestone or carbonaceous mudstones or siltstones. A carbonaceous sedimentary unit can serve as a significant source for carbon to be converted to graphite. The proximity of graphite to the marble supports that the carbon was locally derived.

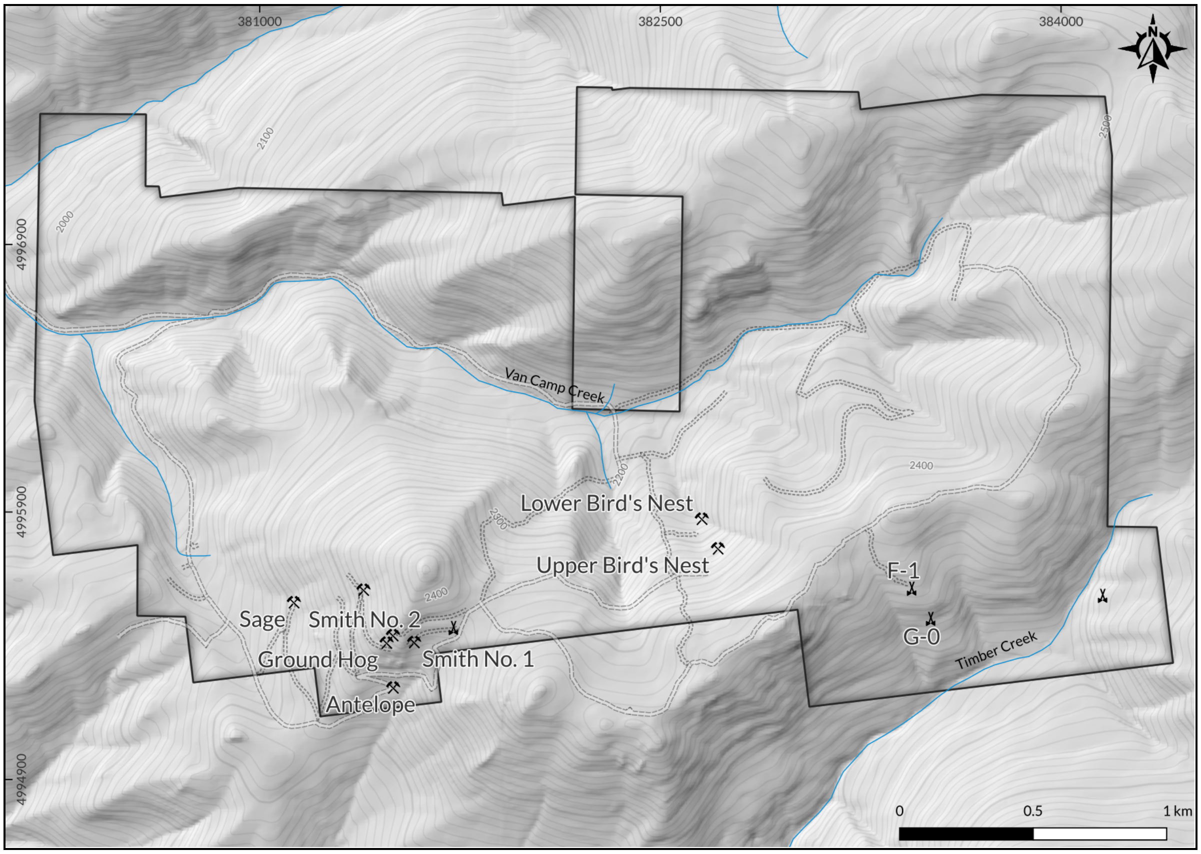


**Figure 23. Historic adits, mines, underground workings, and mineral showings at the Ruby Graphite Project.**

**Figure 24. Graphite in fractures (left), graphite seam near Ground Hog (middle), clotty graphite with pegmatite (right).**

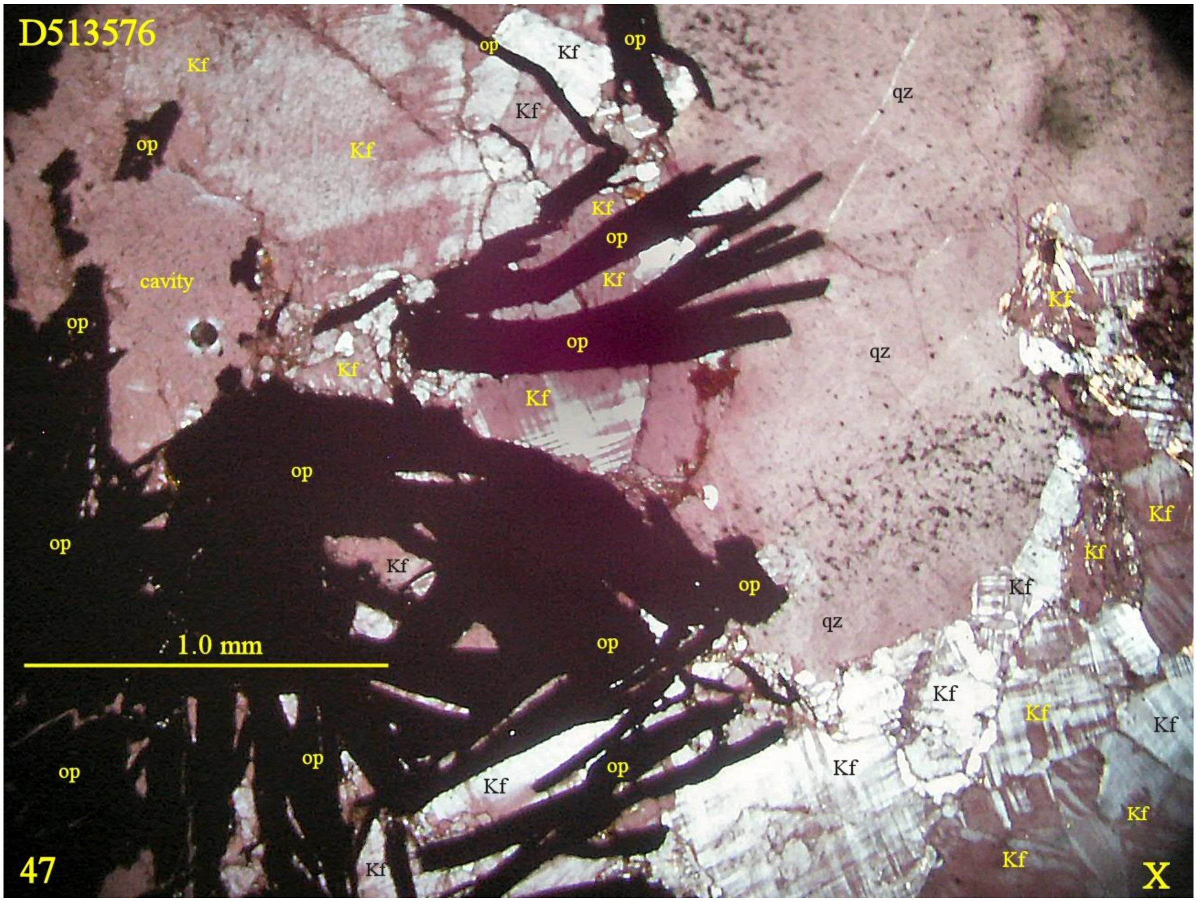


**Figure 25. Photomicrograph of graphite vein in gneiss. Edge of vein of tabular opaque (op) on left (graphite) intergrown with K-feldspar (Kf), to the right; coarse grain of quartz (qz) and very fine to fine grained intergrowth of K-feldspar (Payne, 2023).**

## 7.5 Project Structure

The Project is located within the uplifted Dillon Block that is bound to the north and south by northeast trending thrust faults (Figure 6). The Project contains synform-antiform pairs that are displaced by northwest trending strike-slip faults.

Antiform-synform pairs are the primary structure at the Project, and are isoclinal folds with bedding that dips 40° to 60° to the northwest and strikes to the southwest. The geometry of the antiform-synform pairs form double plunging synforms, creating depressions and culminations (Figure 26). Tight isoclinal microfolds are observed at all scales, and are common in the marble at outcrop scale. The orientation of the microfolds and bedding-foliation intersections indicate closure of the fold across the Saddle trend toward the west.

Many faults transecting the Project at high angles to the strike of geology are right-lateral strike slip faults. The fault that passes through the Van Camp Creek valley at the western margin of the Project crosses the primary fold hinge, and juxtaposes the units with an undetermined amount of displacement. Faults offset the folds in the southeast of the Project. The faults appear to be late and frequently coincide with the northwest trending dikes. Ancient structures including the regional faults bounding the Dillon Block have been reactivated throughout the geologic history of the region and likely terminate the smaller structures identified at the Project.

The cross section A-A' (Figure 27) displays the alternating marble and gneiss units, and the isoclinal fold structure that has similar dip measurements on either side of the hinge. The cross section's location in map view is displayed in Figure 28.

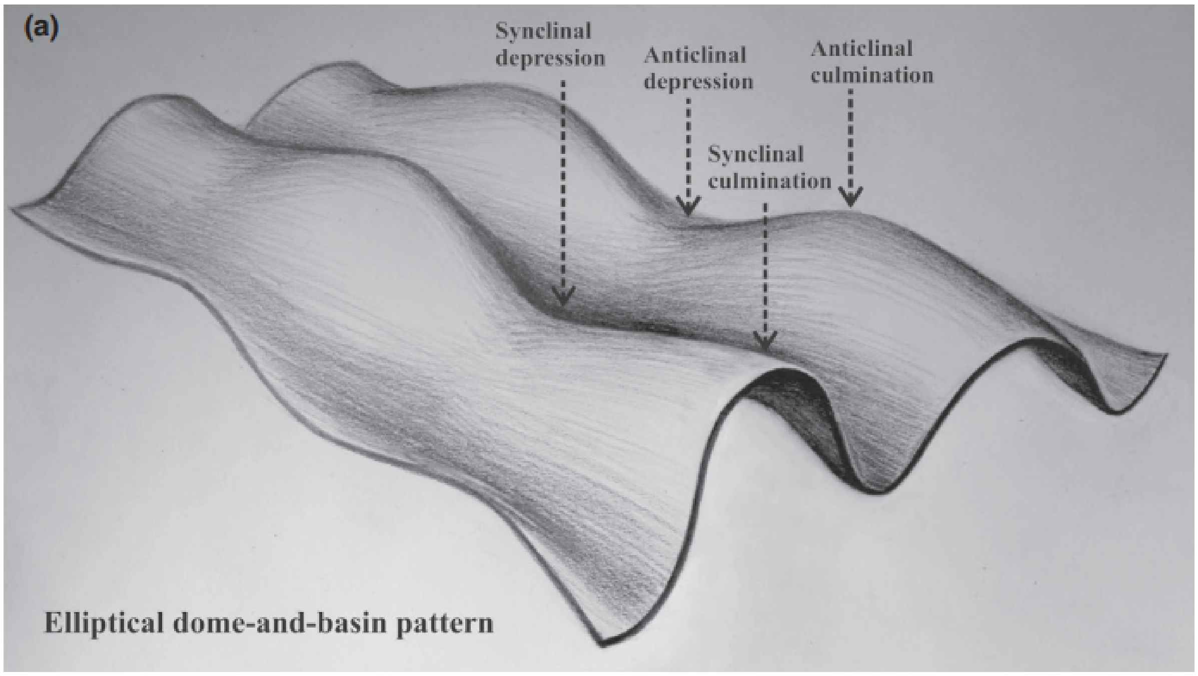


**Figure 26. Schematic of a double plunging synform-antiform pair (Shaocheng and Li, 2020).**

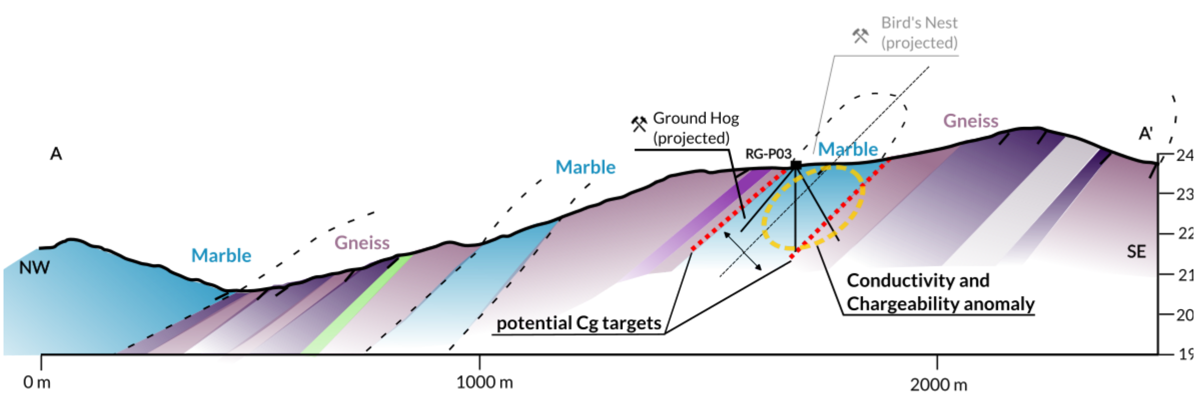


**Figure 27. Interpreted cross section through the Ruby Graphite Project.**

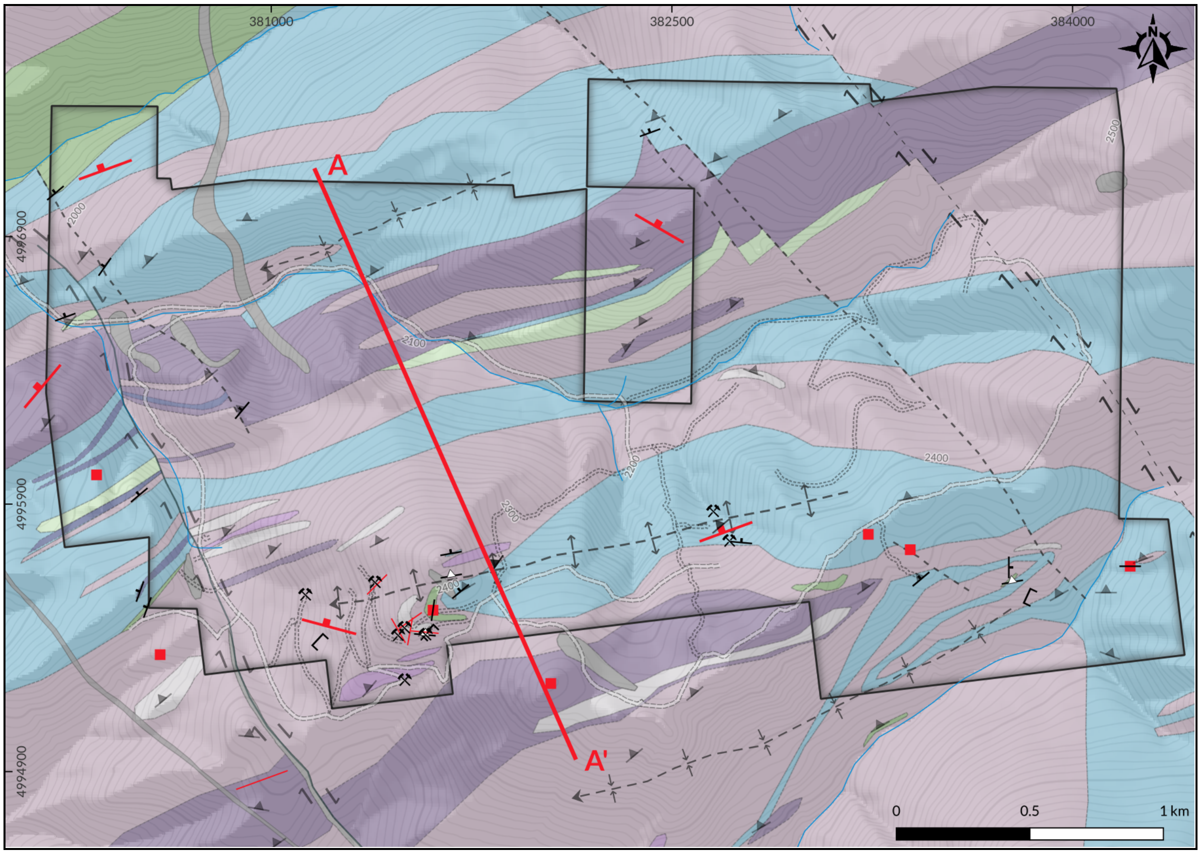


**Figure 28. Map displaying cross section line at Ruby, approximately 400 meters to the east of the Ground Hog mine.**

# 8 DEPOSIT TYPES (GRAPHITE GENESIS)

Graphite deposits are worldwide and found in a variety of geologic settings. An environment for graphite deposition must include:

1. A carbon source; and
2. Conversion of carbon to graphite by temperature and pressure.

## 8.1 Carbon Sources

Carbon is stored in the atmosphere, microorganisms, seawater, rocks and sediments, and the mantle. The carbon cycle explains the transport and continuous flux of carbon between these entities.

The ocean is a large reservoir for carbon deposition and microorganisms produce carbon through living and dying. Accumulation of carbonaceous microorganisms can form microbial mats or carbonaceous sediments (depending on the depositional environment and the amount of oxygen within the atmosphere). Carbon is continuously exchanged between the ocean's surface waters and the atmosphere.

Carbon can also be stored for long periods of time in the ocean. When carbon is deposited in a marine environment, it becomes a component of a sedimentary rock as carbonaceous sediments, limestones, and dolomite.

Volatile carbon from the mantle (often $CO_2$) is introduced terrestrially and subaqueous by volcanic degassing and tectonic degassing. Significant quantities of mantle carbon are released through mid-ocean ridge volcanism (seafloor vents) and volatile $CO_2$ can dissolve in seawater. Additionally, Carbon has a tendency to incorporate into magmas produced by melting peridotite rocks in the upper mantle. Magmas and mantle-derived gasses are effective means of transporting carbon to the earth's surface.

## 8.2 Carbon → Graphite Conversion

Graphite forms when carbon is subject to heat and pressure in the Earth's crust or mantle. Figure 29 illustrates several different source and cooling pathways for the formation of graphite (modified from Luque et al., 2014). Graphite is most often found within metamorphic rocks such as marbles, schists, and gneisses because temperatures and pressures are elevated during metamorphism to convert carbon to graphite. Mobilized Vein graphite is frequently found along structural conduits or lithologic contacts. Graphite veins form through partial volatilization or from carbon-bearing fluids and subsequent recrystallization. Elevated temperatures and pressures within carbon-bearing units release volatiles that mobilize within the host rock as $CO_2$ rich fluids. During transport, wall rocks consume water, and the remaining material precipitates as graphite (Luque et al., 2014).

## 8.3 Isotopic Fractionation

Carbon holds two isotopes- the lighter $^{12}C$ and heavier $^{13}C$. The ratio of $^{13}C/^{12}C$ (indicated by the symbol of $\delta^{13}C$) provides a method to fingerprint the carbon source due to the fractionation of $^{12}C$ and $^{13}C$ both unique to the original source and that can be modified at various phases during the rock cycle. For example, higher values of $\delta^{13}C$ in a rock implies the removal of $^{12}C$ by the loss of methane or carbon dioxide as the rock is reworked by pressure and heat, leaving behind $^{13}C$ and increasing the $^{13}C/^{12}C$ ratio of carbon in the rock. Therefore, graphite generally becomes isotopically heavier as metamorphism progresses (Hoefs and Frey, 1976, Wada et al., 1994).

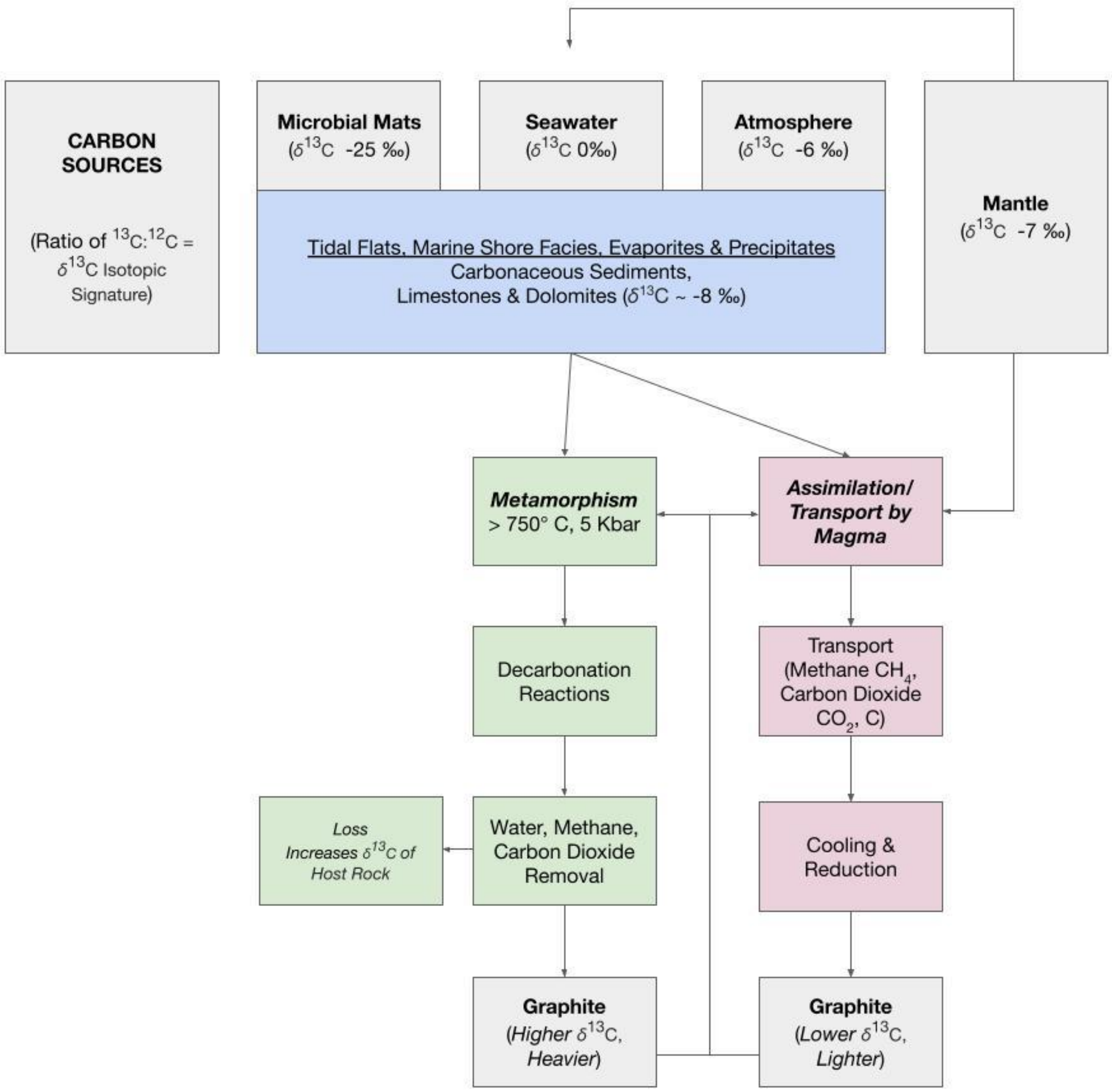


**Figure 29. Generalized diagram displaying several carbon sources, transport mechanisms, formation of graphite and resulting carbon isotope effects (modified from Luque et al., 2014).**

# 9 EXPLORATION

During September 2022, Ethos Geological collected 201 soil samples, 28 rock samples, conducted 18 man-days of field mapping, initiated a drone-based photogrammetry survey, and completed a Project-wide ground electromagnetic survey and a targeted IP survey.

## 9.1 Soil Sampling

Ethos Geological collected 201 soil samples at 25 meter intervals along three transects (Figure 30). Soils were placed in a cloth bag and sent to ALS Minerals in Reno, NV. A duplicate sample was collected for soil pH testing at Ethos Geological in Bozeman, MT.

The soil samples lines are adjacent to known mineralization to identify lateral extension and trends in alteration and mineral composition at the margins of mineralization. They are oriented perpendicular to stratigraphy to fingerprint lithologic units. Because of erosional processes that may move material downslope, soil samples results are not necessarily an exact representation of their underlying geology, and supplemental field mapping observations and other sampling methods are implored for lithologic mapping purposes.

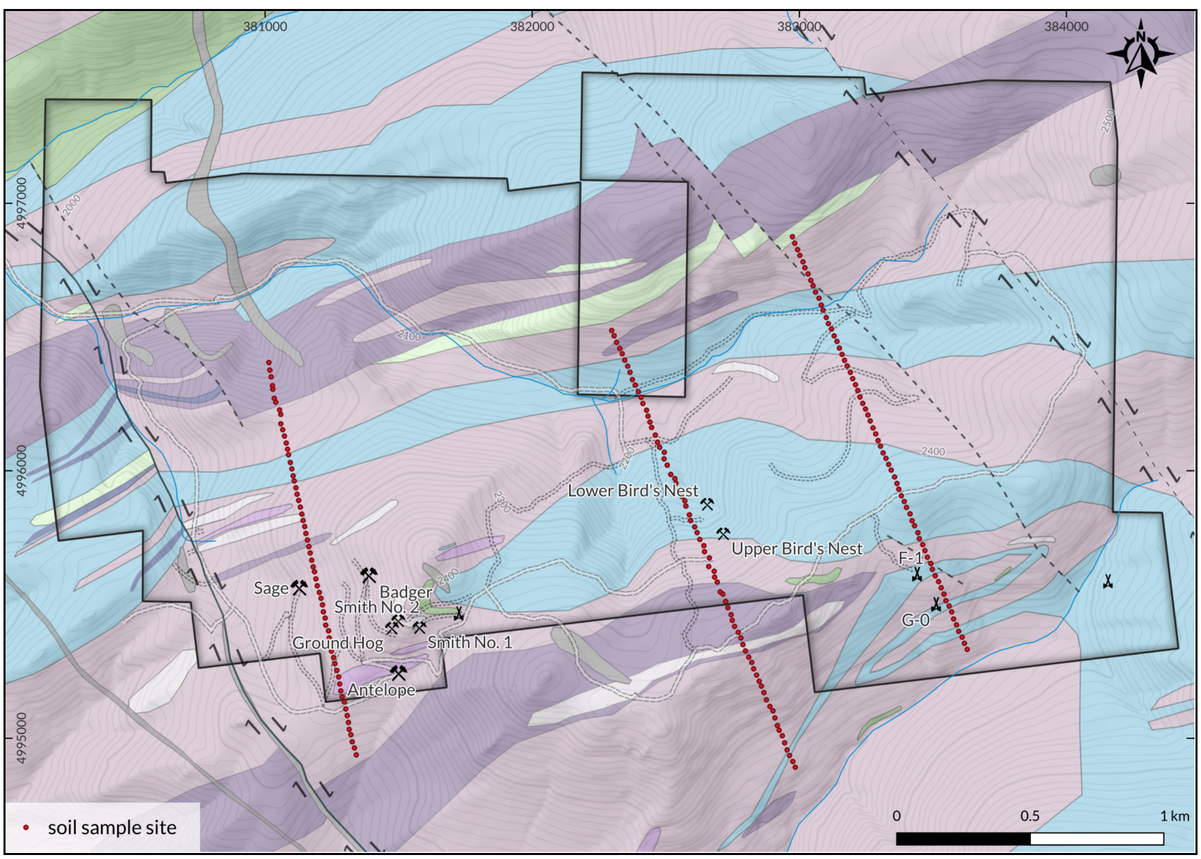


**Figure 30. 2022 soil sample sites.**

### 9.1.1 Results

The soil lines are oriented approximately perpendicular to the strike of geology, therefore delineate approximate lithologic units based on categorized values of elemental abundance. The abundance of rare earth elements in the soils (Figure 31, 32, and 33) are useful for identifying structures and changes in lithology. Each rare earth element (dysprosium, samarium, promethium) displays repeating units across the tight fold in the southeast of the Project and an alternating pattern in the west soil line across the Ground Hog area that mirrors units across the projected hinge of a west plunging fold.

The soil signatures recognize these variations which may not be visible in outcrop. In Figure 31, the southern half of the west soil line displays a sequence of red-yellow-orange-yellow-red (repeating variation in Dysprosium values) in an area mapped as the Quartz Plagioclase K-feldspar gneiss. This repetition implicates a geochemical repetition within the gneiss mirrored across the projected fold hinge. The repeating red and orange in the southern portion of the east line also align with the surface expression of a fold in the marble.

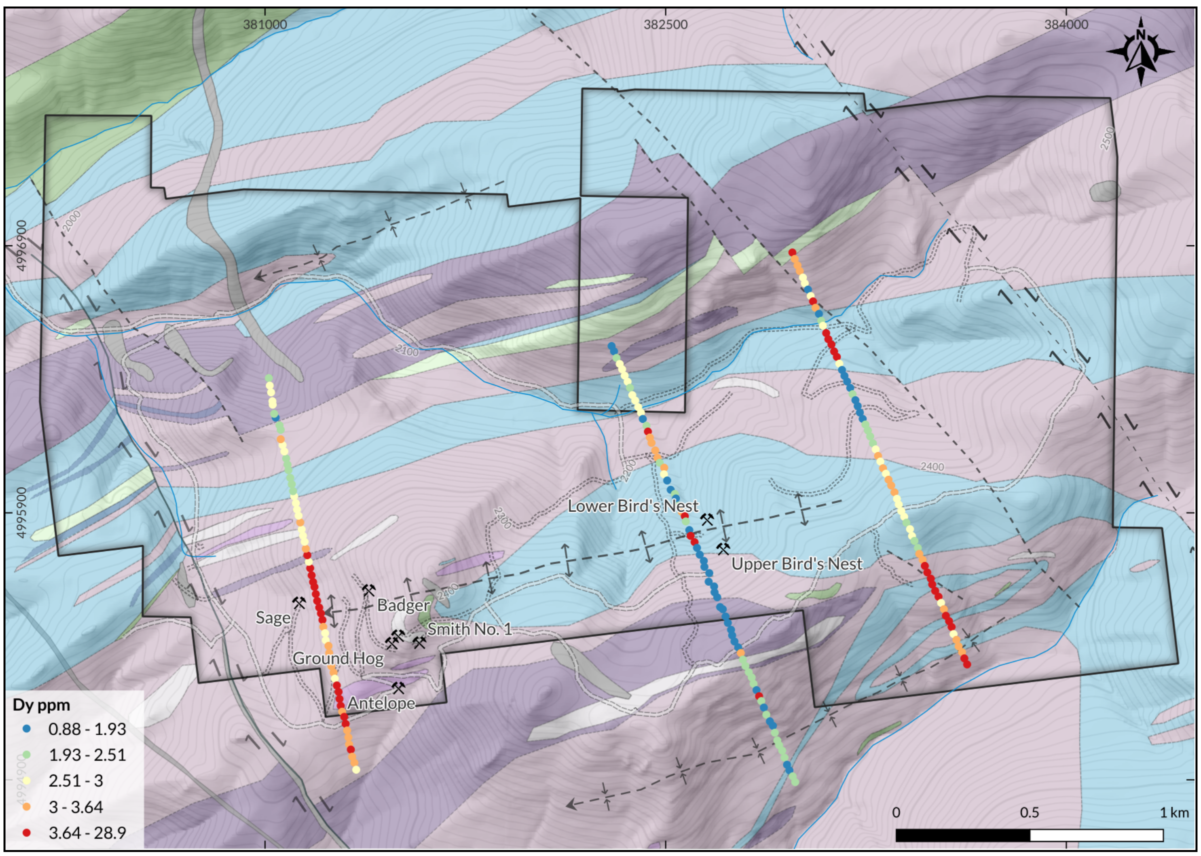


**Figure 31. Dysprosium (Dy), rare earth element ppm values.**

Samarium and promethium geochemical signatures are extremely similar. Figures 32 and 33 display repetition of values in the west line that are expressed by orange-red-orange-red-orange (alternating high Sm/Pr and moderately high Sm/Pr values). The values of samarium and promethium both successfully delineate the fold in the southern portion of the east line as well.

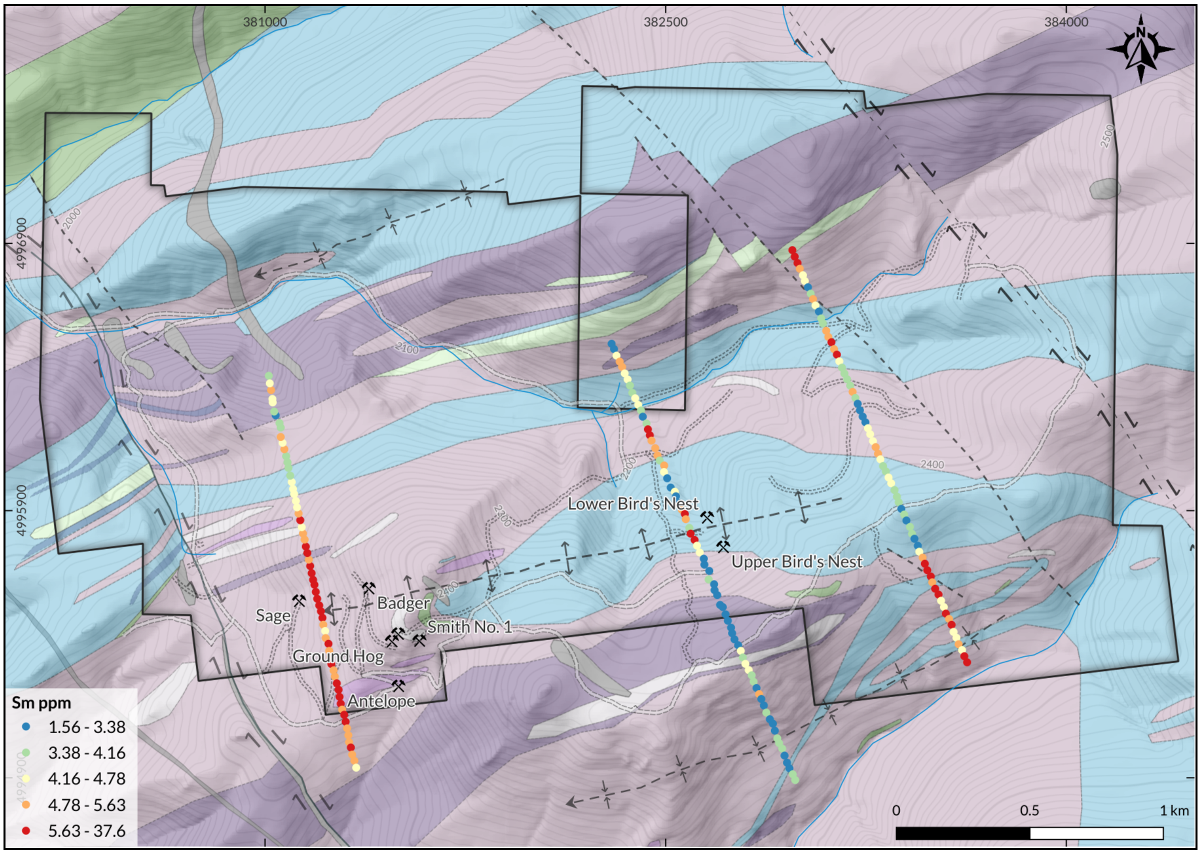


**Figure 32. Samarium (Sm), rare earth element ppm values.**

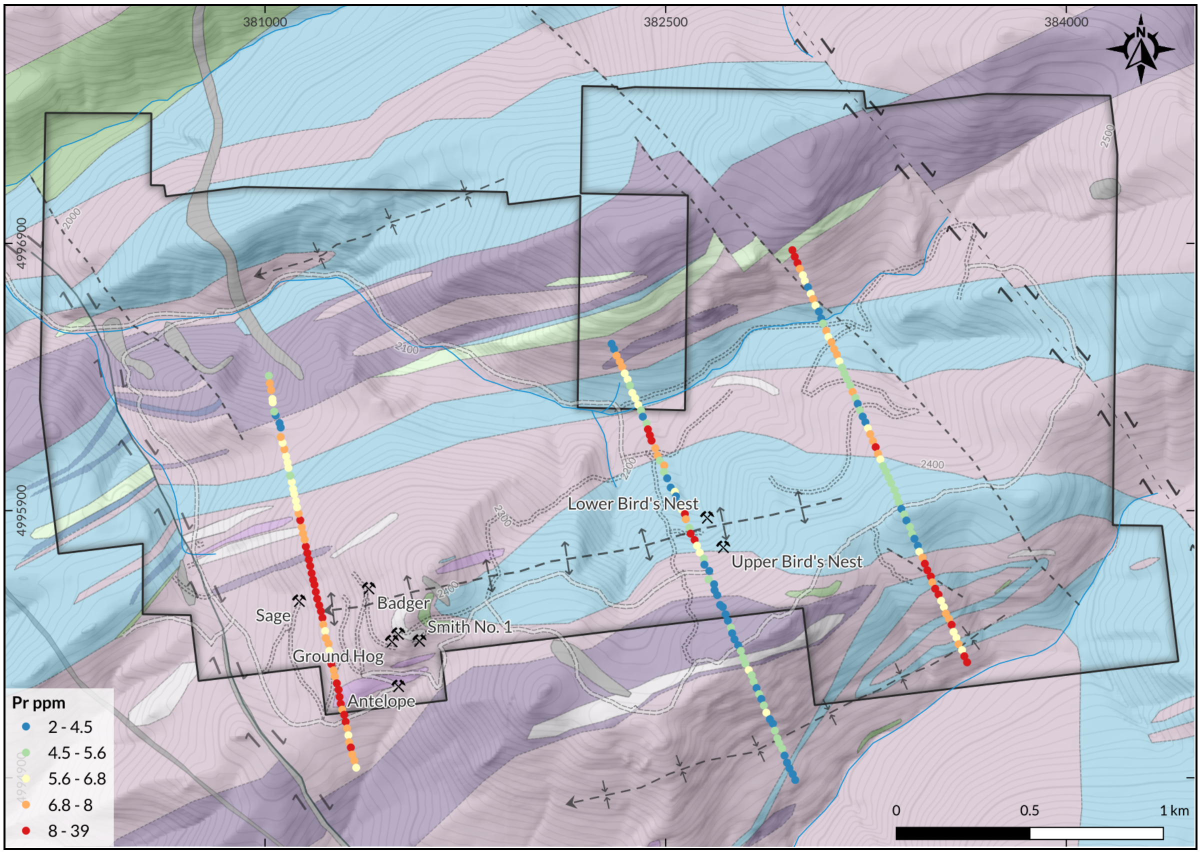


**Figure 33. Promethium (Pr), rare earth element ppm values.**

Calcium in the soils is a useful element to delineate the marble. Calcium in soils identifies marble on the hillside to the north and south of Bird's Nest area, which is predominantly tree-covered and has few outcrops. The high calcium values (>1.18, red) are extensive across the eastern line, less widespread in the middle line, and not present in the west line (Figure 34). The decrease in high calcium at the surface supports a west-plunging antiformal structure. Repeating high values of calcium in the south of the east line correlate with the surface marble outcrops, however calcium does not otherwise recognize repeating units as the rare earth elements do.

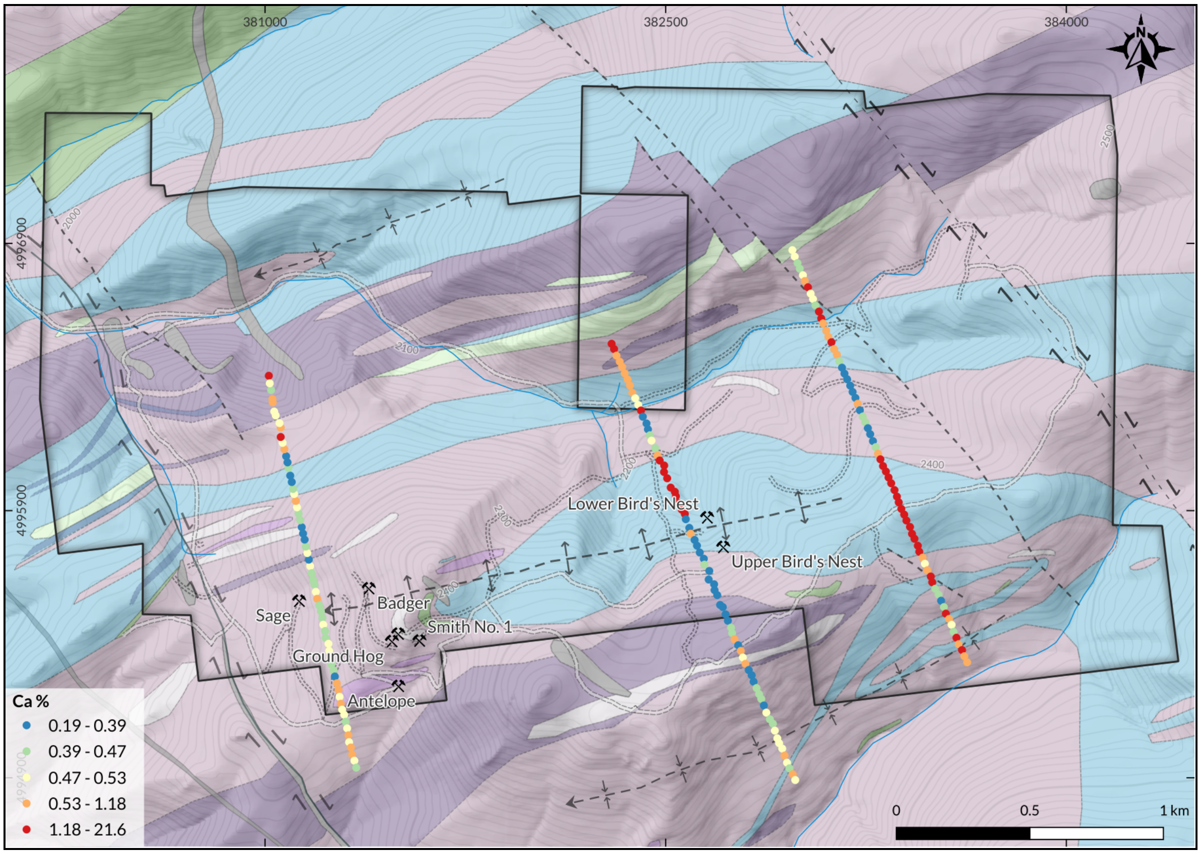


**Figure 34. Calcium percentage in soil assays.**

## 9.2 Rock Sampling

Ethos Geological collected 28 rock samples across the Project (Figure 35). 21 of these samples were sent for assay at ALS Minerals in Twin Falls, Idaho. Full geochemical analysis should identify characteristics of each lithology and determine variation within units.

The analytical process used is a complete characterization package, which is useful for rare earth element fingerprinting to chemically differentiate the gneiss units and determine their protolith. Carbon combustion analysis can assist in understanding the graphite content of the samples, as some were collected from mineral occurrences.

Eighteen of the rock samples were also sent to Vancouver Petrographics, Ltd. in Vancouver, British Columbia, Canada. Selections of these descriptions and images are included in the Project Geology section. The petrographic study identified the mineral composition of each unit.

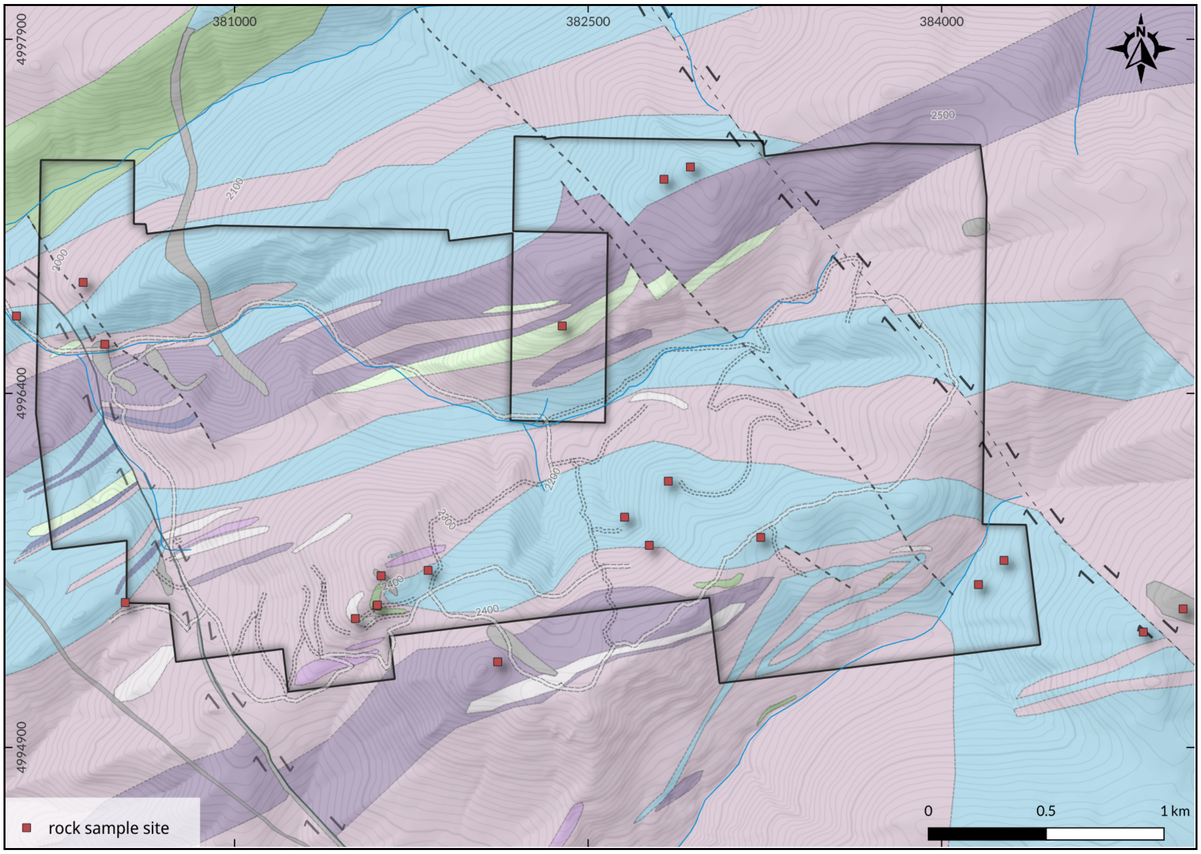


**Figure 35. Rock samples collected in 2022.**

### 9.2.1 Results

Rock samples have been received at the laboratory for analysis and are currently pending; results are expected in March 2023.

## 9.3 Soil pH Analysis (IDH)

Soils pH analysis is an effective and inexpensive tool for examining the effects of hydrothermal fluids through a host rock. As hydrothermal fluids can significantly alter host geochemistry through the exchange of hydrogen ions and water-soluble cations (such as Ca and Mg), concentration or depletion of these elements can be an important vector toward host chemistry and fluid conduits.

Ethos measures this value of H+ ions through analyzing the difference between the starting pH and a buffered pH of each soil sample using a sensitive pH meter. This difference is referred to as the IDH value ("inverse differential hydrogen"). If the pH drops rapidly, the solution is not buffered, indication that there is no Ca.

A hydrothermal conduit (often, a mineralized body) is generally represented by moderation of IDH over a mineralized area, and an IDH peak on either side of the H+ anomalies. The definitive pH signal from a carbonate body is a H+ high over the body, and a Ca high (calcite peak) on either side of the H+. Both of these can be detected with the pH meter.

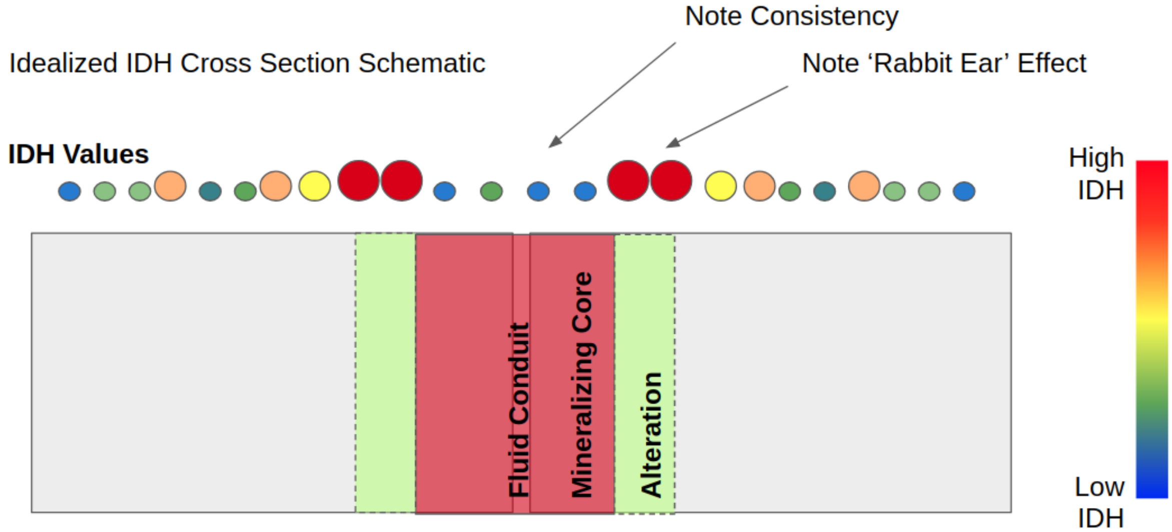


**Figure 36. Simplified IDH schematic illustrating the effects of fluids on soil pH across a hydrothermal conduit.**

The analysis of each sample, in detail, proceeds with mixing a teaspoon of each soil sample with a teaspoon of distilled water for 10 seconds, followed by a pH measurement using digital pH meter (the 'pH' variable). Then, a single drop of hydrochloric acid (10 % HCl) is added to the solution, stirred for 10 seconds and a second pH reading taken (the 'acidified pH', or 'apH' variable).

If the pH drops rapidly, the solution is not buffered, so there is no Ca. If the pH does not appreciably drop after the acid is added, the solution is likely buffered by Ca. In this process, the acidified H+ ('apH') is subtracted from the original H+ ('pH'), and the inverse is calculated to create the IDH variable:

$$IDH = \frac{1}{apH+ - pH+}$$

The objective of the analysis is that samples where there was little change (present Ca buffered the solution as expected along the margins of mineralized bodies) are plotted with their inverse, displaying highs (reds) across any carbonate or Ca-enriched source (Figure 36).

In samples where there is significant change from pH to apH (where there is no Ca buffer present), IDH will display lows over areas lacking in or depleted in Ca.

Areas of consistent suppressed lows or highs reflect stable host rock geochemistry, or underwent moderate, consistent hydrothermal alteration.

### 9.3.1 Results

Identifying precise contacts with the marble unit is crucial to the progress of the Ruby Graphite Project, as graphite mineralization is often found along these contacts and marginal to the carbonate. At Ruby, high IDH values well-define the extent of carbonate bodies underlying the soils (Figure 37).

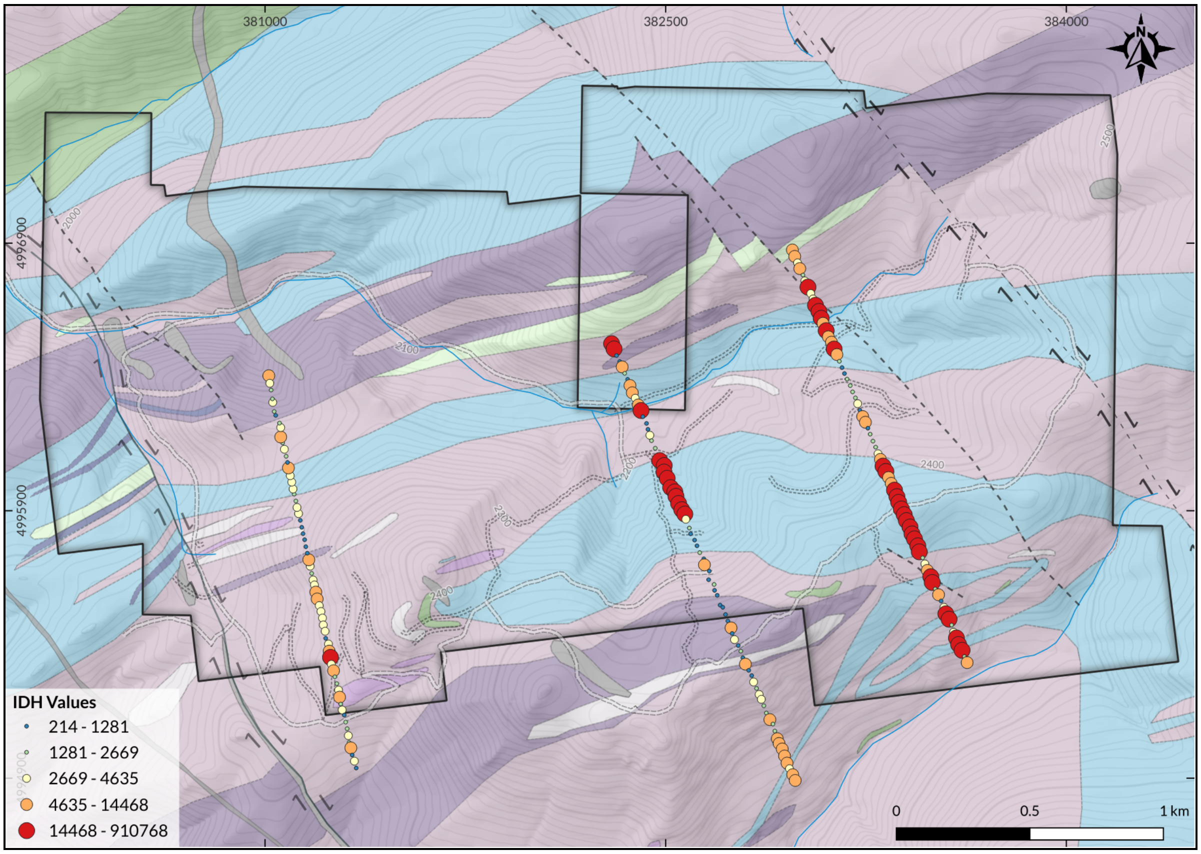


**Figure 37. Soil IDH values showing anomalies overlying carbonates at or near the surface.**

## 9.4 Field Mapping

Ethos Geological personnel conducted 18 man-days of field mapping within two campaigns, August 11-13 and September 5-9. Field mapping targeted historic workings, known graphite mineralization, geologic units and contacts were identified and refined, and structural measurements were collected (Figure 9).

The results from field mapping implicate that previous researchers performed informative work, however,

- lacked detailed rock descriptions
- misinterpreted the rock protoliths

- used igneous-based terminology

2022 field mapping sought to utilize the following methodology:

- Description-based field mapping
- Structural foliation/bedding relationships to determine folding and structural features
- Leverage geologic understanding from adjacent sites (ie. from nearby talc mines)

## 9.5 Drone Photogrammetry Survey

Ethos Geological personnel collected high-resolution drone-based aerial imagery and elevation surveys over the Ruby Graphite Project on August 3-6, 2022. The drone survey photographed 2,709 acres of the Project (Figure 38) at 10 cm/pixel resolution. Ground control points were not collected for the survey.

The purpose of a high resolution survey is to assist in geologic mapping through the increased definition and observation in areas yet mapped, identify subtle lineaments in the elevation relating to geology and structures, and provide a complete set of accurate and precise base data for future mapping and potential mining efforts (volume estimation, infrastructure planning and construction).

Approximately two-thirds of the survey was completed; the survey was hindered by high winds and wildfire smoke present during July and August. Ethos plans to complete the survey in summer 2023.

The collection of the aerial photos was performed at 100 meters greater than the highest point on the project. Pictures were collected using a 20 megapixel resolution gimballed-camera along gridded flight lines with approximately 60% lateral and 70% frontal overlap. These pictures were processed using Pix4D software for the final product using the method of photogrammetry, whereby measurements of each pixel in each photograph are compared from overlapping photographs taken from different angles to determine bare earth, vegetation, and their respective heights and shape. As the location of the drone is known via GPS, the locations of the digital surface model (with vegetation) and digital surface model (bare earth- with vegetation removed), can be precisely determined. Using ground control points to constrict the final model, photogrammetry can produce elevation models with +/- 2cm resolution.

The raw data and survey results for the portions flown are delivered at the resolution as follows:

- Survey extent of 2,709 acres (1,096 ha or 4.23 $mi^2$)
- Aerial orthomosaic imagery - 10 cm/pixel (Figure 38)
- Digital terrain model - 20 cm/pixel
- Digital elevation model - 25 cm/pixel
- Contour lines - 20 cm intervals (Figure 39)

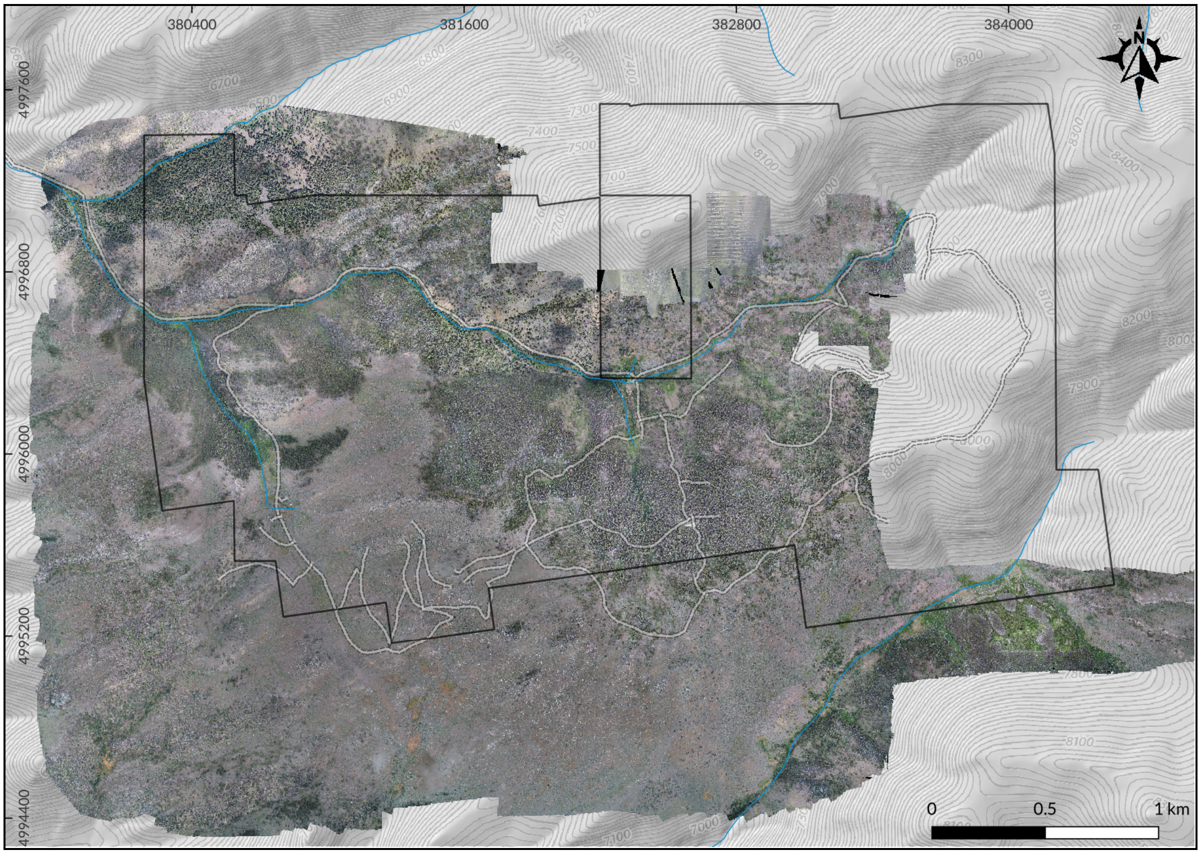


**Figure 38. Aerial mosaic of the Ruby Graphite Project derived from the drone photogrammetry survey.**

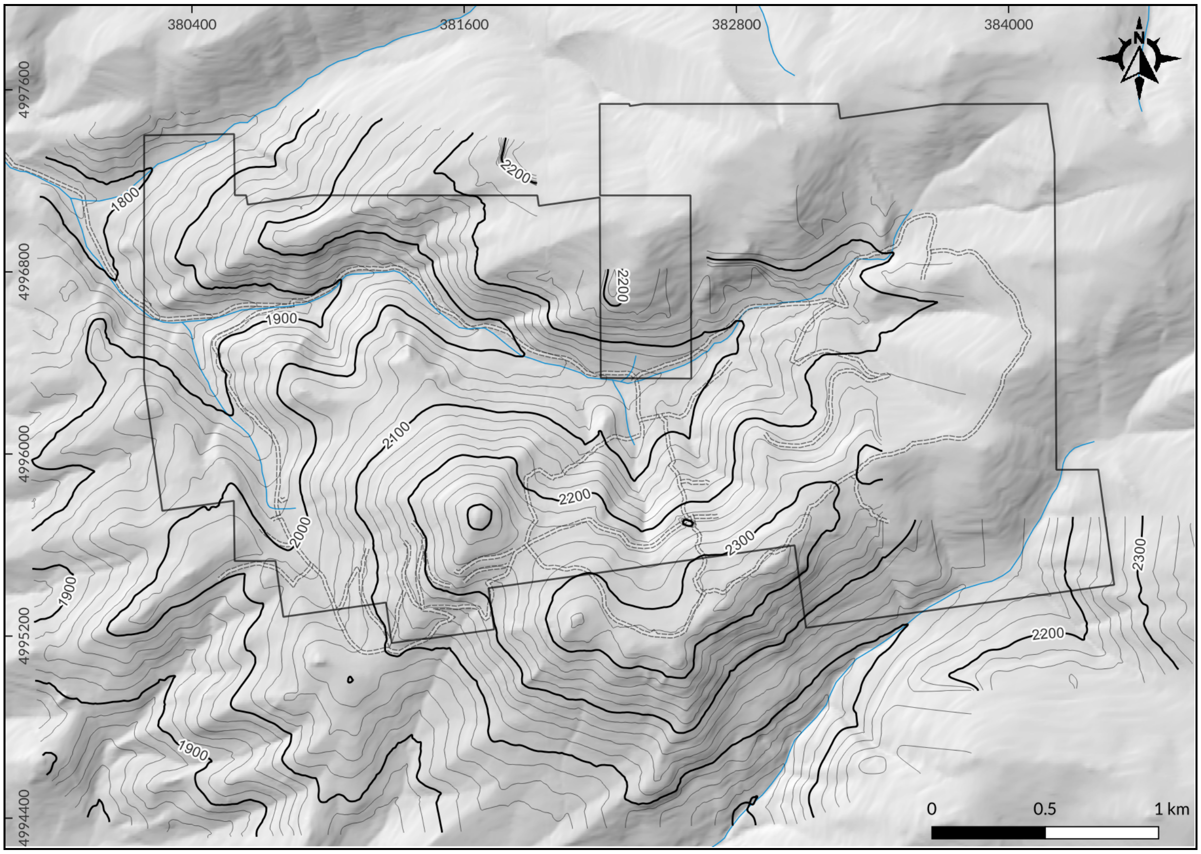


**Figure 39. Contours representing the elevation model for the Ruby Graphite project derived from the drone photogrammetry survey.**

## 9.6 GEM-2 Ski Ground Electromagnetic Survey

Electromagnetic (EM) surveys identify areas of high conductivity, and graphite is a highly conductive mineral. Zones of high conductivity do not exclusively correlate to graphite deposits because other materials such as water and metals also have conductive properties, however the results from the electromagnetic survey can inform prospective areas to be explored. Ethos Geological conducted a ground electromagnetic survey utilizing a GEM-2 Ski handheld conductivity sensor. The GEM-2 Ski enables subsurface scanning to a depth of approximately 10 meters (33 feet) utilizing up to ten frequencies simultaneously. For this survey, four frequencies were sufficient for data acquisition. The survey consisted of 24 northwest-southeast transects at 200 meter (656 ft) line spacing, covering 3087 acres (1,249 ha or 4.82 sq miles).

### 9.6.1 Results

The survey successfully identified conductors coincident with previously known graphite deposits, and further informed projected extension. Three primary trends of conductors were identified (Van

Camp, Cabin, and Saddle); which may represent new graphite discoveries. A fourth conductor may be present to the southeast, named Timber (Figure 40).

In Figure 40, single point anomalies that appear like a 'butterfly' or fan-like features likely indicate a measurement overlying a fault due to the occurrence of clays and fluids along a permeable zone. These anomalies appear like 'butterflies' due to the B-Spline interpolation method used.

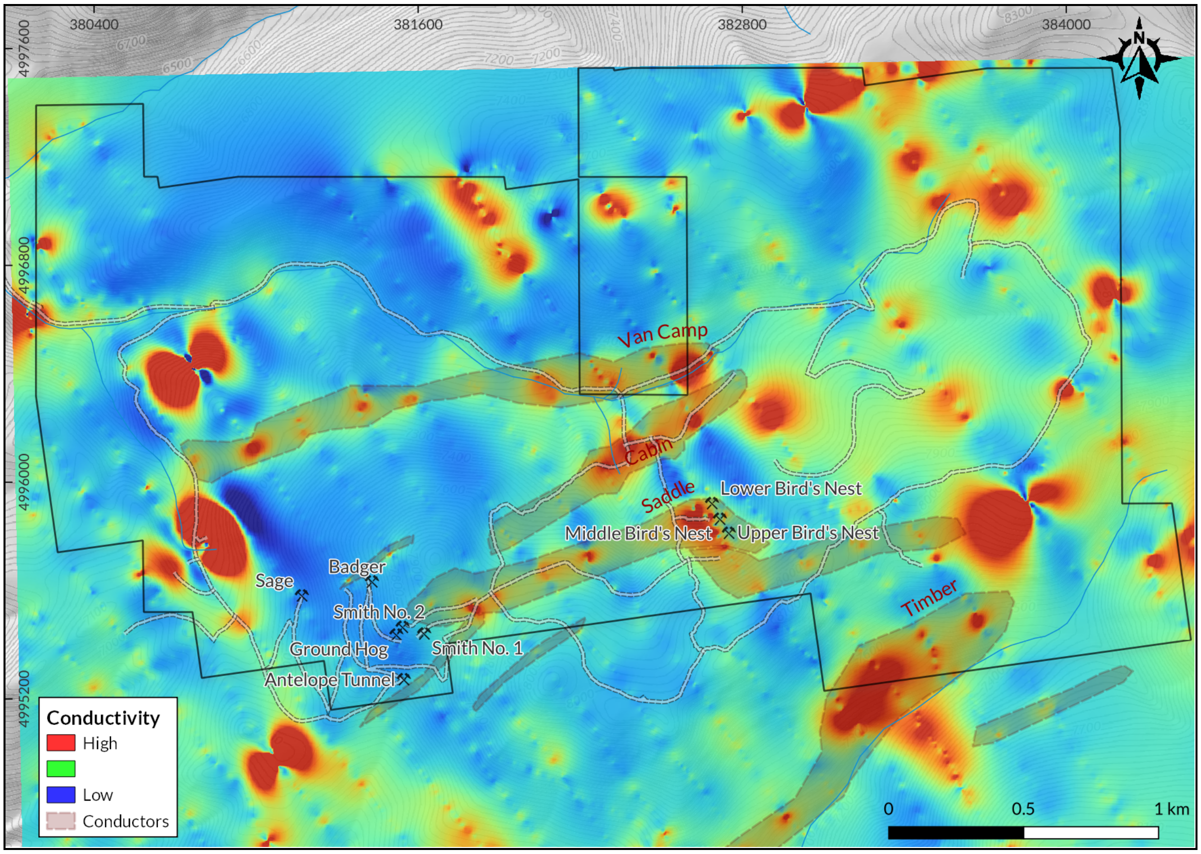


**Figure 40. GEM-2 Ski ground EM survey showing conductivity trends.**

## 9.7 Induced Polarization Geophysical Survey

KLM Geoscience, LLC was contracted to conduct an Induced Polarization and Resistivity (IP/RES) survey November 11 - 26, 2022. A five-person crew collected three 1,600 meter lines, totaling 4.8 line-kilometers (2.98 line-miles) (Figure 41). The three transects were chosen across the Project based on conductors previously identified by the GEM-2 Ski (Figure 40) to improve resolution of faults and conductivity at depth. Standard chargeability and conductivity values are provided for reference (Table 6, 7).

KLM ground crew utilized a 50- meter dipole-dipole array type with a four second time domain. At site, the crew used UTVs, trucks, and humanpower to transport equipment along the lines. Data was collected at the end of each day and provided to a remote analyst for QA/QC and plotting.

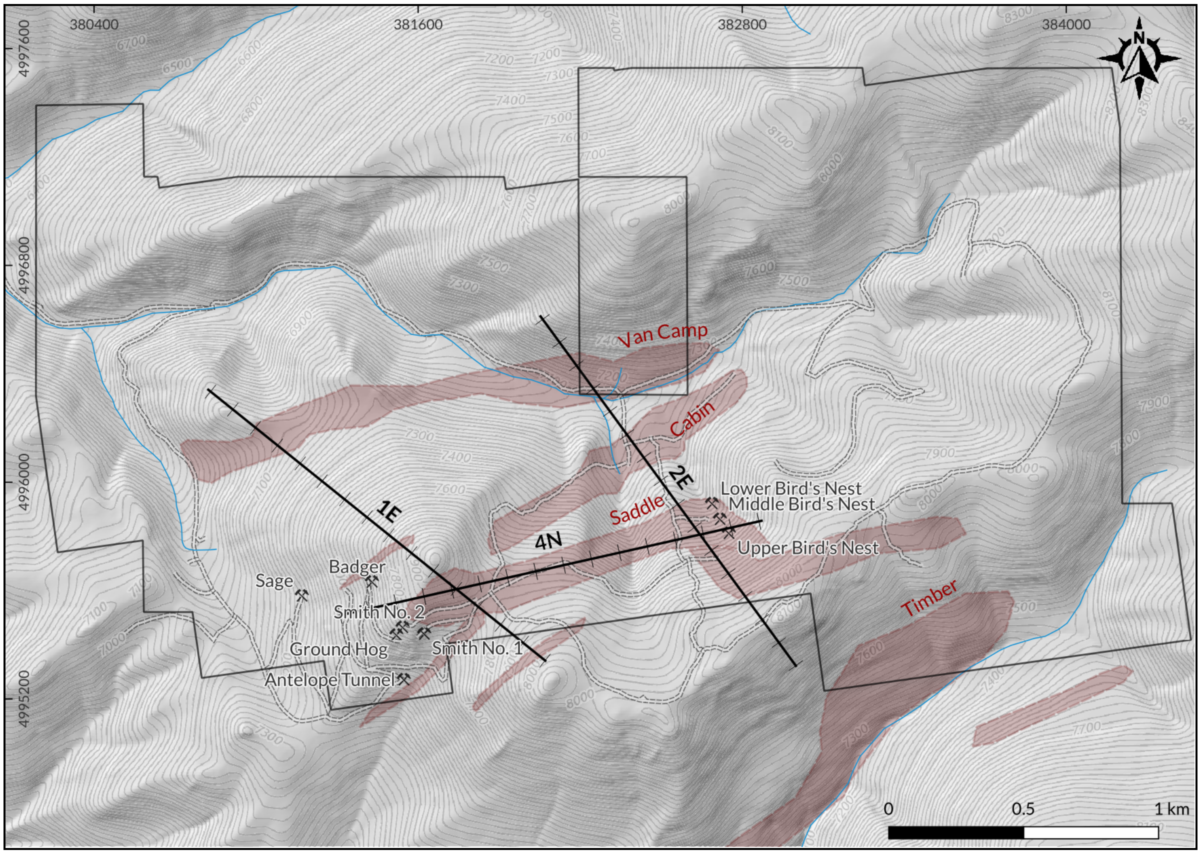


**Figure 41. IP survey completed November 2022: Lines 1E, 2E, and 4N. Conductivity trends are outlined in red.**

### 9.7.1 Results

The IP resistivity and chargeability results were provided by KLM Geoscience, LLC with consistent data scales across the three lines for comparative analyses (Figure 42, 43, and 44). Fewer lines were completed in 2022 than originally proposed due to weather conditions with cold temperatures and snow.

Several conductivity (resistivity) and chargeable anomalies were identified by the surveys and are displayed in the following figures. Conductivity refers to the ability of a material to conduct electricity. In the following figures, the color ramp is inverted on the resistivity scale, visually representing high conductivities in red (low resistivities) and low conductivities (high resistivities) in blue. Chargeability refers to the ability of a material to sustain or dissipate an induced charge. For the chargeability plots, highly-chargeable zones are red and lows are blue.

Zones containing both high conductivity and high chargeability are desirable (Table 6, Table 7), often suggesting the presence of graphite or interconnected sulphides and a high metal content. Zones with low conductivity and chargeability characteristics at Ruby likely indicate marble or barren gneiss or other non-mineralized metamorphic rock.

Care must be applied during interpretation, as other highly conductive materials such as water and clay may also exist and obscure the readings across a given area. Additionally, determination of mineral type on the basis of chargeability alone is not recommended, as the salinity of the surface or groundwater, contaminants within a rock, or a large surface area:volume ratio can all affect a material's chargeability measurements; artificially enhancing the chargeability (increased salinity) or decreasing chargeability (all other items), respectively. For example, water is highly conductive but has a low chargeability; therefore highly chargeable zones in the survey may have a suppressed signature if they are saturated with water, appearing less chargeable.

The following tables display common rock types and their ranges of conductivity and chargeability in a laboratory setting.

**Table 6. Chargeability values for common materials (Telford et al, 1976).**

| Material | Chargeability (ms) | Concentration |
|---|---|---|
| Graphite | 11.2 | 1% |
| Precambrian Gneiss | 6 - 30 | 1% |
| Quartzite | 5 - 12 | 1% |
| Sandstone | 3 - 12 | 1% |
| Ground Water | 0.0 | 1% |

**Table 7. Resistivity (conductivity) values for common materials (Telford et al, 1976).**

| Material | Resistivity (Ωm) | Conductivity (mS/m) |
|---|---|---|
| Graphite | 0.1 - 10 | 10,000 - 100 |
| Mafic Igneous | 2 - 15 | 500 - 67 |
| Ground Water | 2 - 100 | 500 - 10 |
| Felsic Igneous | 15 - 500 | 67 - 2 |
| Metamorphic, weathered | 10 - 2,000 | 100-.5 |
| Permafrost | 500 - 100,000+ | 2 - 0.01 |
| Metamorphic, unweathered | 1,000 - 100,000+ | 1 - 0.01 |
| Dolomite, Limestone | 1,000 - 100,000+ | 1 - 0.01 |
| Marble | ~ 1,000,000,000 | 0.000001 |
| Quartz | ~ 1x10^15 | 0 |

Additional limitations of IP/Res geophysics include the difficulty of the method to resolve areas underlying zones of high conductivity due to the preference of electricity to follow highly-conductive routes. Therefore, zones of apparently-low conductivity underlying zones of high conductivity should be considered suspect and interpreted carefully.

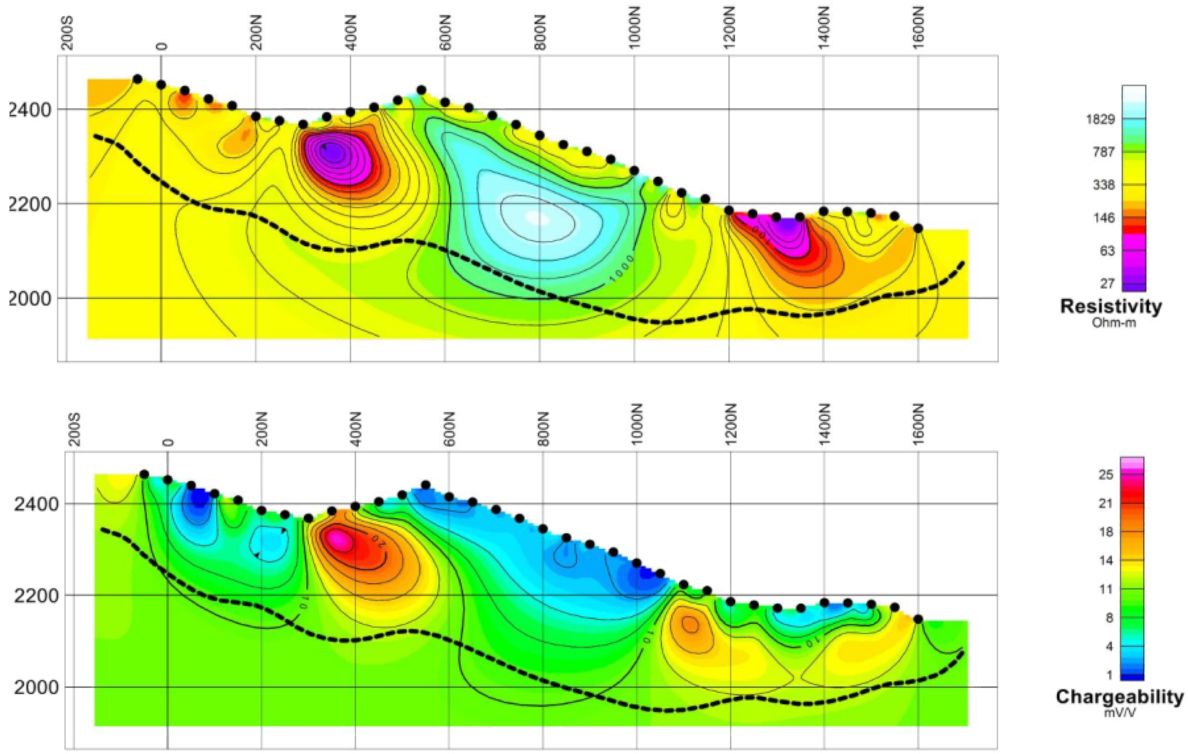


**Figure 42. Resistivity and chargeability for IP/RES Line 1E. The subsurface dashed black line on each model represents the depth of investigation; black dots represent electrode locations.**

Line 1E (Figure 42) displays a highly conductive and chargeable anomaly centered around station 375N, which sits immediately east of and underlying the Ground Hog area and a site of known graphite mineralization. The depth of the anomaly extends approximately 250 meters below the surface, is 250m wide, and dips to the north.

A second conductive anomaly is centered near the 1300N station, implies a north dip, and extends nearly 200m below surface. This anomaly is wrapped by chargeable high, from station 1100N to station 1600N, that may or may not be correlative to the conductive anomaly. This anomaly sits in an area without any historic working or known human disturbance; the apparent U-shape to this chargeable anomaly is likely related to a fault that crosses through the line at approximately 1500N, replicating the rocks and the signature. This anomaly should be investigated.

Two smaller conductive anomalies sit at the surface between 0 and 200N. Though they correlate with chargeable lows, these should be investigated in the field.

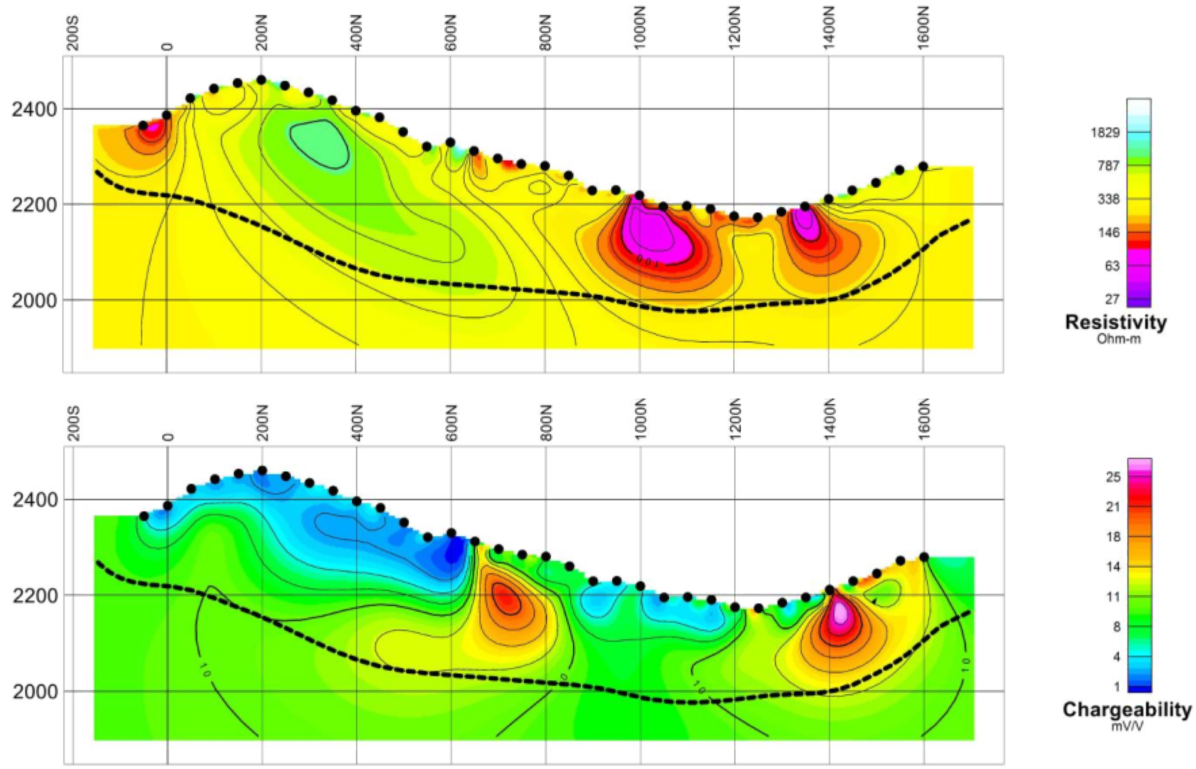


**Figure 43. Resistivity and chargeability for IP/RES Line 2E. The subsurface dashed black line on each model represents the depth of investigation; black dots represent electrode locations.**

Line 2 (Figure 43) displays an anomaly in both conductivity and chargeability centered approximately 1400N, which is located on the hillside to the north of the Smith Cabin and lies near the contact of the calc-mica schist and the marble. The anomaly extends approximately 200 meters deep, and could represent the occurrence of graphite.

To the south of this anomaly (left on the figure), rests a conductive anomaly extending from stations 900N to 1100N. This anomaly, however, correlates with a chargeable low. At surface, the anomaly sits within the Plagioclase Hornblende gneiss (with a low chargeability expected). The anomaly at 1000N also sits south of Van Camp creek in an area containing several springs which could be a source of conductivity.

Finally, Line 2 displays a chargeable anomaly centered at approximately 700N with a distinct pattern; thin at the surface with widening chargeability to nearly 200 meters and slight north-dip, extending to over 250m depth below the surface. Only a small conductivity anomaly overlies this feature at surface. This feature should be investigated.

A long, lowly-chargeable and lowly-conductive anomaly (blue) sits on the south (left) of this line, from stations 0 - 600N. This area coincides with garnet biotite quartz gneiss.

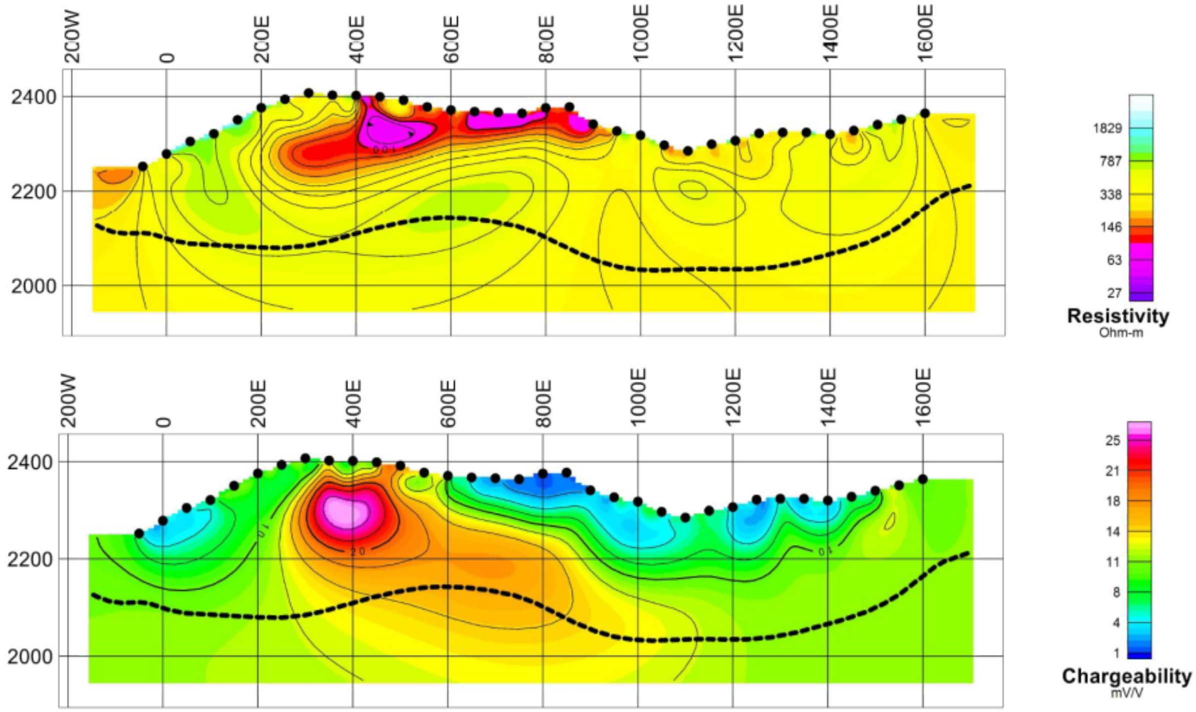


**Figure 44. Resistivity and chargeability for IP/RES Line 4N. The subsurface dashed black line on each model represents the depth of investigation; black dots represent electrode locations.**

Line 4N intersects line 1E and 2E at high angles, and runs approximately west to east across the central portion of the Project (Figure 44). This line exposes a tight, very highly conductive anomaly with a slight westward dip from stations 200E to 1000E. Somewhat coincident with this conductive anomaly is a very broad, wide chargeable anomaly from approximately 250E to 1000E, displaying an apparent east-dip. Though these anomalies are spatially coincident, large, and likely indicating the presence of graphite over a wide area; their differing dips imply a complex structural/mineralogical relationship that should be further explored.

IP geophysical methods struggle to collect measurements underlying zones of high conductivity due to the properties and limitations inherent in their physics. Therefore, it is possible that the conductivity anomaly in Line 4N extends to greater depth than indicated.

## 9.8 VLF/Aerial Geophysical Survey

A drone-based Very-Low Frequency Electromagnetic (UAV-VLF) Survey was initiated in the 2022 field season to define 1) broad-brush identification of additional graphite targets for expanded mineral-rights acquisition, and 2) detailed trends of graphite-bearing zones for identification of specific locations for drilling. However due to manufacturer malfunctions, the survey results are poor and the survey was not completed. The equipment is planned for repair in Q1 2023, and, if completed, will supplement the GEM-2 Ski EM and IP surveys.

# 10 Drilling

*Not applicable at the current stage of the project.*

# 11 Sample Preparation, Analyses, and Security

## 11.1 Sampling Methods

Soil samples are collected from a target depth of 46 centimetres (18 inches) below the ground surface or within the 'C' horizon where appropriate. Sample sites are chosen from pristine settings as much as possible, sourced no closer than 8 metres (25 feet) from active fluvial terrain and away from apparent human disturbance.

Once exposed, approximately 500 grams of sample is sieved through a 0.32 centimeters (0.13 inch) mesh retaining the fraction passing through. The resulting material is placed into specially-designed sample bags with unique sample identification and barcoded tags. This procedure allows the soils to dry and be secured for transport and assay. Sample records include depth, colour, location, sampler name, date, and remarks/site notes.

Rock samples are collected as either; grab, select, chip, float, or channel. Grab samples refer to randomised rocks selected from outcrops with no visual or intentional bias. Select samples are collected from prominent mineralized zones (e.g., mineralized outcrop or a dump pile). Float samples are collected from the ground either adjacent to the outcrops or without a known source.

All rock samples are placed into a sample bag with a unique, barcoded sample ID tag. Rock sample records include location, colour, sampler name, hand sample description, and any additional remarks.

Sample site locations were recorded using a Garmin GPS unit or smartphone-based app (Gaia or OnX maps). All three of these devices express an accuracy of +/- 2m horizontally and +/- 7m vertically, depending on the quality of the GPS signal and the number of available satellites overhead.

## 11.2 Sample Preparation and Analysis

Soil samples were submitted to ALS Global Labs in Reno, Nevada for analysis. At the laboratory, samples are entered into the internal system. Samples are prepared for analysis by drying at <60°C and sieved to -180 microns (-80 mesh). The analytical method used is inductively coupled plasma-mass spectrometry (ICP-MS) with Aqua Regia super trace analysis, and provides extremely low detection limits for the analysis of soils, useful for deep cover exploration. The rare earth elements and lead isotope concentrations are useful for determining pathfinders and fingerprinting hydrothermal fluid history.

Rock samples were submitted to ALS Global Labs in Twin Falls, Idaho for analysis. Samples are entered into the internal system and prepared by fine crushing to 70% passing 2mm (10 mesh). A complete characterization combines whole rock major element analysis by fusion decomposition followed by ICP-AES measurement, total carbon and sulfur by induction furnace/IR, trace elements by lithium borate fusion decomposition followed by acid dissolution and ICP-AES measurement, volatile trace elements by aqua regia digestion followed by ICP-MS measurement, and base metals by four acid digestion followed by ICP-MS measurement to super trace detection levels.

## 11.3 Sample Security

Samples were stored in access-controlled lodging, company vehicles, and/or Ethos Geological's office at 902 N. Wallace, Bozeman, Montana. Sample freight is by USPS, FedEx, or UPS courier to the lab assay destination.

# 12 DATA VERIFICATION

Standard protocol was used for the insertion of standards, blanks, and duplicates at ALS Global Labs for the soils and rock samples.

No verification work was completed for the soil pH analysis, as the results are qualitative and not used for assaying the target mineral.

A quality control program comprising the regular insertion of blank, duplicate and standard samples should be implemented for all future drilling, chip sampling, channel sampling and trenching.

# 13 MINERAL PROCESSING AND METALLURGICAL TESTING

*Not applicable at the current stage of the project.*

# 14 MINERAL RESOURCES ESTIMATE

*Not applicable at the current stage of the project.*

# 15 MINERAL RESERVE ESTIMATE

*Not applicable at the current stage of the project.*

# 16 MINING METHODS

*Not applicable at the current stage of the project.*

# 17 RECOVERY METHOD

*Not applicable at the current stage of the project.*

# 18 PROJECT INFRASTRUCTURE

# 19 MARKET STUDIES AND CONTRACTS

*Not applicable at the current stage of the project.*

# 20 ENVIRONMENTAL STUDIES, PERMITTING AND SOCIAL OR COMMUNITY IMPACT

## 20.1 Environmental Studies

*Not applicable at the current stage of the project*.

## 20.2 Permitting

### 20.2.1 Notice of Intent

A Notice of Intent (NOI) can be used to permit drilling and other exploration work less than five (5) acres of disturbance on BLM surface and subsurface lands. A NOI is planned for submission to the BLM within Q1 2023 for the drill sites on lands with BLM surface and subsurface rights.

### 20.2.2 Plan of Operations

An amendment to the Plan of Operations is currently in progress to submit to the BLM to cover the scope of all proposed exploration activities on the Project sitting on split-estate lands (private surface ownership with BLM subsurface mineral rights). These activities will include use of a drill, the creation of several new spur roads, and the maintenance on existing roads in preparation for a drilling program proposed for 2023.

# 21 CAPITAL AND OPERATING COSTS

Not applicable at the current stage of the project.

# 22 ECONOMIC ANALYSIS

Not applicable at the current stage of the project.

# 23 ADJACENT PROPERTIES

The Ruby Range and greater region hosts a significant concentration of talc mineralization and historic mining, and is one of the leading talc producing areas of the world. Graphite is a common accessory mineral within the talc, and because talc occurs within similar aged rocks and structures as the graphite system at Ruby, several of the adjacent properties are discussed below (Figure 45).

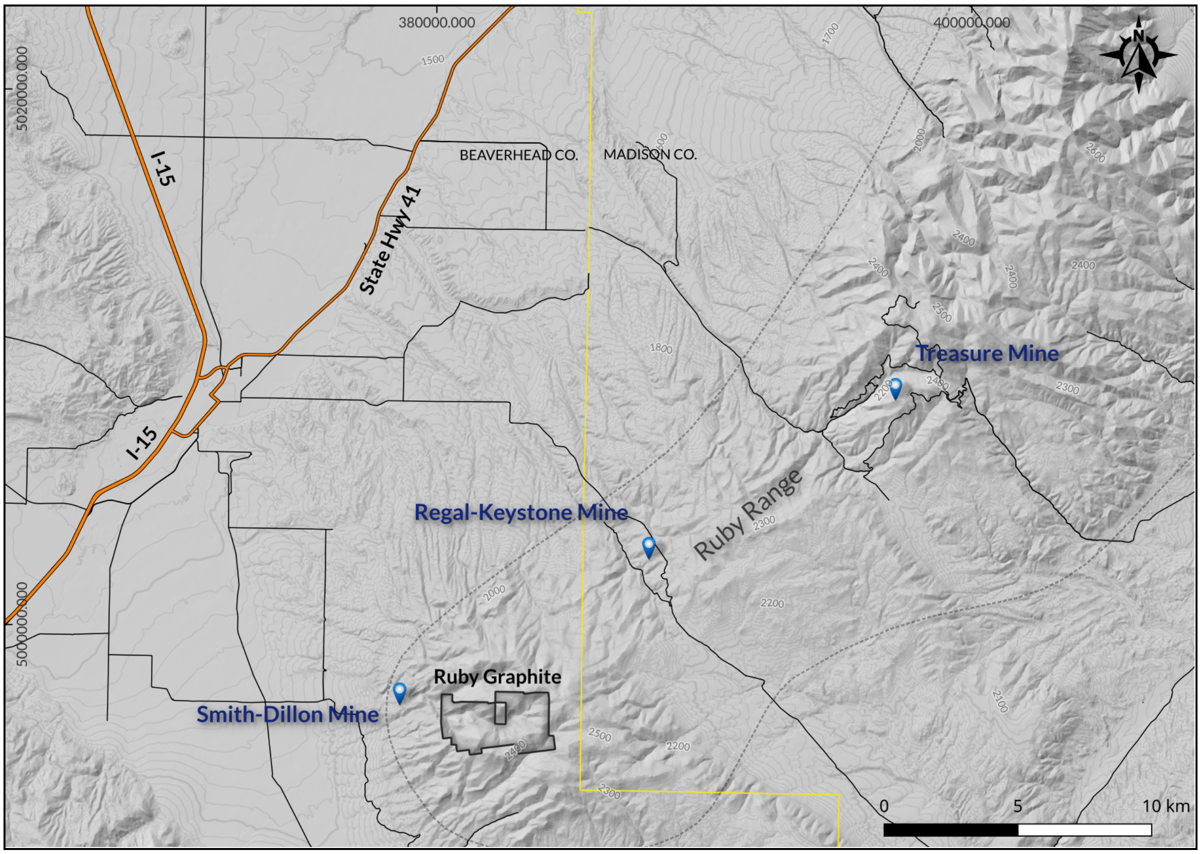


**Figure 45. Properties adjacent to the Ruby Graphite Project.**

Mineralization in the region is generally dominated by talc in a corridor that extends from west to east immediately north of the Project (Figure 46). Anderson (1987) and Childs (2017) suggest that talc formed in, or near, surficial hot springs followed by retrograde metamorphism of Archean rocks.

Metamorphism and preparation of the Archean rocks formed in three periods of recrystallization, characterized by: an initial, high pressure-temperature, amphibolite-grade assemblage; followed by retrograde alteration of the dolomite to form chlorite and serpentine; and finally, select retrograde talc formation from the remaining dolomite. Since talc is not observed to undergo recrystallization to form other phases, this suggests that talc formation is the last major event in the paragenetic history of the hosting marbles (Childs, 2017).

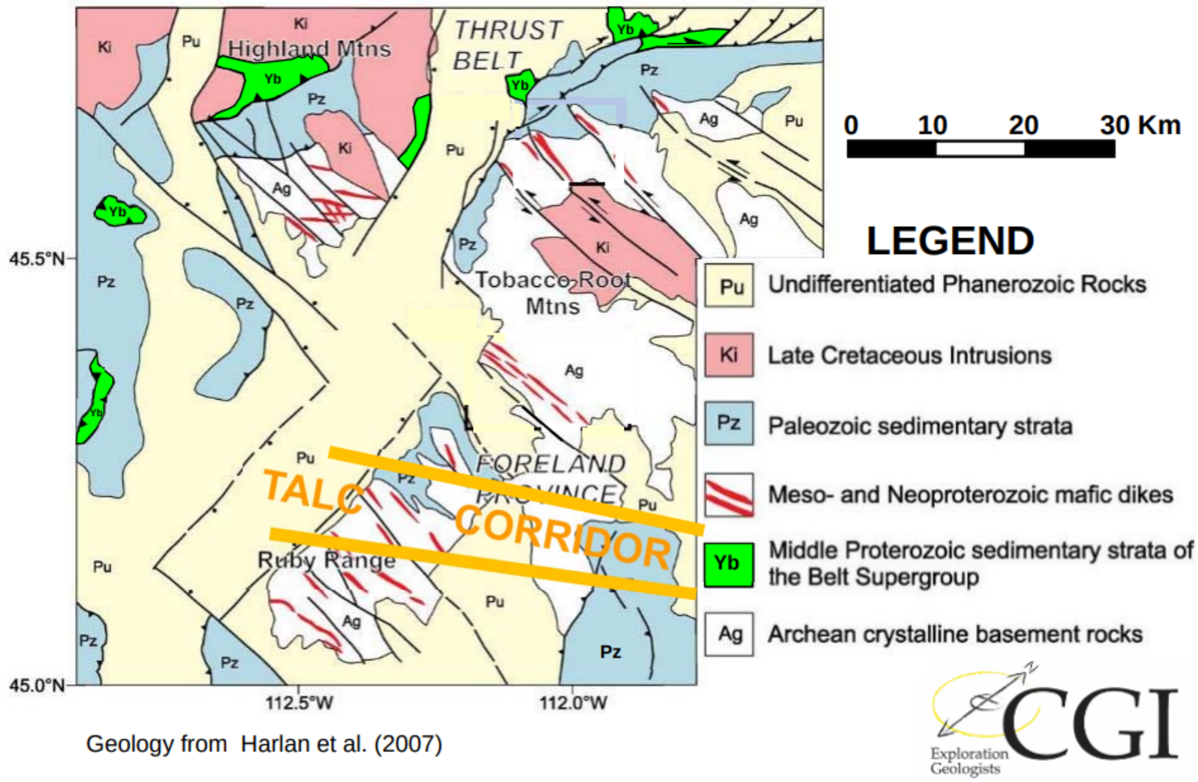


**Figure 46. Talc corridor extending from the northern Ruby Mountains to the southern Tobacco Root Mountains.**

## 23.1 Smith-Dillon Talc Mine

The Smith-Dillon talc mine is a past producer of talc-soapstone in a marble host in the Ruby Mountains in Beaverhead county. It is located in Van Camp Canyon, approximately 1.5 kilometers west of the Project. It was a small deposit owned by Pfizer, Inc. in which production began in 1945. The land is currently owned by Smith Unit, Inc. The deposit was first mined by underground workings, then later by an open pit. It is at a lower elevation than other talc mines in the area. North to northeast trending faults appear to control the talc mineralization. Mineralization is hosted in marble striking northeast and dipping 50 to 70 degrees northwest. (MRDS, 1994)

## 23.2 Regal-Keystone Talc Mine

The Regal-Keystone Talc mine is owned by Pfizer, Inc., on the Christensen Ranch Quadrangle, located 7 kilometers to the Northeast of the Project. This mine is within the 'Talc Corridor', a 65 mile east-west trending deep-seated structural zone containing abundant Archean marble layers (talc host) (Figure 47). It is proposed that the talc formed during development of a southern extension of the Proterozoic Belt Basin. It is suggested that there is a correlation with the northwest trending meso- and neoproterozoic mafic dikes in the region.

The deposit sits close to the core of a tightly refolded synform, the axis of which is oriented northeast with its nose to the southwest, and many faults cut the ore body. The mine area consists of an open-pit mine, approximately 150 meters long and 15 to 35 meters wide, and twenty trenches that range in length from about 15 to 50 meters (Berg, 1977).

The ore body is generally striking SW-NE and dipping 50 degrees to the NW. The underground workings have been inaccessible for many years, recent production has been from the open pit. The talcification process occurred by metasomatism, where dolomite is replaced by talc (Larson, 1991). Pegmatites or quartz-rich rocks are rare and outcrop in small amounts, and are located possibly within the marble. In a thin section analysis, the talc samples show trace graphite, apatite, and tourmaline.

The majority of the marble samples across the study area are dolomitic rather than calcitic. Trace graphite is in both talc and carbonate samples. James (1990) deduced that the origin of graphite results from the fluid mobilization of carbon of originally organic detritus which was later redeposited as graphite under elevated temperatures associated with regional metamorphism (Childs, 2017).

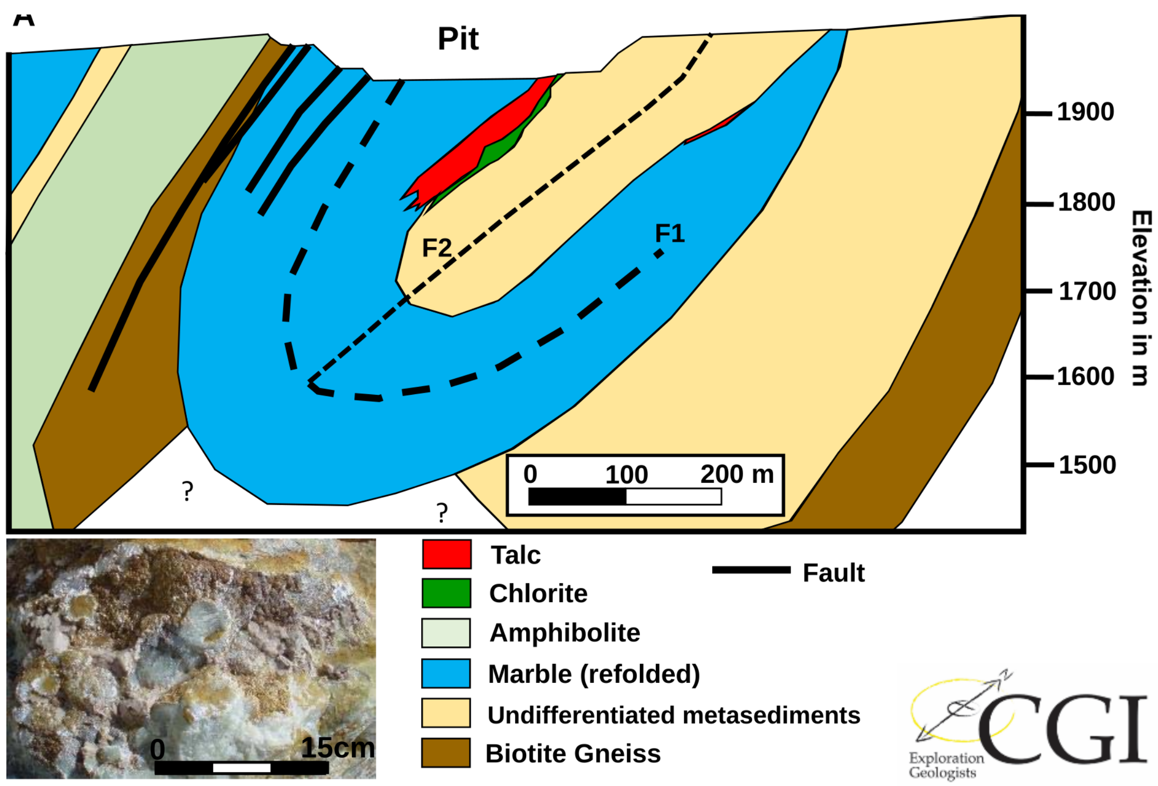


**Figure 47. Cross section through the Regal Talc Mine showing coincidence of marble, talc mineralization and fold axis (Childs, 2017).**

## 23.3 Treasure Mine

The Treasure Chest and Treasure State mines are jointly called the Treasure Mine. The mine is 25 km east of Dillon. Separating these two mines is the vertical, north striking Treasure Fault, which extends up to 245 meters wide. Talc and chlorite mineralization occurs where this structure intersects Pre-Belt marble units. The marble strikes east-west and dips 40 to 60 degrees north. Zones within the talc exhibit metamorphic textures indicating that they were derived from schist and gneiss, and completely replaced by talc (Childs, 2017).

# 24 Other Relevant Data and Information

*All relevant data is included within the Report.*

# 25 Interpretations and Conclusions

The geology, structure, and metamorphic history are important factors in the formation of graphite at Ruby. The region hosts an ideal setting for graphite mineralization due to the presence of marble as the source of carbon for graphite combined with the metamorphic events of the region. Having a widespread potential source for the graphite and widespread metamorphism in the area creates an ideal opportunity for the discovery of a significant size and grade of graphite.

## 25.1 Geologic Setting

### 25.1.1 Protolith

Determining the original setting of the host geology prior to metamorphism (rock 'protolith') is an important foundation for understanding the occurrence, distribution and exploration for graphite. A carbon-rich source that extends throughout the Project has the potential to support a significant volume of graphite.

The geologic units at Ruby are a metamorphic suite composed of gneisses, schists and marbles; Quartz Plagioclase K-Feldspar Gneiss gneiss alternating with less common K-Feldspar Plagioclase Quartz Gneiss, Garnet Biotite Quartz Gneiss, and Plagioclase Hornblende Gneiss outcrop across the Project. The alternating and gradational sequences in this area favor a sedimentary protolith, or sediments derived from a volcanic protolith, that may or may not also contain volcanic hypabyssal sills or dykes. Extension during the Archean would have been able to support a sedimentary and marine platform for the formation of carbonate-bearing sediments (Mogk et al., 1988).

The authors of this report suggest that the gneiss has a primarily sedimentary origin evident by the following field observations:

1) The grain sizes and distributions of quartz, feldspar, micas, amphiboles and pyroxene are similar with those expected from a parent sedimentary quartz sandstone, arkose sandstone, silt, shale and carbonate protolith;

2) Compositional variety within the gneiss, and the presence of intercalated schists and marbles, suggests formation within a dynamic environment such as a near-shore, carbon and organic-rich sedimentary setting;
3) Workers at adjacent talc deposits in the greater region also propose metasediments as a protolith for the gneiss (Childs, 2017); and
4) Rounded zircons are present within the gneisses (sample #D513560).

The intensity of silica in the varying gneiss units suggests that coarse to medium-grained sands were the dominant facies deposited in this part of the basin with layers of silt and mud. The quartz-rich gneisses are likely derived from an arkosic sand, and the mafic sequences are derived from silts and muds interbedded with the sands. The mica schists are derived from a shale, and the marbles derived from carbonate sediments or sourced directly from the marine waters during evaporation. Subsequent periods of regression or transgression form overlapping silt, sand and mud deposits with the carbonate stratigraphy.

The presence of marble indicates episodes of relatively calm, shallow marine paleoenvironment and evaporation at the time of deposition, which could also support the incorporation of organic material (microbial or algal mats) into the shales or carbon directly into the carbonaceous sediments themselves (marbles, schists).

### 25.1.2 Structure

These rocks were subjected to regional fold and thrust events creating a multi-event deformational history. Tight anticline-syncline pairs contribute to a complex geometry at the Project and regional scale. Structural mapping, IP/RES geophysics and soil sample assays suggest that one of the primary structural features is a tight, northwest-dipping and west-plunging antiform in the marble unit that coincides with the graphite horizon, extending eastward from the Ground Hog mine area through the Bird’s Nest showings.

Soil samples from the western-most soil line reflect repeating geochemistry. IDH values (with anomalies coincident with the marbles) also display an anomalous carbonate-like value along the proposed strike of the hingeline west of the Ground Hog area, overlying the proposed fold hinge of the carbonate at depth.

The resistivity values for IP line 4N support this observation, displaying a conductive body dipping to the west. On the same line, however, a large chargeable anomaly dips to the east, and further work is required to determine the conductivity/chargeability/antiformal fold relationship. As discussed prior, multiple episodes of deformation could present more complicated fold orientations than what are currently understood.

Combined, the coincidence of high conductivity anomalies with to the central marble unit, the proposed west-striking antiformal fold, the proximity of graphite mineralization with the marble and adjacent gneiss units, and the alignment of the graphite showings with the antiform itself all imply that the fold itself and associated faults and fractures are sites of transport and deposition for graphite mineralization.

### 25.1.3 Metamorphism

Multiple episodes of metamorphism affected the rocks comprising the Ruby Range and greater region. These events include a preliminary metamorphic event in the early Paleoproterozoic during subduction, crustal shortening and the deformation related to the Trans-Montana fold-thrust belt (1.81-1.76 Ga, Gifford 2020); and a later event in the late Cretaceous related to the Laramide and Sevier orogenies (~65 Ma, Wells et al., 2012).

Graphite mineralization at Ruby likely occurred during the first metamorphic event in the early Paleoproterozoic. Metamorphic assemblages containing graphite, almandine garnet, and secondary K-feldspar require pressures over 4 kbar and over 750°C. Regional metamorphic pressures up to 8 kbar and over 800°C have been well documented during the early Paleoproterozoic from 1.81 - 1.76 Ga (Gifford, 2020). At Ruby, sample #D513578 displays intergrowths of graphite with secondary K-feldspar (Figure 20), and sample #D513577 holds graphite (opaques in thin section) interstitial to and as inclusion within garnet (Figure 18).

The interpretation of graphite formation prior to the Cretaceous is further supported by the carbon isotope analysis of graphite from the Ruby Range (Luque et al., 2012). Values from the Ruby Graphite Project measured ~ -8.6 to -5.8 $C^{13}$ (versus -25 $C^{13}$ for primary graphite), implying that the graphite at Ruby underwent metamorphism and alteration after formation to create heavier carbon isotope signatures through the increased removal of $CH_4$ (Luque et al., 2012).

The diabase dikes that cut the gneisses, marbles and schists are Ruby at high angles were possibly emplaced as early as the Mesoproterozoic (Childs, 2017). The mineral tremolite is a major constituent within both the marble units and the diabase dikes, and secondary talc also exists in the diabase dikes, suggesting a second metamorphic event the Ruby rocks between 400 and 600°C and a range of mild to moderate pressures. A lower-grade metamorphic event is documented by Wells et al (2012) that affected the Ruby area in the Cretaceous during the Laramide and Sevier orogenies.

Therefore the graphite likely formed alongside secondary K-feldspar and garnet during high-grade metamorphism in the early Paleoproterozoic, followed by intrusion of the diabase dykes, then alteration of select minerals within the marble and diabase dikes to tremolite during another metamorphic event in the Cretaceous. Finally, the presence of sustained high temperatures due to the intrusion of the diabase dikes and a second metamorphic episode was likely to have increased the graphite flake size (Ma, et al., 2021).

### 25.1.4 Pegmatites

Several pegmatites outcrop across the Ruby Graphite Project; their relationship with the other rock types and graphite mineralization are unclear. The pegmatites are isolated but host a similar strike as the other geology and have not been observed cross-cutting stratigraphy, a relationship suggesting that they formed at the same time or are syngenetic with the compression that formed the surrounding rocks.

The Authors suggest that the pegmatites formed through anatexis (the process of melting or partial melting of pre-existing solid rocks) during metamorphism in the early Paleoproterozoic at pressures and temperatures capable of mobilizing quartz and feldspars into isolated small horizons through partial melting of the host rock. Therefore, the anatectic pegmatites and graphite likely formed during the same metamorphic event.

## 25.3 Exploration Potential

Historic information and field observations inform that graphite at Ruby occurs near the lithologic contacts of gneiss with marble along fold hinges or parallel structures. These zones are further supported by data derived from the GEM-2 Ski EM and IP Surveys. The grade from historic workings has been estimated to range from 4-29% Cg with averages ranging from 8-16% Cg from underground workings (Giulio, 1945), encountered as flaky plates, acicular, and clotty masses within veins, and disseminated interstitial to crystals within the gneiss.

Multiple exploration targets have been identified across the Project. From north to south, the targets of interest include: Van Camp, Cabin, Saddle, and Timber trends.

The Saddle trend is the primary exploration target, coinciding with the plunging antiform in the marbles and a likely concentrating mechanism for graphite. The west plunging nose of the proposed antiform was previously mined at Ground Hog, and recent exploration suggests that this mineralization trend extends to the east.

The length of the Saddle trend is significant, extending for over one kilometer laterally from its surface expressions at Ground Hog to Bird's Nest The depth of the Saddle trend has yet been tested, however, a very large (250m x 250m) chargeable and conductivity anomaly sits below surface at IP Lines 1 and 4 (Figure 42) and is the primary drill target..

## 25.4 Conclusions

The following is a synopsis of the genesis of the rocks and graphite mineralization at Ruby:

1. Carbon-rich sediments formed within a near-shore environment ~2.6 Ga.
2. Burial, accretion and upper-amphibolite to granulite-facies metamorphism of the rocks occurred ~1.8 Ga, during which:
    a. Pressures and temperatures in rocks of the Ruby Range reached ~ 800°C, and up to nine (9) kbar;
    b. Fold hinges and structural dilation were created during compression event,
    c. Graphite likely formed during devolatilization of the carbonate units,
    d. Graphite may locally concentrate within structural conduits and other dilation zones, and
    e. Pegmatites may have formed during metasomatism and dewatering of the sedimentary protolith.
3. Retrograde metamorphism, cooling and extension of the rocks occurred ~ 1.76-1.71 Ga, during which:
    a. Many of the talc deposits formed along extensional faults in the greater region, and
    b. Secondary tremolite alteration may have formed within the host rocks.
4. Post 1.71 Ga, during the Proterozoic:

   a. Extension of the Ruby Range rocks in a NE-SW direction created NW-striking structures,
   b. Sediments collected during the formation of the Belt Supergroup, and
   c. Diabase dikes intruded many of the Proterozoic rocks.
5. Compression, folding and metamorphism during the Cretaceous subjected the rocks to a second period of alteration, reaching a peak of approximately 6kbar and 600°C.
   a. This metamorphic event modified the graphite's carbon isotope signature, making it heavier, and
   b. May have upgraded the flake size of graphite at Ruby.

Ethos Geological concludes that the Ruby Graphite Project holds significant potential for discovery and exploration success, evident by the following;

- History of mining exposes near-surface lodes containing graphite within veins and seams;
- Identification of trends within geophysical surveys coincident with geological, structural, and/or known graphite rich horizons;
- The primary target (Saddle trend) extends for approximately 1 km along strike NE-SW from the Ground Hog to Bird's Nest claims, overlying a large, 250m x 250m conductive and chargeable anomaly in IP geophysics;
- Additional, parallel trends sit to the north, south, and east of Saddle trend (Van Camp, Cabin, and Timber Creek);
- The carbon-bearing sedimentary protolith is likely extensive, creating significant opportunity for discovery; and
- Year-round access.

# 26 RECOMMENDED FUTURE WORK

Ethos Geological recommends several considerations for future work:

- Carbon isotope analysis of graphite-bearing rocks and marbles;
- Additional IP geophysics;
- High resolution GEM-2 Ski EM surveys targeting definition of newly-identified trends;
- UAV-VLF geophysics survey targeting structures;
- District-scale VTEM survey to explore for additional graphite-bearing horizons;
- 3,500 meters of exploration drilling;
- Outcrop and channel sampling;
- Infill soil sampling; and
- Detailed structural mapping.

## 26.1 Carbon Isotope Analysis

The carbon isotopic weight is useful to help determine the source of the carbon. Biogenic origin of graphite has values -10 % to -35% $\delta C^{13}$, marine sediments 0% +/- 2% $\delta C^{13}$ and magmatic carbon -5%

+/- 2% $\delta C^{13}$ (Ma, 2021). The Authors suggest sampling the graphite in order to further understand the graphite genesis. Graphite becomes isotopically heavier as metamorphism progresses and graphite in high-grade metamorphic rocks becomes heavier than its low-grade counterparts (e.g. Hoefs and Frey, 1976, Wada et al., 1994).

The Authors recommend both: 1) carbon isotope analysis on graphite samples to determine the degree of metamorphism and carbon source (eg. microbial mats, carbonates, primary magma); and 2) carbon isotope analysis of the marble itself, to compare with the graphite samples for similarity of protolith.

## 26.2 Induced Polarization Geophysical Survey

The Authors recommend four additional IP survey lines to improve resolution of the 2022 survey; extension of lines 4N and 2E, adding a northwest-southeast line parallel to line 2E, and adding one line trending north-south to cross the conductors and lines 2E and 4N. The additional IP lines total approximately eight (8) line km (Figure 48).

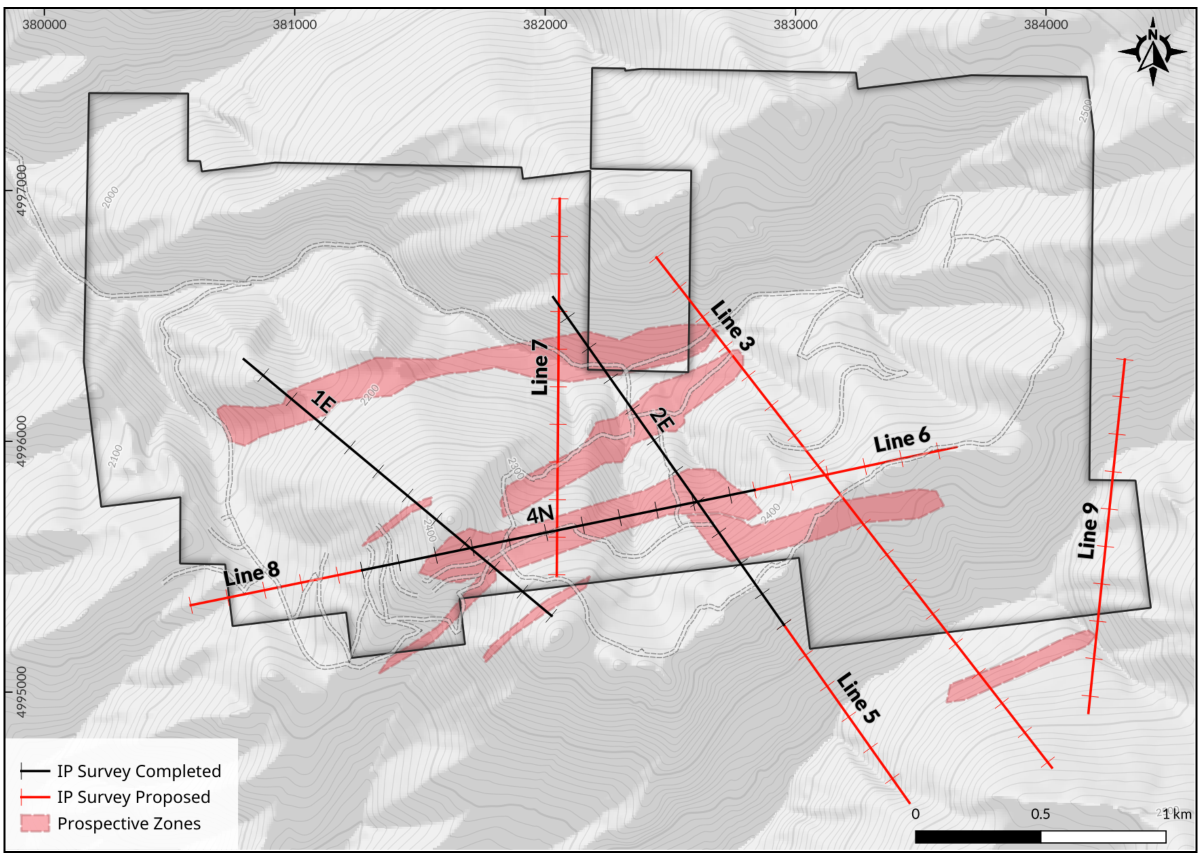


**Figure 48. Proposed additional IP lines (red).**

## 26.3 GEM-2 Ski Ground Electromagnetic Survey

The Authors recommend targeted, higher-resolution GEM-2 Ski surveys along the newly-identified exploration targets (Saddle trends - Figure 41, and around the drill sites - Figure 49) to better determine the continuity of the conductors in these areas in preparation for the drilling campaign. This effort is expected to take approximately two weeks with two field workers, followed by a one to two weeks for data interpretation and mapping program.

## 26.4 UAV-VLF Geophysics Survey

The Authors propose a drone-based Very-Low Frequency Electromagnetic (UAV-VLF) survey to supplement the completed GEM-2 Ski EM and IP surveys and focus on the delineation of structures that may be important conduits for the transport or trap for graphite.

The combination of aerial and progressively-deeper ground-based geophysical surveys will provide broad-brush identification of additional graphite targets for expanded mineral-rights acquisition, and detailed trends of graphite-bearing zones, providing a strategic method for identifying all graphite resources within the Project.

## 26.5 VTEM Survey

The Authors propose a helicopter-born VTEM (Variable Time-Domain EM) survey to further complement other conductivity surveys. VTEM generates currents that diffuse into the earth and take the path of least resistance. Conductive material absorbs the currents and releases a secondary field that the monitor measures. A strong conductor absorbs and releases more or all of the VTEM signal, and a weak conductor absorbs and releases some or none of the VTEM signal. As previously discussed, graphite is a highly conductive material and combining multiple survey methods can assist to delineate the graphite resources within the Project.

## 26.6 Drilling

The Authors recommend a 3,500-meter NQ-core drill program comprising approximately 24 holes at an average depth of 130 meters from 12-15 pads. 26 drill sites are proposed in Figure 49 to target promising geologic horizons and geophysical conductors at surface and depth. A track-mounted drill is recommended to minimize disturbance and reclamation with sumps at each site to host temporary cutting fluids. Permitting for the recommended drilling is underway at the time of this Report.

The drill sites are labeled both by order of importance and by their land ownership classification. The latter classification is useful because several subsets of permits are required based on surface designation, including: BLM- NOI on unpatented claims on BLM land, PL- private mining Lease on patented claims, SE- split estate SRHA lands requiring a PoO (Table 8).

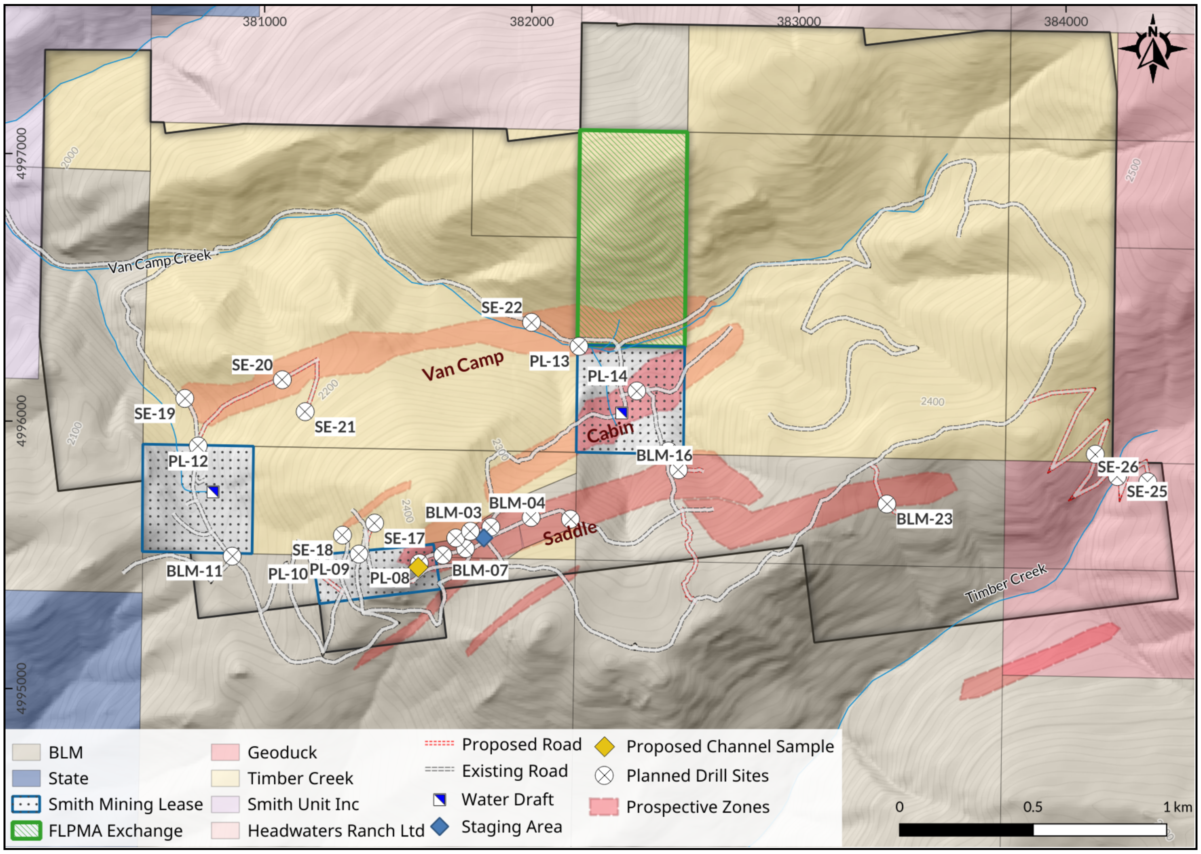


**Figure 49. Map of proposed drill sites for 2023.**

**Table 8. List of proposed drill sites.**

| Drill Site | Easting | Northing | Rationale |
|---|---|---|---|
| BLM-01 | 381715 | 4995563 | Along Saddle Trend; IP and GEM-2 Ski anomaly |
| BLM-02 | 381770 | 4995588 | Along Saddle Trend; IP and GEM-2 Ski anomaly |
| BLM-03 | 381847 | 4995603 | Along Saddle Trend; IP and GEM-2 Ski anomaly |
| BLM-04 | 381998 | 4995639 | Along Saddle Trend; IP and GEM-2 Ski anomaly |
| BLM-05 | 382145 | 4995633 | Along Saddle Trend; IP and GEM-2 Ski anomaly |
| BLM-06 | 381752 | 4995523 | Along Saddle Trend; IP and GEM-2 Ski anomaly |
| BLM-07 | 381667 | 4995499 | Along Saddle Trend; IP and GEM-2 Ski anomaly |
| PL-08 | 381579 | 4995469 | Western extent of Saddle trend, near historic workings |
| PL-09 | 381353 | 4995503 | Near historic workings |
| PL-10 | 381196 | 4995485 | Near historic workings |
| BLM-11 | 380878 | 4995495 | GEM-2 Ski anomaly |

| | | | |
|---|---|---|---|
| PL-12 | 380751 | 4995907 | Western extent of Van Camp trend; on road and Smith Lease |
| PL-13 | 382177 | 4996279 | Along Van Camp trend; IP and GEM-2 Ski anomaly |
| PL-14 | 382393 | 4996112 | Along Cabin trend; GEM-2 Ski and IP conductivity anomaly |
| PL-15 | 382511 | 4995888 | Near historic workings; on road and Smith Lease; IP anomaly |
| BLM-16 | 382549 | 4995817 | Near historic workings; GEM-2 Ski anomaly |
| SE-17 | 381411 | 4995618 | Near historic workings |
| SE-18 | 381291 | 4995573 | Near historic workings |
| SE-19 | 380701 | 4996084 | Western extent of Van Camp trend; GEM-2 Ski anomaly |
| SE-20 | 381066 | 4996154 | Along Van Camp trend; IP conductivity anomaly |
| SE-21 | 381151 | 4996035 | Along Van Camp trend; IP chargeability anomaly |
| SE-22 | 381999 | 4996369 | Along Van Camp trend; IP and GEM-2 SKi anomaly |
| BLM-23 | 383329 | 4995689 | Near historic workings |
| SE-24 | 384110 | 4995876 | New graphite discovery area; along marble-gneiss contact |
| SE-25 | 384192 | 4995792 | New graphite discovery area; along marble-gneiss contact |
| SE-26 | 384306 | 4995773 | New graphite discovery area |

## 26.7 Channel Sampling

The Authors recommend channel sampling of historic mineralized exposures to derive a detailed understanding of graphite concentration and quality over long, exposed intervals (Figure 49). Of particular interest are exposures at the Ground Hog and Bird's Nest workings. A portable diamond saw will be utilized thereby eliminating the need for heavy equipment or significant disturbance.

## 26.8 Soil Sampling

Several additional soil lines cutting across the Project will aid interpretation of the conductive anomalies along the Van Camp trend, provide more information about the extension of the carbonates beyond the current areas of investigation, and further delineate the fold hinge along the Saddle trend. The 288 proposed additional soil samples should have samples spaced every 25 meters (Figure 50). The two western lines will recognize displacement across the fault, the central line can pick up changes in trends between the 2022 soil lines, and the eastern line will inform about marble extension and mineralization to the east.

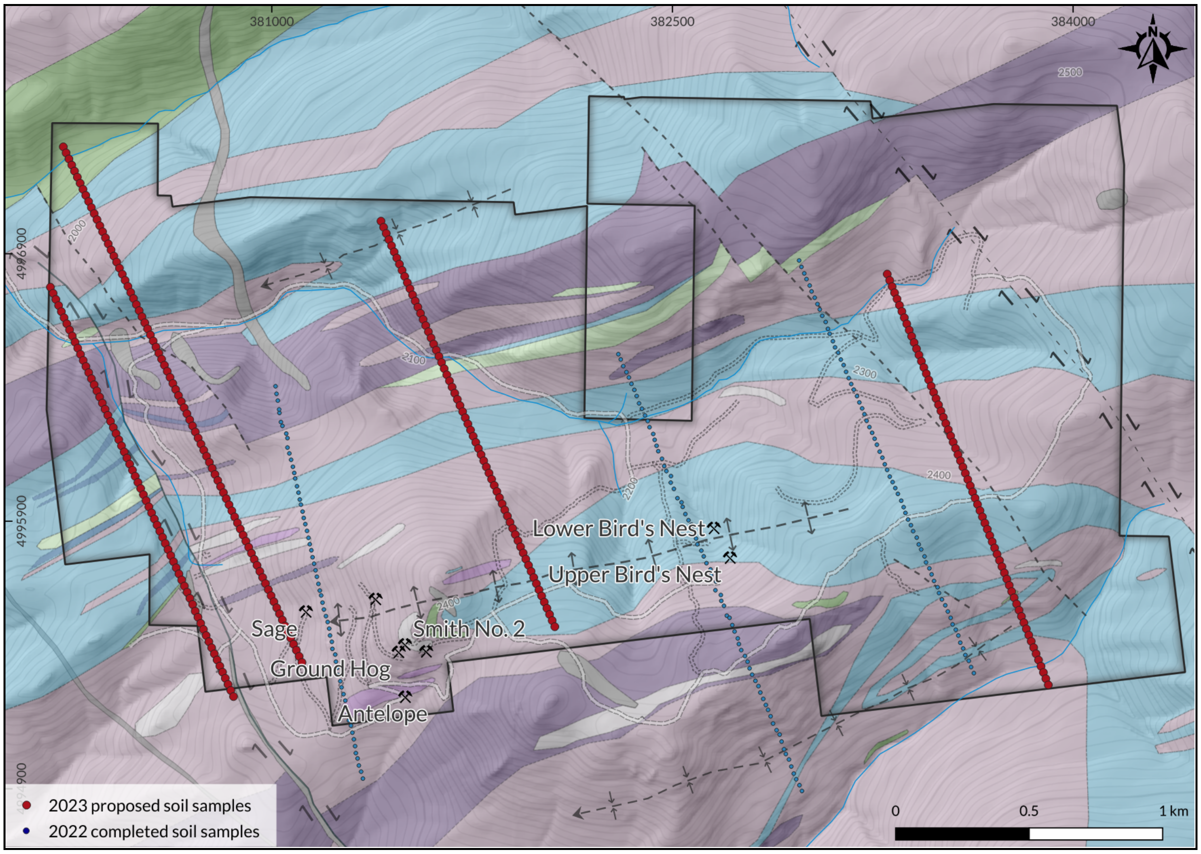


**Figure 50. Proposed soil sites to be sampled in 2023 (red), with existing soil lines (blue).**

## 26.9 Field Mapping

Additional 2023 field mapping is proposed, including:

- Detailed structural mapping to better understand the complex folding and faulting;
- Spatial variability of garnets within gneisses to map the metamorphic gradient; and
- Rock sampling to determine variation within the marble.

# 27 EXPLORATION BUDGET

Table 9 displays the recommended budget for continued exploration at the Ruby Graphite Project. The values are summaries of costs and expenses from experience, current market rates and estimates proposed by the Author(s). In total, a combined geophysics, drilling and field sampling campaign is estimated to cost, with contingency, approximately $2M for a 3,500m of drill core and approximately three (3) months of fieldwork.

**Table 9. Proposed exploration budget for the 2023 calendar year.**

| Year | 2023 |
|---|---|
| Existing Claims | 96 |
| IP Line km | 6.5 |
| Soil Samples | 700 |
| Drill Meters | 3,500 |
| Total Estimate | $1,975,000 |

| Main activity | Sub-activities | 2023 | |
|---|---|---|---|
| Geochemistry | Drill Core Assay | 54,945 | |
| | Rock / Soil Assay | 31,500 | |
| | Other | 53,000 | |
| | *Subtotal Geochemistry* | **139,445** | *7%* |
| Drilling | Diamond Drilling | 1,026,609 | |
| | Mobilization | 6,000 | |
| | Supplies | 102,661 | |
| | *Subtotal Drilling* | **1,135,270** | *58%* |
| Geophysics | Aerial Photo / DEM | 5,000 | |
| | VTEM | 250,000 | |
| | IP / RES | 67,600 | |
| | Drone VLF | 20,000 | |
| | Gem-Ski | 15,000 | |
| | *Subtotal Geophysics* | **357,600** | *18%* |
| Personnel | Geological Personnel | 103,780 | |
| | Field Personnel | 110,670 | |
| | Travel - Non Field Work | 0 | |
| | *Subtotal Personnel* | **214,450** | *11%* |
| Reports & Permitting | Technical Reporting | 25,000 | |
| | Drill Permitting | 5,000 | |
| | Bonds | 45,000 | |
| | *Subtotal Report/Permitting* | **75,200** | *4%* |
| Project Support | Consumables | 20,600 | |
| | Field Supplies | 9,401 | |
| | Field Support | 1,100 | |
| | Freight | 4,000 | |
| | Fuel | 3,000 | |
| | Automobile | 6,120 | |
| | Communication | 3,000 | |
| | *Subtotal Support* | **47,221** | *2%* |
| | *Total* | **$ 1,974,187** | |

# 28 References

Anderson, D., 1987, Timing and Mechanism of Formation of Selected Talc Deposits in the Ruby Range, Southwestern Montana, M.Sc. Thesis, Montana State University Department of Earth Sciences.

Armstrong, F. and Full, R., 1950, Geologic Maps of Crystal Graphite Mine, Beaverhead County, Montana. U.S. Geological Survey Open-File Report 50-26.

Bastin, E., 1912, The Graphite Deposits of Ceylon: A Review of Present Knowledge with a Description of a Similar Graphite Deposit Near Dillon, Montana, Economic Geology: The American Geologist, v. 7, no. 5.

Bell, G. and Van Den Bussche, B., 2018, Competent Persons Technical Report on the Ruby Graphite Project Early-Stage Exploration Target, Ruby Graphite Holdings, LLC., Senergy Engineering.

Bennett, A., 2022, Recent Graphite Price Weakness Masks Phenomenal Demand Growth, Fastmarkets.

Cameron, E., Weis, P., 1960, Strategic Graphite – A Survey: Contributions to Economic Geology, Geological Survey Bulletin 1082-E. U.S. Geological Survey.

Berg, R., 1977, Regal Mine. Mineral Resource Data System, U.S. Geological Survey.

Childs, J. 2017, World Class Talc Deposits of Southwestern Montana, Mine Design Operations and Closure Conference.

Dahl, P.S., 1979, Comparative geothermometry based on major-element and oxygen isotope distributions in Precambrian metamorphic rocks from southwestern Montana: American Mineralogist, v. 64, no. 11–12, p. 1280–1293.

Ford, R., 1954, Occurrence and Origin of the Graphite Deposits Near Dillon, Montana, Economic Geology: Society of Economic Geologists, Inc., v. 49, p. 31-43.

Goss, B., 2013, Graphite Corp: Form 10-K Annual Report for the Period Ending 12/31/12, U.S. Securities and Exchange Commission.

Gifford, J.N., Malone, S.J., and Mueller, P.A., 2020. The Medicine Hat Block and the Early Paleoproterozoic Assembly of Western Laurentia. Geosciences (Switzerland) v 10, no 7, 21pp.

Giulio, S., 1945, Report of Supervising Engineer, Mining Section, Reconstruction Finance Corporation. MBMG Mining Archives Database.

Heinrich, E., 1960, Pre-Beltian Geology of the Cherry Creek and Ruby Mountains Areas, Southwestern, Montana, Part 2 - Geology of the Ruby Mountains, Montana Bureau of Mines and Geology, Memoir No. 38.

James, H. and Hedge, C., 1980, Age of the basement rocks of southwest Montana, Geological Society of America Bulletin, vol. 91, no. 1, p. 11-15.

Larson, A., 1991, Talc Formation in the Regal-Keystone Mine of the Ruby Range, Dillon, Montana: B.A. Thesis, Smith College Geology Department, p. 57.

Luque, F., Crespo-Feo, E., Barrenechea, J., and Ortega, L., 2012, Carbon isotopes of graphite: Implications on fluid history, Geoscience Frontiers, vol. 3(2), p. 197-207.

Luque, F.J., Huizenga, J-M., Crespo-Feo, E., Wada, H., Ortega, L., and Barrenchea, J.F., 2014, Vein Graphite Deposits: Geological Settings, Origin, and Economic Significance, 2013, Miner Deposita, v. 49, p. 261-277.

Ma, Y., Huang, Y., and Liu, L., 2021, Genesis of the Tianping flake graphite deposit at the western margin of Yangtze Block, SW China, Ore Geology Reviews, v. 139.

Mogk, D.W., Henry, D.J. and Ernst, W.G., 1988, Metamorphic petrology of the northern Archean Wyoming province, southwestern Montana: Evidence for Archean collisional tectonics, Metamorphism and crustal evolution of the western United States, Prentice Hall, p. 362-382.

Mitchell, C.J., 1993, Flake Graphite: Industrial Mineral Laboratory Manual, British Geological Survey.

Metamorphism and crustal evolution in the western United States: New York, Prentice-Hall, p. 363-382.

Mueller, P.A., Heatherington, A.L., Kelly, D.M., Wooden, J.L., and Mogk, D.W., 2002, Paleoproterozoic crust within the Great Falls tectonic zone—Implications for the assembly of southern Laurentia: Geology, v. 30, p. 127–130.

Okuma, A., 1971, Structure of the Southwestern Ruby Range near Dillon, Montana: Unpublished Ph.D. Dissertation, Pennsylvania State University, p. 122.

Payne, J., 2023, Petrographic Report 220529 for Ethos Geological, Vancouver Petrographics Ltd.

Perry, E., 1948, Talc, Graphite, Vermiculite and Asbestos Deposits in Montana. Montana Bureau of Mines and Geology, Butte, Montana. Memoir No. 27. pp. 44.

Rumble, D., Duke, E., and Hoering, T., 1986, Hydrothermal Graphite in New Hampshire: Evidence of Carbon Mobility During Regional Metamorphism, Geology 1986, vol. 14, p. 452-455.

Ruppel, E., O'Neill, J., and Lopez, D. 1993, Geologic Map of the Dillon 1 x 2 Quadrangle, Idaho and Montana. U. S. Geological Survey Miscellaneous Investigations Series, Map I-1803-H, scale 1:250,000, 1 sheet.

Schmidt, C.J., Smedes, H.J., and O'Neill, J.M., 1990, Syncompressional emplacement of the Boulder and Tobacco Root batholiths (Montana-U.S.A.) by pull-apart along old fault zones: United Kingdom, University of Liverpool, Geological Journal, v. 25, p. 305–318.

Sinkler, H., 1942, Geology and Ore Deposits of the Dillon Nickel Prospect, Southwestern Montana, Economic Geology, v. 37, p. 136-152.

Smith, L., Hill, C., and Reiten, J., 2020, Quaternary and Late Tertiary of Montana: Climate, Flaciation, Stratigraphic, and Vertebrate Fossils, MBMG Special Publication 122: Geology of Montana, vol. 1: Geologic History, 64 p.

Smith, P., 1900, Declaratory Statement of Lode Mining Claim. Beaverhead County Recorder, bk 46, pp. 465.

Smith, R., 1949, Mine Summary Report for Montana Graphite Inc. Beaverhead County Recorder, Dillon, Montana.

Touzain, P., Balasooriya, N., Bandaranayake, K. and Descolas-Gros, C., 2010, Vein Graphite from the Bogala and Kahatagaha–Kolongaha Mines, Sri Lanka: A Possible Origin, The Canadian Mineralogist, v. 48, pp. 1373-1384.

Vasquez, A., *date unknown*, A Comparative Analysis of Talc Deposits in the Ruby Range, Montana. Department of Geology Amherst College.

Vuke, S., Porter, K., Lonn, J., and Lopez, D., 2007, Geologic Map of Montana: Montana Bureau of Mines and Geology Geologic Map 62-A, pp. 73, scale 1:500,000, 2 sheets.

Wells, M., Holsh, T., Cruz-Uribe, A, and Vervoort, J, 2012, Geodynamics of synconvergent extension and tectonic mode switching: Constraints from the Sevier-Laramide orogen, Tectonics, v. 31, no. 1.

Winchell, A., 1911, A Theory for the Origin of Graphite as Exemplified in the Graphite Deposit Near Dillon, Montana, Economic Geology: Society of Economic Geologists, Inc., v. 6, pp. 218-230.

Winchell, A., 1914, Mining Districts of the Dillon Quadrangle, Montana and Adjacent Areas. U.S. Geological Survey, Bulletin 574.

Winston, D., 1986, Middle Proterozoic tectonics of the Belt basin, western Montana and northern Idaho, in Roberts, S.M., edBelt Supergroup—A guide to Proterozoic rocks of western Montana and adjacent areas: Montana Bureau of Mines and Geology Special Publication 94, p. 245–257.

Unknown, 1901, Crystal Graphite Company. Western Mining World, v. 15, no. 2, pp. 18.

Zazula, J., 1997, On Graphite Transformations and Pressure Induced By Absorption of the LHC Beam, LHC Project Note 78/97, CERN.

Unknown, 2014. Graphite Corp., Form 10-K Annual Report for the Period Ending 12/31/13. U.S. Securities and Exchange Commission.

# Appendix A - Lode Claims

| Claim Name | Location Date | BLM Serial No. | Size (acres) | Claimant |
|---|---|---|---|---|
| RG A-1 | 9/2/2016 | MMC233115 | 20.52 | Ruby Graphite Holdings, LLC. |
| RG A-2 | 6/25/2016 | MMC232732 | 12.46 | Ruby Graphite Holdings, LLC. |
| RG B-0 | 9/2/2016 | MMC233116 | 20.61 | Ruby Graphite Holdings, LLC. |
| RG B-2 | 6/25/2016 | MMC232733 | 19.87 | Ruby Graphite Holdings, LLC. |
| RG C-1 | 6/24/2016 | MMC232734 | 20.57 | Ruby Graphite Holdings, LLC. |
| RG C-2 | 6/23/2016 | MMC232735 | 20.66 | Ruby Graphite Holdings, LLC. |
| RG C-3 | 6/23/2016 | MMC232736 | 20.66 | Ruby Graphite Holdings, LLC. |
| RG D-1 | 6/24/2016 | MMC232737 | 20.66 | Ruby Graphite Holdings, LLC. |
| RG D-2 | 6/23/2016 | MMC232738 | 20.66 | Ruby Graphite Holdings, LLC. |
| RG D-3 | 6/23/2016 | MMC232739 | 10.23 | Ruby Graphite Holdings, LLC. |
| RG E-1 | 9/2/2016 | MMC233117 | 20.66 | Ruby Graphite Holdings, LLC. |
| RG E-2 | 6/26/2016 | MMC232740 | 20.66 | Ruby Graphite Holdings, LLC. |
| RG E-3 | 6/27/2016 | MMC232741 | 18.19 | Ruby Graphite Holdings, LLC. |
| RG F-00 | 9/3/2016 | MMC233118 | 20.66 | Ruby Graphite Holdings, LLC. |
| RG F-0 | 9/3/2016 | MMC233119 | 20.66 | Ruby Graphite Holdings, LLC. |
| RG F-1 | 9/2/2016 | MMC233120 | 20.66 | Ruby Graphite Holdings, LLC. |
| RG F-2 | 6/26/2016 | MMC232742 | 20.66 | Ruby Graphite Holdings, LLC. |
| RG F-3 | 6/27/2016 | MMC232743 | 20.66 | Ruby Graphite Holdings, LLC. |
| RG G-00 | 9/4/2016 | MMC233121 | 20.66 | Ruby Graphite Holdings, LLC. |
| RG G-0 | 9/4/2016 | MMC233122 | 20.66 | Ruby Graphite Holdings, LLC. |
| RG G-1 | 9/4/2016 | MMC233123 | 20.66 | Ruby Graphite Holdings, LLC. |
| RG G-2 | 6/28/2016 | MMC232744 | 20.66 | Ruby Graphite Holdings, LLC. |
| RG G-3 | 6/27/2016 | MMC232745 | 20.66 | Ruby Graphite Holdings, LLC. |
| RG AA-4 | 10/16/2017 | MMC235672 | 16.5 | Ruby Graphite Holdings, LLC. |
| RG AA-5 | 10/17/2017 | MMC235673 | 20.66 | Ruby Graphite Holdings, LLC. |
| RG AA-6 | 10/17/2017 | MMC235674 | 20.66 | Ruby Graphite Holdings, LLC. |
| RG AA-7 | 10/17/2017 | MMC235675 | 20.32 | Ruby Graphite Holdings, LLC. |
| RG AA-8 | 10/17/2017 | MMC235676 | 19.14 | Ruby Graphite Holdings, LLC. |
| RG AA-9 | 10/17/2017 | MMC235677 | 17.91 | Ruby Graphite Holdings, LLC. |
| RG AA-10 | 10/16/2017 | MMC235678 | 16.72 | Ruby Graphite Holdings, LLC. |
| RG AA-11 | 10/17/2017 | MMC235679 | 18.7 | Ruby Graphite Holdings, LLC. |
| RG AA-12 | 10/17/2017 | MMC235680 | 15.59 | Ruby Graphite Holdings, LLC. |
| RG A-3 | 10/13/2017 | MMC235681 | 8.01 | Ruby Graphite Holdings, LLC. |
| RG A-4 | 10/13/2017 | MMC235682 | 13.72 | Ruby Graphite Holdings, LLC. |
| RG A-5 | 10/13/2017 | MMC235683 | 20.66 | Ruby Graphite Holdings, LLC. |
| RG A-6 | 10/13/2017 | MMC235684 | 20.66 | Ruby Graphite Holdings, LLC. |
| RG A-7 | 10/13/2017 | MMC235685 | 20.66 | Ruby Graphite Holdings, LLC. |
| RG A-8 | 10/13/2017 | MMC235686 | 20.66 | Ruby Graphite Holdings, LLC. |
| RG A-9 | 10/17/2017 | MMC235687 | 20.66 | Ruby Graphite Holdings, LLC. |
| RG A-10 | 10/16/2017 | MMC235688 | 20.6 | Ruby Graphite Holdings, LLC. |
| RG B-3 | 10/13/2017 | MMC235689 | 20.61 | Ruby Graphite Holdings, LLC. |
| RG B-4 | 10/13/2017 | MMC235690 | 20.61 | Ruby Graphite Holdings, LLC. |
| RG B-5 | 10/13/2017 | MMC235691 | 20.61 | Ruby Graphite Holdings, LLC. |

| Claim Name | Location Date | BLM Serial No. | Size (acres) | Claimant |
|---|---|---|---|---|
| RG B-6 | 10/13/2017 | MMC235692 | 20.61 | Ruby Graphite Holdings, LLC. |
| RG B-7 | 10/13/2017 | MMC235693 | 20.61 | Ruby Graphite Holdings, LLC. |
| RG B-8 | 10/13/2017 | MMC235694 | 20.61 | Ruby Graphite Holdings, LLC. |
| RG B-9 | 10/17/2017 | MMC235695 | 20.61 | Ruby Graphite Holdings, LLC. |
| RG B-10 | 10/16/2017 | MMC235696 | 16.09 | Ruby Graphite Holdings, LLC. |
| RG C-4 | 10/16/2017 | MMC235697 | 19.15 | Ruby Graphite Holdings, LLC. |
| RG C-5 | 10/18/2017 | MMC235698 | 20.66 | Ruby Graphite Holdings, LLC. |
| RG C-6 | 10/18/2017 | MMC235699 | 20.66 | Ruby Graphite Holdings, LLC. |
| RG C-7 | 10/12/2017 | MMC235700 | 20.66 | Ruby Graphite Holdings, LLC. |
| RG C-8 | 10/12/2017 | MMC235701 | 20.66 | Ruby Graphite Holdings, LLC. |
| RG C-9 | 10/12/2017 | MMC235702 | 20.66 | Ruby Graphite Holdings, LLC. |
| RG C-10 | 10/16/2017 | MMC235703 | 8.94 | Ruby Graphite Holdings, LLC. |
| RG D-4 | 10/18/2017 | MMC235704 | 13.17 | Ruby Graphite Holdings, LLC. |
| RG D-6 | 10/18/2017 | MMC235705 | 8.44 | Ruby Graphite Holdings, LLC. |
| RG D-7 | 10/12/2017 | MMC235706 | 9.53 | Ruby Graphite Holdings, LLC. |
| RG D-8 | 10/12/2017 | MMC235707 | 10.63 | Ruby Graphite Holdings, LLC. |
| RG D-9 | 10/12/2017 | MMC235708 | 11.72 | Ruby Graphite Holdings, LLC. |
| RG D-10 | 10/12/2017 | MMC235709 | 15.86 | Ruby Graphite Holdings, LLC. |
| RG E-4 | 10/8/2017 | MMC235710 | 16.69 | Ruby Graphite Holdings, LLC. |
| RG E-5 | 10/8/2017 | MMC235711 | 15.6 | Ruby Graphite Holdings, LLC. |
| RG E-6 | 10/8/2017 | MMC235712 | 14.5 | Ruby Graphite Holdings, LLC. |
| RG E-7 | 10/11/2017 | MMC235713 | 13.4 | Ruby Graphite Holdings, LLC. |
| RG E-8 | 10/11/2017 | MMC235714 | 12.3 | Ruby Graphite Holdings, LLC. |
| RG E-9 | 10/11/2017 | MMC235715 | 13.63 | Ruby Graphite Holdings, LLC. |
| RG E-10 | 10/11/2017 | MMC235716 | 20.66 | Ruby Graphite Holdings, LLC. |
| RG E-11 | 10/11/2017 | MMC235717 | 18.08 | Ruby Graphite Holdings, LLC. |
| RG F-4 | 10/8/2017 | MMC235718 | 20.66 | Ruby Graphite Holdings, LLC. |
| RG F-5 | 10/8/2017 | MMC235719 | 20.66 | Ruby Graphite Holdings, LLC. |
| RG F-6 | 10/8/2017 | MMC235720 | 20.66 | Ruby Graphite Holdings, LLC. |
| RG F-7 | 10/11/2017 | MMC235721 | 20.66 | Ruby Graphite Holdings, LLC. |
| RG F-8 | 10/11/2017 | MMC235722 | 20.66 | Ruby Graphite Holdings, LLC. |
| RG F-9 | 10/11/2017 | MMC235723 | 20.66 | Ruby Graphite Holdings, LLC. |
| RG F-10 | 10/11/2017 | MMC235724 | 20.66 | Ruby Graphite Holdings, LLC. |
| RG F-11 | 10/11/2017 | MMC235725 | 10.98 | Ruby Graphite Holdings, LLC. |
| RG G-4 | 10/9/2017 | MMC235726 | 20.66 | Ruby Graphite Holdings, LLC. |
| RG G-5 | 10/9/2017 | MMC235727 | 20.66 | Ruby Graphite Holdings, LLC. |
| RG G-6 | 10/9/2017 | MMC235728 | 20.66 | Ruby Graphite Holdings, LLC. |
| RG G-7 | 10/9/2017 | MMC235729 | 20.66 | Ruby Graphite Holdings, LLC. |
| RG G-8 | 10/9/2017 | MMC235730 | 20.66 | Ruby Graphite Holdings, LLC. |
| RG G-9 | 10/11/2017 | MMC235731 | 20.66 | Ruby Graphite Holdings, LLC. |
| RG G-10 | 10/10/2017 | MMC235732 | 20.66 | Ruby Graphite Holdings, LLC. |
| RG H-00 | 10/10/2017 | MMC235733 | 20.66 | Ruby Graphite Holdings, LLC. |
| RG H-0 | 10/10/2017 | MMC235734 | 20.66 | Ruby Graphite Holdings, LLC. |
| RG H-1 | 10/10/2017 | MMC235735 | 19.53 | Ruby Graphite Holdings, LLC. |
| RG H-2 | 10/10/2017 | MMC235736 | 12.98 | Ruby Graphite Holdings, LLC. |
| RG H-3 | 10/10/2017 | MMC235737 | 14.09 | Ruby Graphite Holdings, LLC. |
| RG H-4 | 10/9/2017 | MMC235738 | 15.2 | Ruby Graphite Holdings, LLC. |

| Claim Name | Location Date | BLM Serial No. | Size (acres) | Claimant |
|---|---|---|---|---|
| RG H-5 | 10/9/2017 | MMC235739 | 16.3 | Ruby Graphite Holdings, LLC. |
| RG H-6 | 10/9/2017 | MMC235740 | 17.41 | Ruby Graphite Holdings, LLC. |
| RG H-7 | 10/9/2017 | MMC235741 | 18.52 | Ruby Graphite Holdings, LLC. |
| RG H-8 | 10/9/2017 | MMC235742 | 19.62 | Ruby Graphite Holdings, LLC. |
| RG H-9 | 10/11/2017 | MMC235743 | 20.55 | Ruby Graphite Holdings, LLC. |
| RG H-10 | 10/10/2017 | MMC235744 | 17.28 | Ruby Graphite Holdings, LLC. |